Proceedings of the Mini-Workshop

Quarks and Hadrons

Bled, Slovenia, July 7–14, 2002

Edited by

Bojan Golli
Mitja Rosina
Simon Širca

University of Ljubljana and Jožef Stefan Institute

The Mini-Workshop *Quarks and Hadrons*

was organized by

Jožef Stefan Institute, Ljubljana

Department of Physics, Faculty of Mathematics and Physics, University of Ljubljana

and sponsored by

Department of Physics, Faculty of Mathematics and Physics, University of Ljubljana

Society of Mathematicians, Physicists and Astronomers of Slovenia

Organizing Committee

Simon Širca
Mitja Rosina
Bojan Golli

List of participants

Wojciech Broniowski, Cracow, `b4bronio@cyf-kr.edu.pl`
Veljko Dmitrašinović, Belgrade, `dmitrasin@yahoo.com`
Wojciech Florkowski, Cracow, `florkows@amun.ifj.edu.pl`
Leonid Glozman, Graz, `leonid.glozman@uni-graz.at`
Dubravko Klabučar, Zagreb, `klabucar@phy.hr`
Dirk Merten, Bonn, `merten@isis6.itkp.uni-bonn.de`
Hans-Jürgen Pirner, Heidelberg, `pir@tphys.uni-heidelberg.de`
Bojan Golli, Ljubljana, `bojan.golli@ijs.si`
Damijan Janc, Ljubljana, `damijan.janc@ijs.si`
Milan Potokar, Ljubljana, `milan.potokar@ijs.si`
Mitja Rosina, Ljubljana, `mitja.rosina@ijs.si`
Simon Širca, Ljubljana, `simon.sirca@fmf.uni-lj.si`

Electronic edition

`http://www-f1.ijs.si/BledPub/`

Contents

Preface

The series of mini-workshops at Bled, which started in 1987 with the workshop on *Mesonic Degrees of Freedom in Hadrons*, has established its own character of friendly but productive confrontation of ideas, and has by now become traditional. The scope of this small-scale meeting was to confront people working on closely related problems in hadronic physics and to engage participants in critical discussions without the time constraints of "offical" meetings. We were pleased to see our guests invariably enjoying such a format. The Proceedings, initially published only on the Web, have also evolved into a full-fledged serial publication.

As the town of Bled has also hosted this year's European Conference on Few-Body Problems in Physics (September 8–14, 2002), the population at the Mini-Workshop was slightly reduced. However, even the ghost of the approaching big event during our small event has not deterred us from working hard in a relaxed atmosphere of Villa Plemelj. The beautiful environment of Lake Bled helped brighten up the atmosphere of the presentations while the occasional inclement weather contributed to the patience for long afternoon discussions.

Ljubljana, November 2002

B. Golli
M. Rosina
S. Širca

Workshops organized at Bled

▷ *What Comes beyond the Standard Model* (June 29–July 9, 1998)
    Bled Workshops in Physics **0** (1999) No. 1
▷ *Hadrons as Solitons* (July 6-17, 1999)
▷ *What Comes beyond the Standard Model* (July 22–31, 1999)
▷ *Few-Quark Problems* (July 8-15, 2000)
    Bled Workshops in Physics **1** (2000) No. 1
▷ *What Comes beyond the Standard Model* (July 17–31, 2000)
▷ *Statistical Mechanics of Complex Systems* (August 27–September 2, 2000)
▷ *Selected Few-Body Problems in Hadronic and Atomic Physics* (July 7-14, 2001)
    Bled Workshops in Physics **2** (2001) No. 1
▷ *What Comes beyond the Standard Model* (July 17–27, 2001)
    Bled Workshops in Physics **2** (2001) No. 2
▷ *Studies of Elementary Steps of Radical Reactions in Atmospheric Chemistry*
▷ *Quarks and Hadrons* (July 6-13, 2002)
    Bled Workshops in Physics **3** (2002) No. 3
▷ *What Comes beyond the Standard Model* (July 15–25, 2002)
    Bled Workshops in Physics **3** (2002) No. 4

Also published in this series

▷ Book of Abstracts, *XVIII European Conference on Few-Body Problems in Physics*,
    Bled, Slovenia, September 8–14, 2002, Edited by Rajmund Krivec, Bojan Golli,
    Mitja Rosina, and Simon Širca
    Bled Workshops in Physics **3** (2002) No. 1–2

Thermal model at RHIC *

Wojciech Broniowski and Wojciech Florkowski

H. Niewodniczański Institute of Nuclear Physics, ul. Radzikowskiego 152, 31-342
Kraków, Poland

Abstract. We show that the ratios of the abundances as well as the transverse-momentum
spectra of all hadrons measured at RHIC, including the hyperons, are described very well
in a thermal model assuming the simultaneous chemical and thermal freeze-outs. The
model calculation takes into account all hadronic resonances and uses a simple parametrization of the freeze-out hypersurface.

We present a simple model describing the abundances and the $p_\perp$-spectra
of hadrons measured at RHIC [1,2]. Our approach is a combination of the thermal model, used frequently in the studies of the relative hadron yields [3–11],
with a model of the hydrodynamic expansion of matter at freeze-out. The main
assumptions of the model [12–14] are as follows: *i)* the chemical freeze-out and
the thermal freeze-out occur simultaneously, which means that we neglect elastic
rescattering after the chemical freeze-out, *ii)* all hadronic resonances are included
in both the calculation of the hadron multiplicities and the spectra, and *iii)* a simple form of the freeze-out hypersurface is proposed, which is a generalization of
the Bjorken model [15] (see also [16–21]),

$$\tau = \sqrt{t^2 - x^2 - y^2 - z^2} = \text{const.} \tag{1}$$

The hydrodynamic flow on the freeze-out hypersurface (1) is taken in the form
resembling the Hubble law,

$$u^\mu = \frac{x^\mu}{\tau} = \frac{t}{\tau}\left(1, \frac{x}{t}, \frac{y}{t}, \frac{z}{t}\right). \tag{2}$$

Recently, new arguments have been accumulated in favor of our first assumption. The measurements of the $K^*(892)$ states by the STAR Collaboration
[22] indicate that either the daughter particles from the decay $K^*(892) \to K\pi$ do
not rescatter or the expansion time between the chemical and thermal freeze-out
is short (smaller than the $K^*(892)$ lifetime, τ=4 fm/c). Moreover, the measured
yield of $K^*(892)$ fits very well to the pattern obtained from the thermal analysis
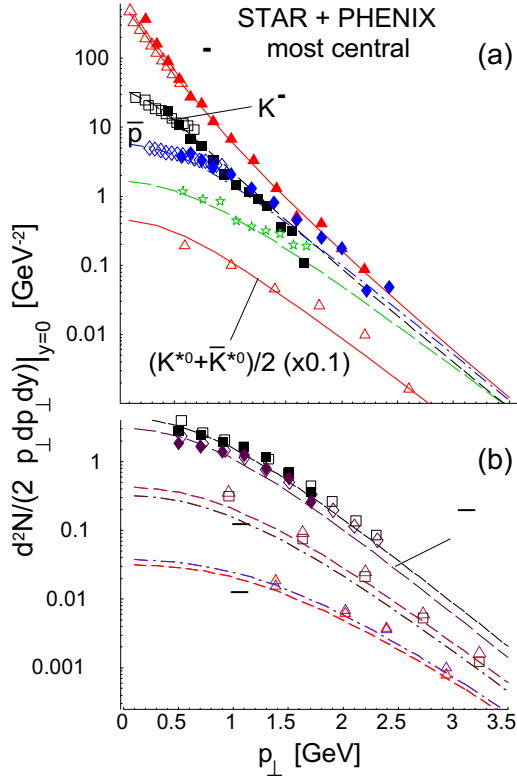
Fig. 1. The $p_\perp$-spectra at midrapidity of $\pi^-, K^-, \bar{p}, \phi$ and $K^*(892)$ in part (a), and of the hyperons Λ, Ξ and Ω in part (b). The model calculation is compared to the PHENIX (filled symbols) and STAR (open symbols) most central data [22,37,28,34,32,33,38–40] from Au + Au collisions at $\sqrt{s_{NN}}$ = 130 GeV. Both the data and the theoretical curves are absolutely normalized (they include full feeding from the weak decays).

of the ratios of hadron abundances. This fact suggests again a short expansion time between the two freeze-outs. The assumption about the single freeze-out also solves the antibaryon puzzle [24]. Since the annihilation cross section for $p\bar{p}$ pairs is much larger than the elastic cross section, most of the protons would annihilate with antiprotons during the long way from the chemical to the thermal freeze-out. Such effect is not seen. In addition, let us mention that the single-freeze-out scenario is natural if the hadronization process occurs in such a way that neither elastic or inelastic processes are effective. An example here is the *sudden-hadronization* model of Ref. [25].

Our model has two thermodynamic and two geometric (expansion) parameters. The two thermodynamic parameters, T = 165 MeV and μ_B = 41 MeV, were obtained from the analysis of the ratios of the hadron multiplicities measured at RHIC [11]. In this calculation the grand-canonical ensemble was used without the strangeness suppression factor (γ_s=1). Since the particle ratios depend weakly on

	Model	Experiment
Fitted thermal parameters		
T [MeV]	165 ± 7	
μ_B [MeV]	41 ± 5	
μ_S [MeV]	9	
μ_I [MeV]	-1	
χ^2/n	0.97	
Ratios used for the fit		
π^-/π^+	1.02	1.00 ± 0.02 [26], 0.99 ± 0.02 [27]
$\overline{p}/\pi^-$	0.09	0.08 ± 0.01 [28]
K^-/K^+	0.92	0.88 ± 0.05 [29], 0.78 ± 0.12 [30] 0.91 ± 0.09 [26], 0.92 ± 0.06 [27]
K^-/π^-	0.16	0.15 ± 0.02 [29]
K_0^*/h^-	0.046	0.060 ± 0.012 [29,31] later: 0.042 ± 0.011 [23]
$\overline{K_0^*}/h^-$	0.041	0.058 ± 0.012 [29,31] later: 0.039 ± 0.011 [23]
$\overline{p}/p$	0.65	0.61 ± 0.07 [28], 0.54 ± 0.08 [30] 0.60 ± 0.07 [26], 0.61 ± 0.06 [27]
$\overline{\Lambda}/\Lambda$	0.69	0.73 ± 0.03 [29]
$\overline{\Xi}/\Xi$	0.76	0.82 ± 0.08 [29]
Ratios predicted		
ϕ/h^-	0.019	0.021 ± 0.001 [32]
ϕ/K^-	0.15	$0.1 - 0.16$ [32]
Λ/p	0.47	0.49 ± 0.03 [33,34]
Ω^-/h^-	0.0010	0.0012 ± 0.0005 [35]
Ξ^-/π^-	0.0072	0.0085 ± 0.0020 [36]
Ω^+/Ω^-	0.85	0.95 ± 0.15 [35]

Table 1. Optimal thermal parameters, ratios $\frac{dN_i/dy}{dN_j/dy}\big|_{y=0}$ used for the fit, and further predicted ratios. The preliminary experimental numbers for $K^*(892)$ [31] have changed [23], and better agreement with the model followed.

the centrality of the collision, we treat the thermodynamic parameters as the universal parameters (independent of centrality).

The results for the particle abundances are collected in Table I.

The two geometric parameters are τ of Eq. (1) and ρ_{max}. The parameter ρ_{max} determines the transverse size of the firecylinder at the freeze-out,

$$\rho = \sqrt{x^2 + y^2} \leq \rho_{max}. \qquad (3)$$

In the natural way, the values of τ and ρ_{max} depend on the considered centrality class of events. For the minimum-bias data, which average over centralities, we find: $\tau = 5.55$ fm and $\rho_{max} = 4.50$ fm, whereas for the most central collisions we find: $\tau = 7.66$ fm and $\rho_{max} = 6.69$ fm [12]. The calculation of the spectra (and determination of the geometric parameters) is based on the standard Cooper-Frye formalism. The details of our method, especially of the technical problems

concerning the treatment of the resonances, are given in the Appendix of Ref. [13].

In Fig. 1 we show our results for the most central collisions. In the upper part (a) we show the spectra of pions, kaons, antiprotons, the ϕ mesons, and the $K^*(892)$ mesons. In the lower part (b) we show the spectra of the hyperons Λ, Ξ and Ω. The model calculation agrees very well with the data. Note, e.g., the convex shape of the pion spectrum, crossing of the pion and the antiproton spectra at $p_\perp \sim 2$ GeV, and the good reproducing of the Ω spectrum. The good agreement between the model calculation and the data supports strongly the idea of thermalization of the hadronic matter produced at RHIC. Let us emphasize that the expansion parameters were fitted in Ref. [12] to the spectra of pions, kaons and protons only. The spectra of other particles were calculated with the same values of the parameters, hence, they are predictions of our model. In view of this fact, the good agreement of the Ω spectrum, predicted before the data were available, is highly non-trivial, especially in the context of the SPS results [14].

A characteristic feature of our approach is a rather high decoupling temperature $T \sim 165$ MeV. However, the (inverse) slope parameters corresponding to this temperature are lowered by the decays of the resonances [11]. This "cooling" of the spectrum by the decays of the resonances explains the difference between the high temperature of the chemical freeze-out and a smaller "apparent" temperature inferred from the shape of the spectra. We note that a similar high decoupling temperature has been found in the full hydrodynamic calculation of Ref. [41], where also a complete set of hadronic resonances is employed. It remains a challenge to check whether our particular freeze-out conditions (shape of the freeze-out hypersurface and Hubble flow) may be obtained as the final stage of hydrodynamic evolution. First steps in this direction have been already made [42].

Let us make a few comments about the size of our geometric parameters. Translated to the measured HBT radii, R_{out} and R_{side}, they turn out to be too small. This problem can be circumvented by the inclusion of the excluded-volume corrections [6] which affect only the overall normalization of the spectra. If we rescale τ and ρ_{max} by about 30%, we obtain a satisfactory agreement with the HBT data. On the other hand, the ratio R_{out}/R_{side} is close to unity in our model, independently of the excluded-volume corrections. The approximate equality of these two radii follows in our model from the fact that the time extension of our system at freeze-out is much shorter than its space extension.

In conclusion, we want to stress that a simple thermal model (with altogether four parameters) reproduces the abundances and the transverse-momentum spectra of all hadrons which have been measured so far at RHIC. This fact brings strong evidence for thermalization of hadronic matter at RHIC and, possibly, indicates that a thermalized system of quarks and gluons was formed at the earlier stages of the collisions.

References

1. Proceedings of the 15th Int. Conference on Ultrarelativistic Nucleus-Nucleus Collisions (Quark Matter 2001), Stony Brook, New York, 15-20 Jan 2001, Nucl. Phys. **A698** (2002).
2. Proceedings of the 16th Int. Conference on Ultrarelativistic Nucleus-Nucleus Collisions (Quark Matter 2002), Nantes, France, 18-24 July 2002, to be published in Nucl. Phys. **A**.
3. J. Rafelski, J, Letessier, and A. Tounsi, Acta Phys. Pol. B **28**, 2841 (1997).
4. J. Cleymans, D. Elliott, H. Satz, and R. L. Thews, Z. Phys. C **74**, 319 (1997).
5. P. Braun-Munzinger, I. Heppe, and J. Stachel, Phys. Lett. B **465**, 15 (1999).
6. G. D. Yen and M. I. Gorenstein, Phys. Rev. C **59**, 2788 (1999).
7. F. Becattini, J. Cleymans, A. Keranen, E. Suhonen, and K. Redlich, Phys. Rev. C **64**, 024901 (2001).
8. M. Gaździcki, Nucl. Phys. A **681**, 153 (2001).
9. J. Rafelski, J. Letessier, and G. Torrieri, Phys. Rev. C **64**, 054907 (2001).
10. P. Braun-Munzinger, D. Magestro, K. Redlich, and J. Stachel, Phys. Lett. B **518**, 41 (2001).
11. W. Florkowski, W. Broniowski, and M. Michalec, Acta Phys. Pol. B **33**, 761 (2002).
12. W. Broniowski and W. Florkowski, Phys. Rev. Lett. **87**, 272302 (2001).
13. W. Broniowski and W. Florkowski, Phys. Rev. C **65**, 064905 (2002).
14. W. Broniowski and W. Florkowski, Proc. of the Int. Workshop XXX on Gross Properties of Nuclei and Nuclear Excitations, Hirschegg, 2002, p. 146, hep-ph/0202059.
15. J. D. Bjorken, Phys. Rev. D **27**, 140 (1983).
16. G. Baym, B. Friman, J.-P. Blaizot, M. Soyeur, and W. Czyż, Nucl. Phys. A **407**, 541 (1983).
17. P. Milyutin and N. N. Nikolaev, Heavy Ion Phys **8**, 333 (1998); V. Fortov, P. Milyutin, and N. N. Nikolaev, JETP Lett. **68**, 191 (1998).
18. P. J. Siemens and J. Rasmussen, Phys. Rev. Lett. **42**, 880 (1979); P. J. Siemens and J. I. Kapusta, Phys. Rev. Lett. **43**, 1486 (1979).
19. E. Schnedermann, J. Sollfrank, and U. Heinz, Phys. Rev. C **48**, 2462 (1993).
20. T. Csörgő and B. Lörstad, Phys. Rev. C **54**, 1390 (1996).
21. D. H. Rischke and M. Gyulassy, Nucl. Phys. A **697**, 701 (1996); Nucl. Phys. A **608**, 479 (1996).
22. P. Fachini, STAR Collaboration, nucl-ex/0203019.
23. C. Adler et al., STAR Collaboration, nucl-ex/0205015.
24. R. Rapp and E. V. Shuryak, Proc. of the Int. Workshop XXX on Gross Properties of Nuclei and Nuclear Excitations, Hirschegg, 2002, p. 130, nucl-th/0202059.
25. J. Rafelski and J. Letessier, Phys. Rev. Let. **85**, 4695 (2000); G. Torrieri and J. Rafelski, New J. Phys. **3**, 12 (2001).
26. B. B. Back, PHOBOS Collaboration, Phys. Rev. Lett. **87**, 102301 (2001).
27. I. G. Bearden, BRAHMS Collaboration, Nucl. Phys. **A698**, 667c (2002).
28. J. Harris, STAR Collaboration, Nucl. Phys. **A698**, 64c (2002).
29. H. Caines, STAR Collaboration, Nucl. Phys. **A698**, 112c (2002).
30. H. Ohnishi, PHENIX Collaboration, Nucl. Phys. **A698**, 659c (2002).
31. Z. Xu, STAR Collaboration, Nucl. Phys. **A698**, 607c (2002).
32. C. Adler et al., STAR Collaboration, Phys. Rev. **C65**, 041901 (2002).
33. C. Adler et al., STAR Collaboration, nucl-ex/0203016.
34. C. Adler et al., STAR Collaboration, Phys. Rev. Lett. **87**, 262302 (2001).
35. C. Suire, STAR Collaboration, in [2].
36. J. Castillo, STAR Collaboration, in [2].

37. J. Velkovska, PHENIX Collaboration, Nucl. Phys. A **698**, 507c (2002).
38. K. Adcox et al., PHENIX Collaboration, Phys. Rev. Lett. **89**, 092302 (2002).
39. J. Castillo, STAR Collaboration, talk presented at SQM2001; see also in [2].
40. B. Hippolyte, STAR Collaboration, talk presented at CRIS2002.
41. K. J. Eskola, H. Niemi, P. V. Ruuskanen, and S. S. Räsänen, hep-ph/0206230; P. V. Ruuskanen, in [2].
42. T. Csörgő, F. Grassi, Y. Hama, and T. Kodama, hep-ph/0204300.

Effective $U_A(1)$ symmetry breaking interactions

V. Dmitrašinović

Vinča Institute of Nuclear Sciences, P.O.Box 522, 11001 Beograd, Yugoslavia

Abstract. We review the phenomenological consequences of various effective $U_A(1)$ symmetry breaking interactions. In particular we look at the baryon spectra. We comment on the recent conjecture that the chiral symmetry might be restored in the higher regions of hadron spectra in the light of our results for scalar mesons and the spectral sum rules.

The so-called "$U_A(1)$ problem" consists of (i) the fact that the sum of the eighth and ninth pseudoscalar meson $\eta(550)$, $\eta^{'}(960)$ masses lies (far) above the flavour $SU(3)$ mass relations prediction of two kaon masses ($2\,m_K$) and (ii) that their mixing angle is far from being the "ideal" one. These two facts imply a large *explicit* $U_A(1)$ symmetry breaking, that is believed to be induced by instantons in QCD. These instanton effects can be described by 't Hooft's $U_A(1)$-symmetry breaking quark flavour determinant effective interaction [1]

$$\begin{aligned}\mathcal{L}_{tH}^{(6)} &= -K_{tH}\left[\det\left(\bar{\psi}(1+\gamma_5)\psi\right) + \det\left(\bar{\psi}(1-\gamma_5)\psi\right)\right]\\ &= -2K_{tH}\mathfrak{Re}\left(\det\bar{\psi}(1+\gamma_5)\psi\right).\end{aligned} \tag{1}$$

Phenomenological consequences of the determinant effective interaction in spinless meson channels of either parity have been studied in Ref. [2], where new effects for the scalar mesons were reported. In the same place the strength K of the 't Hooft interaction was also fixed in terms of the pseudoscalar (PS) meson properties as

$$-12K_{tH}\langle\bar{q}q\rangle^3 = f_\eta^2\left[m_{\eta'}^2 + m_\eta^2 - 2m_K^2\right]. \tag{2}$$

Equivalent results for scalar mesons have been reported in Ref. [3] using directly the instanton-induced (II) interaction with a finite spatial range.

There is another $U_A(1)$ symmetry breaking effective interaction that is proportional to the squared imaginary part of the determinant

$$\begin{aligned}\mathcal{L}_{VW}^{(12)} &= K_{VW}\left[\det\left(\bar{\psi}(1+\gamma_5)\psi\right) - \det\left(\bar{\psi}(1-\gamma_5)\psi\right)\right]^2\\ &= -4K_{VW}\left(\mathfrak{Im}\det\bar{\psi}(1+\gamma_5)\psi\right)^2.\end{aligned} \tag{3}$$

as well as the analogues of the above two with antisymmetric Pauli tensors inserted between the Dirac spinors [4].

1 Mesons

The role of $U_A(1)$ symmetry breaking in meson spectra has been extensively studied over the past 10 years [2–7]; a brief review of the field can be found in Ref. [8]. There scalar meson spectra and the V - A spectral sum rules were discussed. Considering the fact that the recent parity-doubling/chiral symmetry restoration (χSR) conjecture [9] uses several methods and/or results obtained or used in the aforementioned studies, this seems like a good place to make several comments of direct relevance to this conjecture, rather than to review again some established facts. This is by no means to be understood as a polemic, but rather as a part of an academic dialogue: It is an observation on matters not discussed by Glozman that could potentially have serious implications for the viability of this idea.

1. **An explicit counterexample** to the claim that asymptotic restoration of chiral $SU_L(N_f) \times SU_R(N_f)$ symmetry implies parity doubling in meson spectra is the original form of the second Weinberg sum rule: Even with as strong an assumption as the vanishing of the zeroth moment of the spectral density difference (that later proved to be false in QCD), Weinberg still had to assume another ("KSFR") relation (connecting the widths of the vector and axial-vector states) before he could turn his assumption into a prediction of the vector/axial-vector meson mass ratio (that turned out to be $1/\sqrt{2}$ rather than unity, as conjectured by Glozman!). Now, one may object that these are only the ground state mesons, that are not subject of the χSR conjecture. But, as one increases the number of states in the spectra, the number of new "radially excited state KSFR" relations, that are necessary to calculate the V/A mass ratios, also grows. Clearly, more is necessary for parity doubling of vector (V) and axial-vector (A) mesons than mere asymptotic equality of spectral functions. If that were not enough, it has been shown [4] that the second spectral sum rule is not only sensitive to $SU_L(N_f) \times SU_R(N_f)$ chiral symmetry breaking (χSB), but rather to nonconservation of the "larger" (enveloping) $U_L(2N_f) \times U_R(2N_f)$ *current algebra*. Thus, one may have χSR and still have a nonvanishing second spectral sum. In other words, spectral functions do *not* depend only on *chiral* symmetry, as assumed by Glozman, but also on higher current algebras.

2. **Technical objections** to the way $U_A(1)$ symmetry breaking was treated. (i) $U_A(1)$ symmetry breaking depends (sensitively) on the number of (light) flavours, c.f. Ref. [2]. Glozman uses two-flavour mass formulas for "realistic" purposes (to compare with experimental spectra), instead of the three flavour ones. This is inadmissible and only hides other shortcomings of this scheme: (a) Too few flavour singlets are predicted: some observed states must be assigned to glueballs, so it is not clear which states are radial excitations; (b) not all of the suggested mass differences may serve as measure of $U_A(1)$ symmetry breaking: In this regard we have shown in Ref. [6] that the scalar meson mass difference may vanish even with 't Hooft force turned on, depending on the strength of the vector/axial-vector interaction, i.e. on the admixing of pseudo-vector component to the pseudoscalar mesons. (ii) An oversimplified assignment of mesons to chiral symmetry irreducible representations (irreps)

has been made in Ref. [9]: mixings of pseudoscalar (PS) and axial vector (A), scalar (S) and vector (V), V and tensor (T), A and pseudotensor (PT) have been ignored. As we have shown in Ref. [6], mixing of PS and A mesons substantially changes the scalar meson mass difference that was used as a measure of $U_A(1)$ symmetry restoration by Glozman. Indeed the said mass difference can be made arbitrarily close to zero, even in the presence of $U_A(1)$ symmetry breaking interaction, by means of changing the amount of the PS-A mixing. Other mixings, mentioned above, may well have similarly dramatic effects.

3. **Objections to the identification procedure** for chiral multiplets. Even if the experimental interpretation in Ref. [9] were correct, the conclusion that chiral symmetry restoration-induced parity doublets have already been observed would still be invalid. Rather, the "observed" parity doubling would be purely accidental. This is so because members of *different* chiral multiplets have been compared (see below) in Glozman's putative scheme [9]. That is, of course, inadmissible: chiral restoration implies parity doubling within the same chiral multiplet, not among members of two different multiplets (which doubling may indeed occur, but only due to random coincidence) [10]. In a logically consistent check of chiral restoration one must first positively identify the purported members of chiral multiplets going from the bottom up, i.e. starting with the ground state and then matching corresponding excited states. One must not start at some high-lying set of (accidental) parity doublets and then move down until one arbitrarily declares victory and all states lying below that arbitrary line as being beyond the reach of the conjecture, as was done in Ref. [9]. As one moves down in mass from the alleged parity doubled chiral partners in Glozman's proposed scheme, one finds that some chiral multiplets are incomplete: for example, the (well established) $\pi(1300)$ state does not have a scalar partner in the observed spectrum, according to Glozman's scheme. This proves that a misidentification of chiral multiplets has taken place, which fact negates all claims relating to chiral symmetry restoration in meson spectra at high masses.

2 Baryons

More recently, significant effects due to the instanton-induced interaction have been reported in baryon spectroscopy [11]. In this note we wish to give a simple explanation of the 't Hooft quark flavour-determinant effective interaction's effects in baryon spectroscopy. We confirm the results of earlier studies [11], with one distinction: we have no free parameters to adjust in our calculation because we take the value of the 't Hooft coupling constant K as constrained above by the meson spectra.

The effective two-body 't Hooft interaction leads to the following two-quark potential

$$V_{12} = 4K \langle \bar{q}q \rangle_0 P_{12}^{\bar{3}} \left(1 + \gamma^5{}_1 \gamma^5{}_2 \right) \delta(\mathbf{r}_1 - \mathbf{r}_2)$$
$$P_{12}^{\bar{3}} = \left[\frac{1}{3} - \frac{1}{4} \boldsymbol{\lambda}_1 \cdot \boldsymbol{\lambda}_2 \right]. \tag{4}$$

The flavour dependence of this potential is proportional to the $\bar{\mathbf{3}}$ projection operator $P_{12}^{\bar{3}}$, i.e., it only operates in the flavour antisymmetric state. Note, however, that in the $q\bar{q}$ channels the same flavour factor is *not exactly* a flavour singlet projector any more.

The 't Hooft interaction also leads to the following three-quark potential

$$V_{123} = 12KP_{123}^1 \left(1 + \sum_{i<j}^3 \gamma^5{}_i\gamma^5{}_j \right) \delta(\mathbf{r}_1 - \mathbf{r}_2)\delta(\mathbf{r}_3 - \mathbf{r}_2)$$

$$12P_{123}^1 = \left[\frac{4}{9} - \frac{1}{3}\sum_{i<j}^3 \boldsymbol{\lambda}_i \cdot \boldsymbol{\lambda}_j + d^{abc}\lambda_1^a\lambda_2^b\lambda_3^c \right]. \tag{5}$$

As can be seen from Eq. (5) the flavour dependence of the 't Hooft three-quark potential is just the flavour SU(3) singlet projection operator P_{123}^1 [8] for three quarks. Thus the 't Hooft three-quark potential contributes only in the flavour singlet q^3 channel, as already noticed in Ref. [11]. As the lowest lying flavour singlet is necessarily a P-wave state (due to the Pauli principle) and the spatial part of the three-body potential Eq. (5) contains two Dirac delta functions, its matrix element is zero.

We use the constituent quark model [12] with the harmonic oscillator Hamiltonian to calculate the basic effects of the 't Hooft interaction. This model is clearly rather simple, but should be adequate for the purpose of identifying the qualitative features and making first estimates of the 't Hooft interaction effects in baryons. In the following we shall keep only the leading-order ($\mathcal{O}(1)$) terms in the nonrelativistic [NR] expansion, i.e. we do not keep the spin dependent parts. In this spirit we have also neglected the strong-hyperfine ("Breit") interaction in the constituent quark Hamiltonian [12], that is believed to be an important part of the (extended) constituent quark model, but that also suffers from several shortcomings, an excessively large coupling constant being one. We shall show that some of the best known effects associated with the strong Breit force are reproduced by the 't Hooft interaction.

With these assumptions we can calculate the three-quark system spectra in different flavour channels. But as the 't Hooft potential is a contact term, one cannot separate the resulting Schrödinger equation exactly. So, we must use some approximate method, e.g. perturbation theory. We find the following 't Hooft potential flavour space matrix elements

$$\langle V \rangle_1 = 12K\langle \bar{q}q \rangle_0 \langle \delta(\mathbf{r}_1 - \mathbf{r}_2) \rangle_1 \tag{6}$$

$$\langle V \rangle_8 = 6K\langle \bar{q}q \rangle_0 \langle \delta(\mathbf{r}_1 - \mathbf{r}_2) \rangle_8 \tag{7}$$

$$\langle V \rangle_{10} = 0 \tag{8}$$

The reason for the last line is that the flavour singlet **1** three-quark system cannot have a completely symmetric spin-spatial wave function, the way the ground state octet and decimet do, due to the Pauli principle and the complete antisymmetry of the singlet's flavour- and colour wave functions.
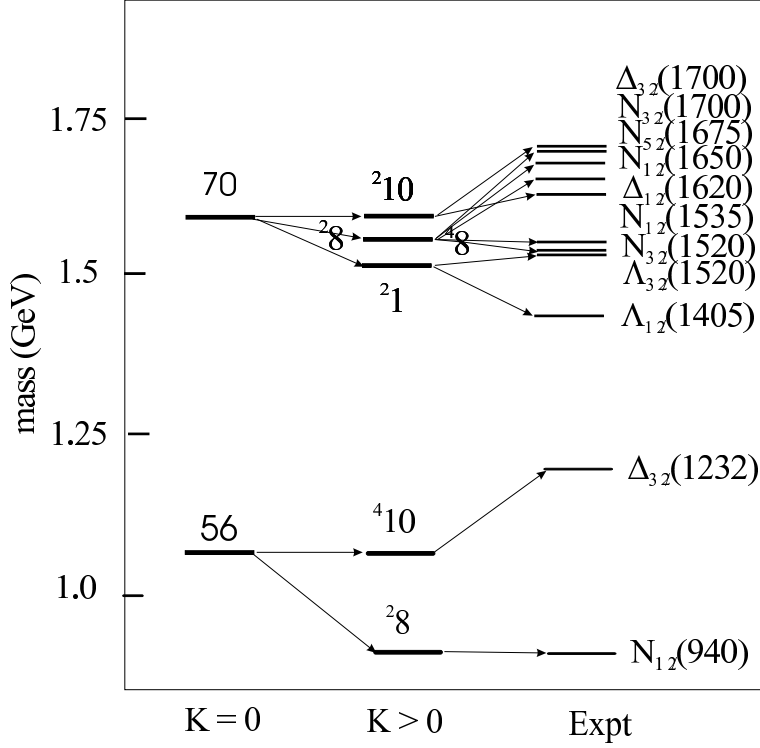
Fig. 1. Baryon mass spectrum as calculated in the nonrelativistic quark model with harmonic oscillator confinement without (K = 0) and with (K $\neq$ 0) 'tHooft interaction for the two lowest lying shells (N = 0,1); the prediction for the Roper resonance (N = 2) is not shown. Also shown are the observed baryon states (expt).

In the first approximation with all spin-spin interactions neglected,

$$\langle \Psi_S(N=0)|\delta(\mathbf{r}_1 - \mathbf{r}_2)|\Psi_S(N=0)\rangle = \langle \delta(\mathbf{r}_1 - \mathbf{r}_2)\rangle_{8\subset 56} = \langle \delta(\mathbf{r}_1 - \mathbf{r}_2)\rangle_{10\subset 56}$$

$$\equiv I = \left(\frac{m_q \omega}{\sqrt{2\pi}}\right)^{3/2} \tag{9}$$

$$\langle \Psi_P(N=1)|\delta(\mathbf{r}_1 - \mathbf{r}_2)|\Psi_P(N=1)\rangle = \langle \delta(\mathbf{r}_1 - \mathbf{r}_2)\rangle_{1\subset 70} = \frac{1}{2}\sum_M \langle \psi_{1M}^\lambda|\delta(\mathbf{r}_1 - \mathbf{r}_2)|\psi_{1M}^\lambda\rangle$$

$$= \frac{1}{2}I = \frac{1}{2}\left(\frac{m_q \omega}{\sqrt{2\pi}}\right)^{3/2} \tag{10}$$

$$\langle \Psi_S'(N=2)|\delta(\mathbf{r}_1 - \mathbf{r}_2)|\Psi_S'(N=2)\rangle = \langle \delta(\mathbf{r}_1 - \mathbf{r}_2)\rangle_{8\subset 56}$$

$$= \frac{5}{4}I = \frac{5}{4}\left(\frac{m_q \omega}{\sqrt{2\pi}}\right)^{3/2}, \tag{11}$$

where ω = 500 MeV is the oscillator frequency in the model, and the constituent quark mass, $m_q = 313 MeV$, is approximately one third of the nucleon's. Thus we find the following energy shifts

$$\delta E_{1\subset 70}(N=1) = \delta E_{8\subset 56}(N=0) = 6K\langle \bar{q}q\rangle_0 I \tag{12}$$

$$\delta E_{\mathbf{8} \subset \mathbf{70}}(N = 1) = 3K\langle \bar{q}q \rangle_0 I \tag{13}$$

$$\delta E_{\mathbf{8} \subset \mathbf{56}}(N = 2) = \frac{15}{2}K\langle \bar{q}q \rangle_0 I \tag{14}$$

$$\delta E_{\mathbf{10}} = 0. \tag{15}$$

Inserting into Eq. (2) the experimental value for the ps meson masses and decay constants, as well as the quark condensate $\langle \bar{q}q \rangle = -(225\text{MeV})^3$, the 't Hooft coupling constant becomes $K = 390\text{GeV}^{-5}$, we find the baryon spectrum shown in Fig. 1. The second radially excited state (the Roper resonance) mass moves down by about 130MeV, but is still too large to be visible in Fig. 1. There one can see that about one third of the observed positive parity ground state $\mathbf{8} - \mathbf{10}$ mass splitting and about one half of the observed negative parity $\mathbf{1} - \mathbf{10}$ mass splitting are reproduced by 't Hooft interaction. Admittedly, one cannot describe the fine structure (LS splitting) of the spectra (as yet), but that ought to be possible with the inclusion of spin-dependent forces. In particular these results show that 't Hooft's interaction causes a significant part (at least a half) of the $\Lambda_0(1405)$ and $\Lambda_0(1520)$'s mass shifts to anomalously low masses compared with other P-wave baryons. [Remember that $N^*(1535)$ and $N^*(1520)$ ought to be about 130 MeV lighter than the corresponding Λ_0's, due to one strange quark in the latter, in the absence of 't Hooft's interaction.] This mass shift was first pointed out in Ref. [11]. Finally, the mystery of the Roper resonance's abnormally low mass now seems within the reach of rational explanation starting from QCD.

References

1. G. 't Hooft, Phys. Rev. D **14**, 3432 (1976), (E) *ibid.* **18**, 2199 (1978);
2. V. Dmitrašinović, Phys. Rev. **C 53**, 1383 (1996).
3. E. Klempt, B. C. Metsch, C. R. Münz, and H. R. Petry, Phys. Lett. **B 361**, 160 (1995).
4. V. Dmitrašinović, Phys. Rev. D **56**, 247 (1997).
5. V. Dmitrašinović, Phys. Rev. **D 57**, 7019 (1998).
6. V. Dmitrašinović, Nucl. Phys. **A 686**, 377 (2001).
7. V. Dmitrašinović, Phys. Rev. **D 62**, 096010(8) (2000).
8. V. Dmitrašinović, p. 46 - 53 in "Hadrons and Nuclei: First International Symposium", AIP Conf. Proc. 594; ed. I-T. Cheon, T. Choi, S.-W. Hong and S.H. Lee, American Institute of Physics, Melville, N.Y., (2001).
9. L. Ya. Glozman, hep-ph/0205072 and these proceedings.
10. D. Jido, Y. Nemoto, M.Oka and A. Hosaka, Nucl. Phys. **A 671**, 471 (2000).
11. U. Löring, B.Ch. Metsch, and H.R. Petry,Eur. Phys. J. **A 10**, 395 (2001); *ibid.***A 10**, 447 (2001).
12. A. Le Yaouanc, L L. Oliver, O. Pène and J.-C. Raynal, *Hadron Transitions in the Quark Model*, (Gordon and Breach, New York, 1988).

Clustering, colour SU(3) symmetry and confinement in the $q^2\bar{q}^2$ system

V. Dmitrašinović

Vinča Institute of Nuclear Sciences, P.O.Box 522, 11001 Beograd, Yugoslavia

Abstract. We examine the clustering properties, or "colour saturation" of the $q^2\bar{q}^2$ system in the presence of SU(3) symmetric two- and three-quark interactions proposed to enforce confinement (Phys. Lett. **B 499**, 135 (2001)). We assume the most general SU(3) transformation properties of the four-quark interaction and then show that at least some four-quark interaction is necessary to ensure clustering of the $q^2\bar{q}^2$ system into two $q\bar{q}$ mesons, though that also leads to a breakdown of confinement, and *vice versa*.

The SU(3) colour degree of freedom was introduced in the mid-60's with the intention of alleviating the need for quark (rank-3) para-statistics [1,2]. The working assumption has been that confinement allows only colour singlet states to exist, or put differently, that the colour singlet states would be the lowest ones in energy, perhaps with an infinitely, or at least very large energy gap to the coloured states. In few-quark systems with the number of constituent quarks + antiquarks larger than three ($n \geq 4$), however, there are multiple colour singlets, that have not been experimentally observed (as yet). Thus, it appears that the above working assumption is insufficient to explain the paucity of observed states, i.e. we may have to look for an additional selection rule or a new dynamical principle.

In a recent attempt to ensure confinement of quarks with general SU(3) symmetric colour dynamics, we were forced to modify the usual $F_i \cdot F_j$ two-quark interaction and to introduce a new three-quark one [3]. This new interaction ensures that the colour singlets are the lowest energy states in both the $q\bar{q}$ and the q^3 systems in addition to confinement of these systems. In the $q^2\bar{q}^2$ system this three-quark force splits the energies of the two colour singlet states, as it does in the q^6 system [4]. That is, however, not enough to make this dynamics viable: it has to allow for the observed clustering of quarks and antiquarks into mesons (and baryons) at asymptotic center-of-mass (CM) separations. [1]

We shall start here the study of clustering in the simplest nontrivial system: $q^2\bar{q}^2$ ought to cluster into two $q\bar{q}$ mesons. Clustering is automatic with the $F_i \cdot F_j$ two-quark interaction, but the new colour-independent two-body interaction is additive, i.e. it does not saturate. The new three-quark interaction introduced in Ref. [3] does saturate, indeed it vanishes entirely in the two-meson colour-singlet state [4]. Thus, we must look for other ways to cancel the additive two-quark force

---

[1] This property sometimes goes by the name of "colour saturation", for historical reasons, named after similarity to the nuclear interaction saturation.

in this channel. Several possibilities arise: 1) a non-saturating three-quark force, which, however, would spoil the good confinement properties of the q^3 system, or 2) a non-saturating four-quark force. We shall focus here on the latter.

In the $q^2 \bar{q}^2$ system, there are two linearly independent colour singlets. One can separate them according to their symmetry properties under the interchange of the two quark/antiquark indices: one state ($|6_{12} \bar{6}_{34}\rangle$) is symmetric, another ($|\bar{3}_{12} 3_{34}\rangle$) antisymmetric. The asymptotic "two meson" colour singlet state is a linear combination of the two: $|1_{13} 1_{24}\rangle = \frac{1}{\sqrt{3}} |\bar{3}_{12} 3_{34}\rangle + \sqrt{\frac{2}{3}} |6_{12} \bar{6}_{34}\rangle$. Clustering means that "two meson" colour singlet state expectation value of the (total) potential must be proportional to the sum of two two-body potentials in the limit of asymptotically large CM separations:

$$\lim_{R \to \infty} \left(\langle V \rangle_{11} \equiv \langle 1_{13} 1_{24} | V | 1_{13} 1_{24} \rangle \right) \simeq \mathcal{V}_{13} + \mathcal{V}_{24} \tag{1}$$

where

$$V = V^{2b} + V^{3b} + V^{4b} \tag{2}$$

$$V^{2b} = \sum_{i<j}^{4} V_{ij}, \tag{3}$$

$$V^{3b} = \sum_{i<j<k}^{4} V_{ijk}, \tag{4}$$

$$V^{4b} = V_{1234} . \tag{5}$$

In order to verify the clustering condition Eq. (1) in QCD, one must know the exact forms of the two-, three- and four-body potentials, which is impossible at this stage, both empirically and theoretically. In Ref. [3] we made some simple Ansätze for the two- and three-quark potentials, and constrained them by the requirement of confinement in the $q\bar{q}$ and q^3 systems. Thus we found

$$V_{ij} = \sum_{\alpha} \mathcal{C}_{ij}^{\alpha} \mathcal{V}_{ij} = \left[c_1 + \frac{4}{3} + F_i \cdot F_j \right] \mathcal{V}_{ij} \tag{6}$$

$$V_{ijk} = \sum_{\alpha} \mathcal{C}_{ijk}^{\alpha} \mathcal{V}_{ijk} = c d^{abc} F_i^a F_j^b F_k^c \mathcal{V}_{ijk} . \tag{7}$$

where c_1 and c are constants. With the Ansatz

$$\mathcal{V}_{ijk} = \sum_{i<j}^{k} {}' \mathcal{V}_{ij} \equiv \mathcal{V}_{ij} + \mathcal{V}_{jk} + \mathcal{V}_{ik}, \tag{8}$$

and the harmonic oscillator form for the potential $\mathcal{V}_{ij}$, they are constrained to be $c_1 > 0$, usually taken as $c_1 = 1$, or $\frac{4}{3}$, and $\frac{2}{5} > c > -\frac{3}{2}$. Straightforward evaluation of the two- and three-quark parts of the potential yield

$$\langle V \rangle_{11}^{2b+3b} = \langle 1_{13} 1_{24} | V^{2b} + V^{3b} | 1_{13} 1_{24} \rangle$$

$$= \left(c_1 + \frac{4}{3} \right) \sum_{i<j}^{4} \mathcal{V}_{ij} - \frac{4}{3} \left(\mathcal{V}_{13} + \mathcal{V}_{24} \right) . \tag{9}$$

This potential manifestly does not satisfy the clustering condition, Eq. (1), except when $c_1 = -\frac{4}{3}$, which is excluded by the requirement of confinement in the $q\bar{q}$ sector. Thus we must conclude that either some modification of the three-quark potential, or a (new) four-quark potential is necessary. The former would spoil the confinement of the q^3 system, see Ref. [3], so the latter is left as our only choice.

First we shall make a general SU(3) symmetric Ansatz for the four-quark potential. Then we'll show that several kinds of a four-quark force lead to clustering of $q^2\bar{q}^2$. The four-quark potential can be factored into a colour part $\mathcal{C}_{1234}$ and the spin-spatial part $\mathcal{V}_{1234}$:

$$V_{1234} = \sum_{\alpha} \mathcal{C}^{\alpha}_{1234} \mathcal{V}_{1234}. \tag{10}$$

We shall take only colour factors $\mathcal{C}^{\alpha}_{1234}$ that are symmetric under the interchange of any pair of indices $i \leftrightarrow j$. Then the corresponding spin-spatial potentials $\mathcal{V}_{1234}$ must also be symmetric under the same interchange. Then the following 4-body SU(3) symmetric colour factors may be written down

$$\mathcal{C}_{1234} = \begin{cases} a_4 \sum_{i<j}^{4} F_i \cdot F_j \\ b_4 \sum_{i<j<k}^{4} d^{abc} F_i^a F_j^b F_k^c \\ c_4 \sum_{i<j<k<l}^{4} (F_i \cdot F_j)(F_k \cdot F_l) \\ d_4 \sum_{i<j<k<l}^{4} d^{abf} F_i^a F_j^b d^{cdf} F_k^c F_l^d \end{cases} \tag{11}$$

where $F^a = \frac{1}{2}\lambda^a$ is the quark colour charge, the lower index indicates the number of the quark, λ^a are the Gell-Mann matrices, d^{abc} are the symmetric SU(3) structure constants defined by the anticommutators of the Gell-Mann matrices, and summation over repeated SU(3) indices is understood.

Only three of the four colour factors in Eq. (11) are linearly independent, however, as the following identity holds

$$\sum_{i<j<k<l}^{4} d^{abf} F_i^a F_j^b d^{cdf} F_k^c F_l^d = \frac{1}{3} \sum_{i<j<k<l}^{4} (F_i \cdot F_j)(F_k \cdot F_l). \tag{12}$$

For this reason we may set $d_4 \equiv 0$ without loss of generality. The remaining three colour operators can be expressed in terms of the two Casimir operators as follows

$$\sum_{i<j}^{4} F_i \cdot F_j = \frac{1}{2} C^{(1)}_{1+2+3+4} - \frac{8}{3} \tag{13}$$

$$\sum_{i<j<k}^{4} d^{abc} F_j^a F_j^b F_k^c = \frac{1}{6} \left[C^{(2)}_{1+2+3+4} - \frac{5}{2} C^{(1)}_{1+2+3+4} + \frac{80}{9} \right] \tag{14}$$

$$\sum_{i<j<k<l}^{4} (F_i \cdot F_j)(F_k \cdot F_l) = \frac{1}{8} \left(C^{(1)}_{1+2+3+4} \right)^2 - \frac{19}{24} C^{(1)}_{1+2+3+4} - \frac{1}{4} C^{(2)}_{1+2+3+4} + \frac{10}{9}, \tag{15}$$

where $1 + 2 + 3 + 4$ stands for the (total) colour of the four-quark state and the two Casimir operators are defined by

$$C^{(1)} = F^a F^a \equiv F \cdot F \equiv F^2, \tag{16}$$

$$C^{(2)} = d^{abc} F^a F^b F^c, \tag{17}$$

where F^a are the SU(3) group generators and d^{abc} are as above.

Having constructed an SU(3) symmetric four-quark potential, we turn to its application in the $q^2 \bar{q}^2$ system and ask how it affects clustering. Taking into account the C-conjugation properties discussed in Ref. [3] we must use

$$\bar{C}_{123} = \begin{cases} -d^{abc} F_1^a F_2^b \bar{F}_3^c \\ \ d^{abc} F_1^a \bar{F}_2^b \bar{F}_3^c \end{cases} \tag{18}$$

in the definition of the colour factor

$$\sum_{i<j<k}^{4} \bar{C}_{ijk} = d^{abc} \left(F_1^a + F_2^a \right) \bar{F}_3^b \bar{F}_4^c - d^{abc} \left(\bar{F}_3^a + \bar{F}_4^a \right) F_1^b F_2^c, \tag{19}$$

where the anti-quark colour factor is defined by

$$\bar{F}^a = -\frac{1}{2} \lambda^{aT} = -\frac{1}{2} \lambda^{a*}. \tag{20}$$

Once again, we can express the three independent SU(3) invariant colour factors in Eq. (11) in terms of the two Casimir operators. The first factor remains unchanged:

$$\sum_{i<j}^{4} F_i \cdot F_j = \frac{1}{2} C^{(1)}_{1+2+3+4} - \frac{8}{3}, \tag{21}$$

whereas the second one can be evaluated using Eqs. (23) and (25) in Ref. [3], and the third one is

$$\sum_{i<j<k<l}^{4} (F_i \cdot F_j)(F_k \cdot F_l) = \frac{1}{8} \left(C^{(1)}_{1+2+3+4} - \frac{16}{3} \right)^2$$

$$+ \frac{5}{24} \left(C^{(1)}_{1+2+3+4} - C^{(1)}_{1+2} - C^{(1)}_{3+4} \right)$$

$$+ \frac{1}{2} \sum_{i<j<k}^{4} \bar{C}_{ijk} - \frac{1}{6} \sum_{i<j}^{4} F_i \cdot F_j - \frac{2}{3} \tag{22}$$

where $1 + 2 + 3 + 4$ stands for the (total) colour of the four-quark state. This leads to

$$\langle V \rangle_{11} = \langle 1_{13} 1_{24} | V | 1_{13} 1_{24} \rangle$$

$$= \left[c_1 + \frac{4}{3} \right] \sum_{i<j}^{4} V_{ij} - \frac{4}{3} \left[V_{13} + V_{24} \right] + \left[-\frac{8}{3} a_4 + \frac{20}{9} c_4 \right] V_{1234}. \tag{23}$$

Making the Ansatz $\mathcal{V}_{1234} = \sum_{i<j}^{4} \mathcal{V}_{ij}$, we find the saturation condition

$$c_1 + \frac{4}{3} - \frac{8}{3}a_4 + \frac{20}{9}c_4 = 0, \tag{24}$$

which is the principal result of this paper. Note the consequences of Eq. (24):

1. Some four-quark interaction is necessary to achieve clustering: one cannot satisfy Eq. (24) with $a_4 = c_4 = 0$, because $c_1 > 0$. Note that one may have exact cluster separation of the Hamiltonian at all distances, and not only asymptotically. That, however, would also imply absence of interaction between the two $q\bar{q}$ clusters (mesons). One may, however, modify the $\mathcal{V}_{1234} = \sum_{i<j}^{4} \mathcal{V}_{ij}$ Ansatz at short distances to introduce some meson-meson interaction without spoiling clustering.

2. Of all the $q^2\bar{q}^2$ states the "two-meson" colour singlet $|1_{13}1_{24}\rangle$ has the lowest energy. Unfortunately this state is also deconfined (due to the minus sign in Eq. (23)): each of the two independent $q\bar{q}$ pairs is unbound in an "upside-down" confining (concave) two-body potential. This problem is inevitable: if we change the overall sign of the colour dependent two-body interaction, the colour octet $q\bar{q}$ state becomes deconfined. Thus we have found a paradox: if both colour singlet and octet $q\bar{q}$ pairs are to be confined by two-body forces, then two colour singlet $q\bar{q}$ pairs are deconfined due to the influence of the four-quark force. If we eliminate the four-quark force, then the $q^2\bar{q}^2$ system, though confined, *cannot* cluster into two mesons. These constraints are only a consequence of the assumed SU(3) symmetry.

3. Clearly the clustering condition Eq. (23) is met by a continuous infinity of a_4, c_4 coefficients/four-body potentials. In order to narrow down this (theoretical) uncertainty one may play the same kind of game as with the three-quark potential: constrain the free parameters by demanding proper ordering of coloured states. That procedure, however, *cannot* solve the problem in point 2., as that depends only on the two-quark interaction.

4. Even if one had clustering in the $q^2\bar{q}^2$ system, that would not necessarily ensure the $q^4\bar{q} \to (q^3) + (q\bar{q})$ clustering, nor that of $q^6 \to (q^3) + (q^3)$. Thus we may have to consider the latter two cases separately and introduce a five- and a six-quark interaction to ensure clustering.

Our results appear to be general, as they depend only on the assumption of exact colour SU(3) symmetry and that quarks transform as the fundamental irrep. (**3**) of SU(3). Thus, our results must hold in all SU(3) symmetric theories, *inter alia* also in QCD, no matter what the spatial parts of the potentials may be. (The assumption of additivity of few-quark potentials is sufficient, though perhaps not necessary to achieve clustering.) The conflict between clustering and confinement found here was unexpected, at least for the present author. Clearly new ideas are necessary here.

References

1. Y. Nambu, in *Preludes in Theoretical Physics*, ed. A. de Shalit et al., North Holland, Amsterdam, (1966).

2. O.W. Greenberg, and D. Zwanziger, Phys. Rev. **150**, 1177 (1966).
3. V. Dmitrašinović, Phys. Lett. **B 499**, 135 (2001).
4. S. Pepin and Fl. Stancu, Phys. Rev. D **65**, 054032 (2002).

Chiral and $U(1)_a$ restorations in hadrons

L. Ya. Glozman

Institute for Theoretical Physics, University of Graz, Universitätsplatz 5, A-8010 Graz, Austria

Abstract. The evidence and the theoretical justification of chiral and $U(1)_A$ symmetry restoration in high-lying hadrons is presented.

It has recently been suggested that the parity doublet structure seen in the spectrum of highly excited baryons may be due to effective chiral symmetry restoration for these states [1]. This phenomenon can be understood in very general terms from the validity of the operator product expansion (OPE) in QCD at large space-like momenta and the validity of the dispersion relation for the two-point correlator, which connects the spacelike and timelike regions (i.e. the validity of Källen-Lehmann representation) [2,3].

Consider a two-point correlator of the current (that creates from the vacuum the hadrons with the given quantum numbers) at large spacelike momenta Q^2, where the language of quarks and gluons is adequate and where the OPE is valid. The only effect that chiral symmetry breaking can have on the correlator is through the nonzero value of condensates associated with operators which are chirally active (*i.e.* which transform nontrivially under chiral transformations). To these belong $\langle \bar{q}q \rangle$ and higher dimensional condensates that are not invariant under axial transformation. At large Q^2 only a small number of condensates need be retained to get an accurate description of the correlator. Contributions of these condensates are suppressed by inverse powers of Q^2. At asymptotically high Q^2, the correlator is well described by a single term—the perturbative term. The essential thing to note from this OPE analysis is that the perturbative contribution knows nothing about chiral symmetry breaking as it contains no chirally nontrivial condensates. In other words, though the chiral symmetry is broken in the vacuum and all chiral noninvariant condensates are not zero, their influence on the correlator at asymptotically high Q^2 vanishes. This is in contrast to the situation of low values of Q^2, where the role of chiral condensates is crucial.

This shows that at large spacelike momenta the correlation function becomes chirally symmetric. The dispersion relation provides a connection between the spacelike and timelike domains. In particular, the large Q^2 correlator is completely dominated by the large s spectral density. (The spectral density has the physical interpretation of being proportional to the probability density that the current when acting on the vacuum creates a state of a mass of $\sqrt{s}$.) Hence the large s spectral density must be insensitive to the chiral symmetry breaking in the vacuum. This is in contrast to the low s spectral function which is crucially

dependent on the quark condensates in the vacuum. This manifests a smooth chiral symmetry restoration from the low-lying spectrum, where the chiral symmetry breaking in the vacuum is crucial for physics, to the high-lying spectrum, where chiral symmetry breaking becomes irrelevant and the spectrum is chirally symmetric.

Microscopically this is because the typical momenta of valence quarks should increase higher in the spectrum and once it is high enough the valence quarks decouple from the chiral condensates of the QCD vacuum and the dynamical (quasiparticle or constituent) mass of quarks drops off and the chiral symmetry gets restored [1,4]. This phenomenon does not mean that the spontaneous breaking of chiral symmetry in the QCD vacuum disappears, but rather that the chiral asymmetry of the vacuum becomes irrelevant sufficiently high in the spectrum. The physics of the highly-excited states is such as if there were no chiral symmetry breaking in the vacuum. One of the consequences is that the concept of constituent quarks, which is adequate low in the spectrum, becomes irrelevant high in the spectrum.

If high in the spectrum (i.e. where the chiral symmetry is approximately restored) the spectrum is still quasidiscrete, then the phenomenological manifestation of the chiral symmetry restoration would be that the highly excited hadrons should fall into the representations of the $SU(2)_L \times SU(2)_R$ group, which are compatible with the definite parity of the states - the parity-chiral multiplets [2,3]. In the case of baryons in the N and Δ spectra these multiplets are either the parity doublets $((1/2, 0) \oplus (0, 1/2)$ for N^* and $(3/2, 0) \oplus (0, 3/2)$ for $\Delta^*)$ that are not related to each other, or the multiplets $(1/2, 1) \oplus (1, 1/2)$ that combine one parity doublet in the nucleon spectrum with the parity doublet in the delta spectrum with the same spin.

Summarizing, the phenomenological consequence of the effective restoration of chiral symmetry high in N and Δ spectra is that the baryon states will fill out the irreducible representations of the parity-chiral group. If $(1/2, 0) \oplus (0, 1/2)$ and $(3/2, 0) \oplus (0, 3/2)$ multiplets were realized in nature, then the spectra of highly excited nucleons and deltas would consist of parity doublets. However, the energy of the parity doublet with given spin in the nucleon spectrum *a-priori* would not be degenerate with the doublet with the same spin in the delta spectrum; these doublets would belong to different representations , *i.e.* to distinct multiplets and their energies are not related. On the other hand, if $(1/2, 1) \oplus (1, 1/2)$ were realized, then the highly lying states in N and Δ spectrum would have a N parity doublet and a Δ parity doublet with the same spin and which are degenerate in mass. In either of cases the highly lying spectrum must systematically consist of parity doublets. We stress that this classification is the most general one and does not rely on any model assumption about the structure of baryons.

What is immediately evident from the empirical low-lying spectrum is that positive and negative parity states with the same spin are not nearly degenerate. Even more, there is no one-to-one mapping of positive and negative parity states of the same spin with masses below 1.7 GeV. This means that one cannot describe the low-lying spectrum as consisting of sets of chiral partners. The absence of systematic parity doublets low in the spectrum is one of the most direct

pieces of evidence that chiral symmetry in QCD is spontaneously broken. However, as follows from the discussion above, there are good reasons to expect that chiral symmetry breaking effects become progressively less important higher in the spectrum. As a phenomenological manifestation of this smooth chiral symmetry restoration one should expect an appearance of systematic parity-chiral multiplets high in the spectrum.

Below we show all the known N and Δ resonances in the region 2 GeV and higher and include not only the well established baryons ("****" and "***" states according to the PDG classification), but also "**" states that are defined by PDG as states where "evidence of existence is only fair". In some cases we will fill in the vacancies in the classification below by the "*" states, that are defined as "evidence of existence is poor". We mark both the 1-star and 2-star states in the classification below.

$$J = \frac{1}{2} : N^+(2100) \; (*), \; N^-(2090) \; (*), \; \Delta^+(1910) \quad , \; \Delta^-(1900)(**);$$

$$J = \frac{3}{2} : N^+(1900)(**), \; N^-(2080)(**), \; \Delta^+(1920) \quad , \; \Delta^-(1940) \; (*);$$

$$J = \frac{5}{2} : N^+(2000)(**), \; N^-(2200)(**), \; \Delta^+(1905) \quad , \; \Delta^-(1930) \quad ;$$

$$J = \frac{7}{2} : N^+(1990)(**), \; N^-(2190) \quad , \; \Delta^+(1950) \quad , \; \Delta^-(2200) \; (*);$$

$$J = \frac{9}{2} : N^+(2220) \quad , \; N^-(2250) \quad , \; \Delta^+(2300)(**), \; \Delta^-(2400)(**);$$

$$J = \frac{11}{2} : \qquad ? \qquad , \; N^-(2600) \quad , \; \Delta^+(2420) \quad , \qquad ? \qquad ;$$

$$J = \frac{13}{2} : N^+(2700)(**), \qquad ? \qquad , \qquad ? \qquad , \; \Delta^-(2750)(**);$$

$$J = \frac{15}{2} : \qquad ? \qquad , \qquad ? \qquad , \; \Delta^+(2950)(**), \qquad ? \qquad .$$

The data above suggest that the parity doublets in N and Δ spectra are approximately degenerate; the typical splitting in the multiplets are $\sim$ 200 MeV or less, which is within the decay width of those states. Of course, as noted above,"nearly degenerate" is not a truly well-defined idea. In judging how close to degenerate these states really are one should keep in mind that the extracted resonance masses have uncertainties which are typically of the order of 100 MeV.

If the mass degeneracy between N and Δ doublets is accidental, then the baryons are organized according to $(1/2, 0) \oplus (0, 1/2)$ for N and $(3/2, 0) \oplus (0, 3/2)$ for Δ parity-chiral doublets. This possibility is supported by the fact that one observes systematic parity doublets in the nucleon spectrum as low as at $M \sim 1.7$ GeV, while there are no doublets at this mass in the Δ spectrum. If the mass degeneracy between the highly-lying nucleon and delta doublets is not accidental, then the highly lying states are organized according to $(1/2, 1) \oplus (1, 1/2)$ representation. It can also be possible that in the narrow energy interval more than one parity doublet in the nucleon and delta spectra is found for a given spin. This would then mean that different doublets would belong to different parity-chiral multiplets.

While a discovery of states that are marked by (?) would support the idea of effective chiral symmetry restoration, a definitive discovery of states that are beyond the systematics of parity doubling, would certainly be strong evidence against it. The nucleon states listed above exhaust all states ("****", "***", "**", "*") in this part of the spectrum included by the PDG. However, there are some additional candidates (not established states) in the Δ spectrum. In the $J = 5/2$ channel there are two other candidate states $\Delta^+(2000)(**)$ and $\Delta^-(2350)(*)$; there is another candidate for $J = 7/2$ positive parity state - $\Delta^+(2390)(*)$ as well as for $J = 1/2$ negative parity state $\Delta^-(2150)(*)$. Certainly a better exploration of the highly lying baryons is needed. This task is just for the facilities like in JLAB, BNL, SAPHIR, SPRING-8 and similar.

Recent data on the highly excited mesons give a very strong evidence of chiral symmetry restoration in meson spectra too [4]. Consider, as example, the pseudoscalar and scalar mesons π, f_0, a_0, η within the two-flavor QCD. The corresponding currents (interpolating fields) belong to the $(1/2, 1/2) \oplus (1/2, 1/2)$ irreducible representation of the $U(2)_L \times U(2)_R = SU(2)_L \times SU(2)_R \times U(1)_V \times U(1)_A$ group. If the vacuum were invariant with respect to $U(2)_L \times U(2)_R$ transformations, then all four mesons, π, f_0, a_0 and $\bar{\eta}$ would be degenerate (as well as all their excited states). Once the $U(1)_A$ symmetry is broken explicitly through the axial anomaly, but the chiral $SU(2)_L \times SU(2)_R$ symmetry is still intact in the vacuum, then the spectrum would consist of degenerate (π, f_0) and $(a_0, \bar{\eta})$ pairs. If in addition the chiral $SU(2)_L \times SU(2)_R$ symmetry is spontaneously broken in the vacuum, the degeneracy is also lifted in the pairs above and the pion becomes a (pseudo)Goldstone boson. Indeed, the masses of the lowest mesons are

$$m_\pi \simeq 140 MeV, \; m_{f_0} \simeq 400 - 1200 MeV, \; m_{a_0} \simeq 985 MeV, \; m_{\bar{\eta}} \simeq 782 MeV.$$

This immediately tells that both $SU(2)_L \times SU(2)_R$ and $U(1)_V \times U(1)_A$ are broken in the QCD vacuum to $SU(2)_I$ and $U(1)_V$, respectively.

Systematic data on highly excited mesons are still missing in the PDG tables. We will use the recent results of the partial wave analysis of mesonic resonances from 1.8 GeV to 2.4 GeV obtained in $p\bar{p}$ annihilation at LEAR [5,6]. We note that the f_0 state at 2102 ± 13 MeV is *not* considered by the authors as a $q\bar{q}$ state (but rather as a candidate for glueball) because of its very unusual decay properties

and very large mixing angle. This is in contrast to all other f_0 mesons in this region, for which the mixing angles are small. Therefore these mesons are regarded as predominantly $u, d = n$ states. Hence, in the following we will exclude the f_0 state at 2102 ± 13 from our analysis which applies only to $n\bar{n}$ states.

The prominent feature of the data is an approximate degeneracy of the three highest states in the pion spectrum with the three highest states in the f_0 spectrum:

$$\pi(1801 \pm 13) - f_0(1770 \pm 12), \tag{1}$$

$$\pi(2070 \pm 35) - f_0(2040 \pm 38), \tag{2}$$

$$\pi(2360 \pm 25) - f_0(2337 \pm 14). \tag{3}$$

This can be considered as a manifestation of chiral symmetry restoration high in the spectra. The approximate degeneracy of these physical states indicates that the chiral $SU(2)_L \times SU(2)_R$ transformation properties of the corresponding currents are not violated by the vacuum. This means that the chiral symmetry breaking of the vacuum becomes irrelevant for the high-lying states and the physical states above form approximately the chiral pairs in the $(1/2, 1/2)$ representation of the chiral group. The physics of the highly excited hadrons is such as if there were no chiral symmetry breaking in the vacuum.

A similar behaviour is observed from a comparison of the a_0 and η masses high in the spectra:

$$a_0(2025 \pm ?) - \eta(2010^{+35}_{-60}). \tag{4}$$

Upon examining the experimental data more carefully one notices not only a degeneracy in the chiral pairs, but also an approximate degeneracy in $U(1)_A$ pairs (π, a_0) and (f_0, η) (in those cases where the states are established). If so, one can preliminary conclude that not only the chiral $SU(2)_L \times SU(2)_R$ symmetry is restored high in the spectra, but the whole $U(2)_L \times U(2)_R$ symmetry of the QCD Lagrangian. Then the approximate $(1/2, 1/2) \oplus (1/2, 1/2)$ multiplets of this group are given by:

$$\pi(1801 \pm 13) - f_0(1770 \pm 12) - a_0(?) - \eta(?); \tag{5}$$

$$\pi(2070 \pm 35) - f_0(2040 \pm 40) - a_0(2025 \pm ?) - \eta(2010^{+35}_{-60}); \tag{6}$$

$$\pi(2360 \pm 25) - f_0(2337 \pm 14) - a_0(?) - \eta(2285 \pm 20). \tag{7}$$

This preliminary conclusion would be strongly supported by a discovery of the missing a_0 meson in the mass region around 2.3 GeV as well as by the missing a_0 and η mesons in the 1.8 GeV region. We have to stress, that the $U(1)_A$ restoration high in the spectra does not mean that the axial anomaly of QCD

vanishes, but rather that the specific gluodynamics (e.g. instantons) that are related to the anomaly become unimportant there. It should also be emphasized that the only restoration of $U(1)_V \times U(1)_A$ symmetry (without the $SU(2)_L \times SU(2)_R$) is impossible. This was discussed in ref. [2]. The reason is that even if the effects of the explicit $U(1)_A$ symmetry breaking via the axial anomaly vanish, the $U(1)_V \times U(1)_A$ would still be spontaneously broken once the $SU(2)_L \times SU(2)_R$ were spontaneously broken. This is because the same quark condensates in the QCD vacuum that break $SU(2)_L \times SU(2)_R$ do also break $U(1)_V \times U(1)_A$.

The phenomenon of parity doubling and of chiral symmetry restoration high in the spectra rules out the potential description of highly lying hadrons in the spirit of the constituent quark model. Clearly, the chiral symmetry restoration by itself implies that the concept of constituent quarks (whoose mass is directly related to spontaneous chiral symmetry breaking in the vacuum) becomes inadequate high in the spectrum, though it is a fruitful concept for the low-lying hadrons. That the potential description is incompatible with the parity doubling also follows from the following simple consideration.

Within the potential description of mesons the parity of the state is unambiguously prescribed by the relative orbital angular momentum L of quarks. For example, all the states on the radial pion Regge trajectory are $^1S_0$ $q\bar{q}$ states, while the members of the f_0 trajectory are the $^3P_0$ states. Clearly, such a picture cannot explain the *systematical* parity doubling as it would require that the stronger centrifugial repulsion in the case of $^3P_0$ mesons (as compared to the $^1S_0$ ones) as well as the strong and attractive spin-spin force in the case of $^1S_0$ states (as compared to the weak spin-spin force in the $^3P_0$ channel) must systematically lead to an approximate degeneracy for all radial states. This is very improbable.

The potential picture also implies strong spin-orbit interactions between quarks while the spin-orbit splittings are absent or very small for excited mesons and baryons in the u, d sector. The strong spin-orbit interactions inevitably follow from the Thomas precession (once the confinement is described through a scalar confining potential)[1], and this very strong spin-orbit force must be practically exactly compensated by other strong spin-orbit force from e.g. the one-gluon-exchange interaction in this picture. In principle such a cancellation could be provided by tuning the parameters for some specific (sub)families of mesons. However, in this case the spin-orbit forces become very strong for other (sub)families. This is a famous spin-orbit problem of constituent quark model.

This picture should be contrasted with the string description of highly excited hadrons [7]. Within the latter picture the hadrons are relativistic strings (with the color-electric field in the string) with practically massless quarks at the ends; these massless quarks are combined into parity-chiral multiplets. The string picture is compatible with the chiral symmetry restoration because there always exists a solution for the right-handed and left-handed quarks at the end of the string with exactly the same energy and total angular momentum. Since the nonperturbative field in the string is pure electric and the electric field is "flavor-

---

[1] Note also that a scalar potential explicitly breaks the chiral symmetry in contradiction to the requirement that the chiral symmetry must be restored high in the spectra.

blind", the string dynamics itself is not sensitive to the specific flavor of a light quark once the chiral limit is taken. This picture explains the empirical parity-doubling because for every intrinsic quantum state of the string there necessarily appears parity doubling of the states with the same total angular momentum of hadron. Hence the string picture is compatible not only with the $SU(2)_L \times SU(2)_R$ restoration, but more generally with the $U(2)_L \times U(2)_R$ one. In addition, there is no spin-orbit force at all once the chiral symmetry is restored. This is because the helicity operator does not commute with the spin-orbit operator and the motion of the quark with the fixed helicity is not affected by the spin-orbit force.

References

1. L. Ya. Glozman, Phys. Lett. **B475** (2000) 329.
2. T. D. Cohen and L. Ya. Glozman, Phys. Rev. **D65** (2002) 016006.
3. T. D. Cohen and L. Ya. Glozman, Int. J. Mod. Phys. **A17** (2002) 1327.
4. L. Ya. Glozman, Phys. Lett. **B539** (2002) 257.
5. A. V. Anisovich et al, Phys. Lett. **B491** (2000) 47.
6. A. V. Anisovich et al, Phys. Lett. **B517** (2001) 261.
7. L. Ya. Glozman, Phys. Lett. **B541** (2002) 115.

Phenomenological Schwinger-Dyson approach to η-η′ mass matrix[⋆]

D. Kekez[a] and D. Klabučar[b]

[a] Rudjer Bošković Institute, P.O.B. 180, 10002 Zagreb, Croatia
[b] Physics Department, Faculty of Science, Zagreb University Bijenička c. 32, Zagreb 10000, Croatia

Abstract. It is reviewed pedagogically how a very successful description of the η–η′ mass matrix can be achieved in the consistently coupled Schwinger-Dyson and Bethe-Salpeter approach in spite of the limitations of the ladder approximation. This description is in agreement with both phenomenology and lattice results.

The Schwinger-Dyson and Bethe-Salpeter (SD-BS) approach is the bound-state approach that is chirally well-behaved. (For example, see Ref. [1–3] for recent reviews, and references therein for various phenomenological and other applications of SD-BS approach.) Therefore, among the bound-state approaches it is probably the most suitable one to treat the light pseudoscalar mesons. One solves the Schwinger-Dyson (SD) equation for dressed propagators of the light u, d and s quarks using a phenomenologically successful interaction. These light-quark propagators are then employed in consistent solving of Bethe-Salpeter (BS) equations for various quark-antiquark ($q\bar{q}$) relativistic bound states. Namely, in both SD and BS equations we employ the same, ladder approximation, and the same interaction due to an effective, *dressed* gluon exchange. In the chiral limit (and *close* to it), light pseudoscalar (P) meson $q\bar{q}$ bound states ($P = \pi^{0,\pm}, K^{0,\pm}, \eta$) then **simultaneously** manifest themselves also as (*quasi-*)Goldstone bosons of dynamically broken chiral symmetry. This resolves the dichotomy "$q\bar{q}$ bound state *vs.* Goldstone boson", enabling one to work with the mesons as explicit $q\bar{q}$ bound states (for example, in Refs. [4–11]) while reproducing (even analytically, in the chiral limit) the famous results of the axial anomaly for the light pseudoscalar mesons, namely the amplitudes for $P \rightarrow \gamma\gamma$ and $\gamma^\star \rightarrow P^0 P^+ P^-$ [12]. This is unique among the bound state approaches – for example, see Refs. [1,6,12] and references therein. Nevertheless, one keeps the advantage of bound state approaches that from the $q\bar{q}$ substructure one can calculate many important quantities (such as the pion decay constant f_π) which are just parameters in most of other chiral approaches to the light-quark sector. The description [5,8–10] of η–η′ complex is especially noteworthy, as it is very successful in spite of the limitations of the SD-BS approach in the ladder approximation.

For the description of η and η′, the crucial issues are the meson mixing and construction of physical meson states. They are formulated in Refs. [5,8,9] for the

---

[⋆] Talk delivered by D. Klabučar

SD-BS approach, where solving of appropriate BS equations yields the eigenvalues of the squared masses, $M_{u\bar{u}}^2, M_{d\bar{d}}^2, M_{s\bar{s}}^2$ and $M_{u\bar{s}}^2$, of the respective quark-antiquark bound states $|u\bar{u}\rangle, |d\bar{d}\rangle, |s\bar{s}\rangle$ and $|u\bar{s}\rangle$. The last one is simply the kaon, and $M_{u\bar{s}}$ is its mass M_K. Nevertheless, the first three do not correspond to any physical pseudoscalar mesons. Thus, $M_{u\bar{u}}^2, M_{d\bar{d}}^2, M_{s\bar{s}}^2$ do not automatically represent any physical masses, although the mass matrix (actually, to be precise, the non-anomalous part of the mass matrix) is simply $\hat{M}_{NA}^2 = \text{diag}(M_{u\bar{u}}^2, M_{d\bar{d}}^2, M_{s\bar{s}}^2)$ in the basis $|q\bar{q}\rangle, (q = u, d, s)$. However, the flavor SU(3) quark model leads one to recouple these states into the familiar octet-singlet basis of the zero-charge subspace of the light unflavored pseudoscalar mesons:

$$|\pi^0\rangle = \frac{1}{\sqrt{2}}(|u\bar{u}\rangle - |d\bar{d}\rangle) , \tag{1}$$

$$|\eta_8\rangle = \frac{1}{\sqrt{6}}(|u\bar{u}\rangle + |d\bar{d}\rangle - 2|s\bar{s}\rangle) , \tag{2}$$

$$|\eta_0\rangle = \frac{1}{\sqrt{3}}(|u\bar{u}\rangle + |d\bar{d}\rangle + |s\bar{s}\rangle) . \tag{3}$$

With $|u\bar{u}\rangle$ and $|d\bar{d}\rangle$ being practically chiral states as opposed to a significantly heavier $|s\bar{s}\rangle$, Eqs. (1–3) do not define the octet and singlet states of the exact SU(3) flavor symmetry, but the *effective* octet and singlet states. However, as pointed out by Gilman and Kauffman [13] (following Chanowitz, their Ref. [8]), in spite of this flavor symmetry breaking by the s quark, these equations still implicitly assume nonet symmetry in the sense that the same states $|q\bar{q}\rangle$ $(q = u, d, s)$ appear in both the octet member η_8 (2) and the singlet η_0 (3). Nevertheless, in order to avoid the $U_A(1)$ problem, this symmetry must ultimately be broken by gluon anomaly at least at the level of the masses of pseudoscalar mesons.

In the basis (1–3), the non-anomalous part of the (squared-)mass matrix of π^0 and etas is

$$\hat{M}_{NA}^2 = \begin{pmatrix} M_\pi^2 & 0 & 0 \\ 0 & M_{88}^2 & M_{80}^2 \\ 0 & M_{08}^2 & M_{00}^2 \end{pmatrix} . \tag{4}$$

The η_8 "mass" $M_{88} \equiv M_{\eta_8}$ can be related to the kaon mass through the Gell-Mann–Okubo (GMO) relation, although the kaon does not appear in this scheme as it obviously cannot mix with π^0 and etas, since it is strangely flavored. Equation (4) shows that also the isospin $I = 1$ state π^0 decouples from any mixing with the $I = 0$ states η_8 and η_0, thanks to our working in the isospin limit throughout. Therefore, we are concerned only with the diagonalization of the 2×2 submatrix in the subspace of etas in order to find their physical masses and corresponding $q\bar{q}$ content. In the isospin limit, obviously $M_{u\bar{u}} = M_{d\bar{d}}$, which we then can strictly identify with our model π^0 mass M_π. Since in this model we can also calculate $M_{s\bar{s}}^2 = \langle s\bar{s}|\hat{M}_{NA}^2|s\bar{s}\rangle$, this gives us our calculated entries in the mass matrix:

$$M_{88}^2 \equiv \langle \eta_8|\hat{M}_{NA}^2|\eta_8\rangle \equiv M_{\eta_8}^2 = \frac{2}{3}\left(M_{s\bar{s}}^2 + \frac{1}{2}M_\pi^2\right) , \tag{5}$$

$$M_{80}^2 \equiv \langle \eta_8|\hat{M}_{NA}^2|\eta_0\rangle = M_{08}^2 = \frac{\sqrt{2}}{3}\left(M_\pi^2 - M_{s\bar{s}}^2\right) , \tag{6}$$

$$M_{00}^2 \equiv \langle \eta_0 | \hat{M}_{NA}^2 | \eta_0 \rangle = \frac{2}{3} (\frac{1}{2} M_{s\bar{s}}^2 + M_\pi^2) . \tag{7}$$

The last one, M_{00}, is the *non-anomalous part* of the η_0 "mass" M_{η_0}. Namely, all the model masses $M_{q\bar{q}'}$ ($q, q' = u, d, s$) and corresponding $q\bar{q}'$ bound state amplitudes are obtained in the ladder approximation, and thus (irrespective of what the concrete model could be) with an interaction kernel which cannot possibly capture the effects of gluon anomaly. Fortunately, the large N_c expansion indicates that the leading approximation in that expansion describes the bulk of main features of QCD. The gluon anomaly is suppressed as $1/N_c$ and is viewed as a perturbation in the large N_c expansion. It is coupled *only* to the singlet combination η_0 (3); only the η_0 mass receives, from the gluon anomaly, a contribution which, unlike quasi-Goldstone masses $M_{q\bar{q}'}$'s comprising $\hat{M}_{NA}^2$, does *not* vanish in the chiral limit. As discussed in detail in Sec. V of Ref. [5], in the present bound-state context it is thus best to adopt the standard way (see, e.g., Refs. [14,15]) to *parameterize* the anomaly effect. We thus break the $U_A(1)$ symmetry, and avoid the $U_A(1)$ problem, by shifting the η_0 (squared) mass by an amount denoted by 3β (in the notation of Refs. [8,9]). The complete mass matrix is then $\hat{M}^2 = \hat{M}_{NA}^2 + \hat{M}_A^2$, where

$$\hat{M}_A^2 = \begin{pmatrix} 0 & 0 & 0 \\ 0 & 0 & 0 \\ 0 & 0 & 3\beta \end{pmatrix} , \tag{8}$$

and where the value of the anomalous η_0 mass shift 3β is related to the topological susceptibility of the vacuum, but in the present approach must be treated as a parameter to be determined outside of our bound-state model, i.e., fixed by phenomenology or taken from the lattice calculations [16].

We could now go straight to the nonstrange-strange (NS-S) basis, but before doing this, it may be instructive to rewrite for a moment the matrix (8) in the flavor, $|q\bar{q}\rangle$ basis, where

$$\hat{M}_A^2 = \beta \begin{pmatrix} 1 & 1 & 1 \\ 1 & 1 & 1 \\ 1 & 1 & 1 \end{pmatrix} , \tag{9}$$

since for some readers it may be the best place to introduce the effect of flavor symmetry breaking. Namely, Eq. (9) tells us that due to the gluon anomaly, there are transitions $|q\bar{q}\rangle \rightarrow |q'\bar{q}'\rangle$; $q, q' = u, d, s$. However, the amplitudes for the transition from, and into, light $u\bar{u}$ and $d\bar{d}$ pairs need not be the same as those for the significantly more massive $s\bar{s}$. The modification of the anomalous mass matrix (9) which allows for possible effects of the breaking of the SU(3) flavor symmetry is then

$$\hat{M}_A^2 = \beta \begin{pmatrix} 1 & 1 & X \\ 1 & 1 & X \\ X & X & X^2 \end{pmatrix} . \tag{10}$$

There are arguments [8,9], supported by phenomenology, that the transition suppression is estimated well by the nonstrange-to-strange ratio of respective constituent masses, $X \approx \mathcal{M}_u / \mathcal{M}_s$, or, as commented below, of respective decay constants, $X \approx f_\pi / f_{s\bar{s}}$.

After adding the anomalous contribution (8) to Eq. (4), pion still remains decoupled and we obviously still can restrict ourselves to 2×2 submatrix in the subspace of etas. However, when dealing with quark degrees of freedom when the symmetry between the nonstrange (*NS*) and strange (*S*) sectors is broken as described above, the most suitable basis for that subspace is the so-called *NS-S* basis:

$$|\eta_{NS}\rangle = \frac{1}{\sqrt{2}}(|u\bar{u}\rangle + |d\bar{d}\rangle) = \frac{1}{\sqrt{3}}|\eta_8\rangle + \sqrt{\frac{2}{3}}|\eta_0\rangle \,, \tag{11}$$

$$|\eta_S\rangle = |s\bar{s}\rangle = -\sqrt{\frac{2}{3}}|\eta_8\rangle + \frac{1}{\sqrt{3}}|\eta_0\rangle \,. \tag{12}$$

The η–η′ mass matrix in this basis is

$$\hat{M}^2 = \begin{pmatrix} M^2_{\eta_{NS}} & M^2_{\eta_S \eta_{NS}} \\ M^2_{\eta_{NS} \eta_S} & M^2_{\eta_S} \end{pmatrix} = \begin{pmatrix} M^2_{u\bar{u}} + 2\beta & \sqrt{2}\beta X \\ \sqrt{2}\beta X & M^2_{s\bar{s}} + \beta X^2 \end{pmatrix} \xrightarrow{\phi} \begin{pmatrix} M^2_{\eta} & 0 \\ 0 & M^2_{\eta'} \end{pmatrix} \,, \tag{13}$$

where the indicated diagonalization is given by the *NS–S* mixing relations[1]

$$|\eta\rangle = \cos\phi|\eta_{NS}\rangle - \sin\phi|\eta_S\rangle \,, \quad |\eta'\rangle = \sin\phi|\eta_{NS}\rangle + \cos\phi|\eta_S\rangle \,, \tag{14}$$

rotating η_{NS}, η_S to the mass eigenstates η, η′. Now the *NS–S* mass matrix (13) tells us that due to the gluon anomaly, there are transitions $|\eta_{NS}\rangle \leftrightarrow |\eta_S\rangle$. However, the amplitude for the transition from, and into, η_{NS}, need not be the same as those for the more massive η_S. The role of the flavor-symmetry-breaking factor X is to allow for that possibility. As remarked little earlier, there are arguments [8,9], supported by phenomenology, that the transition suppression is estimated well by the nonstrange-to-strange ratio of respective quark constituent masses, $\mathcal{M}_u$ and $\mathcal{M}_s$. Due to the Goldberger-Treiman relation, this ratio is essentially equal [5,8,9] to the ratio of η_{NS} and η_S pseudoscalar decay constants $f_{\eta_{NS}} = f_\pi$ and $f_{\eta_S} = f_{s\bar{s}}$ which are calculable in the SD-BS approach. Same as $\mathcal{M}_u$ and $\mathcal{M}_s$, they were found in our earlier papers, especially [5,8,9]. In other words, we can estimate the flavor-symmetry-breaking suppression factor as $X \approx \mathcal{M}_u/\mathcal{M}_s$, or equivalently, as $X \approx f_\pi/f_{s\bar{s}}$. Our model results $\mathcal{M}_u/\mathcal{M}_s = 0.622$ and $f_\pi/f_{s\bar{s}} = 0.689$ are in both cases reasonably close to $X_{exp} \approx 0.78$ extracted phenomenologically [8,9] from the *empirical* mass matrix $\hat{m}^2_{exp}$ featuring experimental pion and kaon masses, or, after diagonalization, η and η′ masses – see Eq. (7) in Ref. [9]. (In our model calculations below, we use $X = f_\pi/f_{s\bar{s}} = 0.689$ to show the robustness of our approach to slight variations. Namely, our earlier works [8,9,17] mostly presented results based on slightly different values of X obtained with the help of ratios of γγ amplitudes, which is yet another, but again related way of obtaining X.)

In our present notation, capital M_a's denote the calculated, model pseudoscalar masses, whereas lowercase m_a's denote the corresponding empirical

---

[1] The effective-singlet-octet mixing angle θ, defined by analogous relations where $\eta_{NS} \to \eta_8, \eta_S \to \eta_0, \phi \to \theta$, is related to the *NS–S* mixing angle φ as $\theta = \phi - \arctan\sqrt{2} = \phi - 54.74°$. The relation between our approach and the two-mixing-angle scheme is clarified in the Appendix of Ref. [8].

masses. The empirical mass matrix $\hat{m}_{exp}^2$ can be obtained from the calculated, model one in Eq. (13) by *i)* obvious substitutions $M_{u\bar{u}} \equiv M_\pi \to m_\pi$ and $M_{s\bar{s}} \to m_{s\bar{s}}$, and *ii)* by noting that $m_{s\bar{s}}$, the "empirical" mass of the unphysical $s\bar{s}$ pseudoscalar bound state, is given in terms of masses of physical particles as $m_{s\bar{s}}^2 = 2m_K^2 - m_\pi^2$ due to the Gell-Mann-Oakes-Renner (GMOR) relation. Since $M_{u\bar{u}}$, obtained by solving the BS equation, is identical to our model pion mass M_π, it was fitted to the empirical pion mass m_π, *e.g.*, in Ref. [8]. Similarly, $M_{u\bar{s}} \equiv M_K$ is fitted to the empirical kaon mass m_K. Therefore we also have $M_{s\bar{s}}^2 \approx 2m_K^2 - m_\pi^2$, since our model has good chiral behavior and also satisfies the GMOR relation, thanks to which we have $M_{s\bar{s}}^2 = 2M_K^2 - M_\pi^2$ in a very good approximation. We thus see that in our model mass matrix, the parts stemming from its *non-anomalous* part $\hat{M}_{NA}^2$ (4) are already close to the corresponding parts in $\hat{m}_{exp}^2$. We can thus expect a good overall description of the masses in η and η′ complex. We now proceed to verify this expectation.

The *anomalous* entry β is fixed phenomenologically to be $\beta_{exp} \approx 0.28$ GeV^2, along with $X_{exp} \approx 0.78$, by requiring that trace and determinant of $\hat{m}_{exp}^2$ have their experimental values. But, this can be done also with our calculated, model mass matrix $\hat{M}^2$. Requiring that the empirical value of the trace $m_\eta^2 + m_{\eta'}^2 \approx 1.22$ GeV^2 be fixed by Eq. (13), yields

$$\beta = \frac{1}{2 + X^2}[(m_\eta^2 + m_{\eta'}^2)_{exp} - (M_{u\bar{u}}^2 + M_{s\bar{s}}^2)] \tag{15}$$

where $X = f_\pi/f_{s\bar{s}} = 0.689$ and $M_{u\bar{u}} = 0.1373$ GeV and $M_{s\bar{s}} = 0.7007$ GeV are now our model-calculated [8] quantities, giving us $\beta = 0.286$ GeV^2. Since $(M_{u\bar{u}}^2 + M_{s\bar{s}}^2) = 2m_K^2$ holds to a very good approximation, our approach satisfies well the first equality (from the matrix trace) in

$$2\beta + \beta X^2 = m_\eta^2 + m_{\eta'}^2 - 2m_K^2 = \frac{2N_f}{f_\pi^2}\chi, \tag{16}$$

where the second equality is the Witten-Veneziano (WV) formula [18], with χ being the topological susceptibility of the pure Yang-Mills gauge theory. Our model values of X and β (f_π is fitted to its experimental value) thus imply $\chi = (178\,\text{MeV})^4$, in excellent agreement with the lattice result $\chi = (175 \pm 5\,\text{MeV})^4$ of Alles *et al.* [16].

The mixing angle is then determined to be $\phi = 43.2°$ (or equivalently, $\theta = -11.5°$), for example through the relation

$$\tan 2\phi = \frac{2\sqrt{2}\beta X}{M_{\eta_S}^2 - M_{\eta_{NS}}^2}, \tag{17}$$

where

$$M_{\eta_{NS}}^2 = M_{u\bar{u}}^2 + 2\beta = M_\pi^2 + 2\beta = 0.592\,\text{GeV}^2 = (769\,\text{MeV})^2 \tag{18}$$

and

$$M_{\eta_S}^2 = M_{s\bar{s}}^2 + \beta X^2 = 0.627\,\text{GeV}^2 = (792\,\text{MeV})^2 \tag{19}$$

are our *calculated* η_{NS} and η_S masses. They have reasonable values, in a good agreement with, *e.g.*, η_{NS} and η_S masses calculated in the dynamical SU(3) linear σ model [17].

The diagonalization of the NS-S mass matrix gives us the η and η′ masses:

$$M_\eta^2 = \cos^2 \phi \, M_{\eta_{NS}}^2 - \sqrt{2}\beta X \sin 2\phi + \sin^2 \phi \, M_{\eta_S}^2 \qquad (20)$$

$$M_{\eta'}^2 = \sin^2 \phi \, M_{\eta_{NS}}^2 + \sqrt{2}\beta X \sin 2\phi + \cos^2 \phi \, M_{\eta_S}^2 \ . \qquad (21)$$

Plugging in the above predictions for $\beta, X, M_{\eta_{NS}}$ and M_{η_S}, our model η and η′ masses then turn out to be $M_\eta = 575$ MeV and $M_{\eta'} = 943$ MeV. This is in good agreement with the respective empirical values of 547 MeV and 958 MeV.

However, the above is not all that can be said about agreement with experiment and other approaches. The second thing we may point out is the reasonable agreement we find if we insert our values of β, X and $M_{q\bar{q}}$'s into our model mass matrix and compare it with the η-η′ mass matrix obtained on lattice by UKQCD collaboration [19].

Third, Ref. [8] clearly shows that our approach and results are not in conflict, but in fact agree very well with results in the two-mixing-angle scheme (reviewed and discussed in, *e.g*, Ref. [20]). Actually, our results can also be given [8,21] in the two-mixing-angle scheme.

Fourth, what we found from the mass matrix is consistent with what we found in the same SD-BS approach through another route, *i.e.* from $\eta, \eta' \to \gamma\gamma$ processes [5,8–10].

The above shows that the consistently coupled SD-BS approach provides a surprisingly satisfactory description of the η-η′ complex, especially if one recalls that β, parameterizing the anomalous η_0 mass shift, was the only new parameter. Namely, all other model parameters were fixed already by Ref. [22] providing the model we used in Refs. [4–10]. Nevertheless, we would like to point out that even this one parameter, β, can be fixed beforehand. Instead of being a parameter, β can be obtained through WV formula (16) from the lattice results on the topological susceptibility χ. The central value of widely accepted $\chi = (175 \pm 5\,\text{MeV})^4$ [16] would lead to β less than 7% below our model value, which is within upper error bar anyway. Thus, we can eliminate β as a free parameter and still achieve almost as satisfactory description as the one given above.

References

1. C. D. Roberts, arXiv:nucl-th/0007054.
2. R. Alkofer and L. von Smekal, Phys. Rept. **353** (2001) 281 [arXiv:hep-ph/0007355].
3. C. D. Roberts and S. M. Schmidt, Prog. Part. Nucl. Phys. **45** (2000) S1 [arXiv:nucl-th/0005064].
4. D. Kekez and D. Klabučar, Phys. Lett. B **387** (1996) 14 [arXiv:hep-ph/9605219].
5. D. Klabučar and D. Kekez, Phys. Rev. D **58** (1998) 096003 [arXiv:hep-ph/9710206].

6. D. Kekez, B. Bistrović and D. Klabučar, Int. J. Mod. Phys. A **14** (1999) 161 [arXiv:hep-ph/9809245].

7. D. Kekez and D. Klabučar, Phys. Lett. B **457** (1999) 359 [arXiv:hep-ph/9812495]. See also D. Klabučar and D. Kekez, arXiv:hep-ph/9905251, hep-ph/9907537, hep-ph/9909273.

8. D. Kekez, D. Klabučar and M. D. Scadron, J. Phys. G **26** (2000) 1335 [arXiv:hep-ph/0003234].

9. D. Klabučar, D. Kekez and M. D. Scadron, arXiv:hep-ph/0012267; published in "Rostock 2000/Trento 2001, Exploring quark matter", p. 145.

10. D. Kekez and D. Klabučar, Phys. Rev. D **65** (2002) 057901 [arXiv:hep-ph/0110019].

11. B. Bistrović and D. Klabučar, Phys. Lett. B **478**, 127 (2000) [arXiv:hep-ph/9912452]. (For completeness, see also B. Bistrović and D. Klabučar, Phys. Rev. D **61** (2000) 033006 [arXiv:hep-ph/9907515].)

12. R. Alkofer and C. D. Roberts, Phys. Lett. B **369** (1996) 101 [arXiv:hep-ph/9510284], and references therein.

13. F. J. Gilman and R. Kauffman, Phys. Rev. D **36** (1987) 2761 [Erratum-ibid. D **37** (1988) 3348].

14. V. A. Miransky, "Dynamical Symmetry Breaking In Quantum Field Theories," *World Scientific Publishing Co., Singapore (1993)*.

15. J. F. Donoghue, E. Golowich and B. R. Holstein, "Dynamics Of The Standard Model," Cambridge Monogr. Part. Phys. Nucl. Phys. Cosmol. **2** (1992) 1.

16. B. Alles, M. D'Elia and A. Di Giacomo, Nucl. Phys. B **494** (1997) 281 [arXiv:hep-lat/9605013].

17. D. Kekez, D. Klabučar, and M. D. Scadron, J. Phys. G **27** (2001) 1775 [arXiv:hep-ph/0101324].

18. E. Witten, Nucl. Phys. B **156** (1979) 269;
G. Veneziano, Nucl. Phys. B **159** (1979) 213.

19. C. McNeile and C. Michael [UKQCD Collaboration], Phys. Lett. B **491** (2000) 123 [arXiv:hep-lat/0006020].

20. Th. Feldmann, Int. J. Mod. Phys. A **15** (2000) 159.

21. D. Klabučar and D. Kekez, in the proceedings of XVIIIth European Conference on Few-Body Problems in Physics, 8 - 14 September 2002, Bled, Slovenia, to appear in Few-Body Systems, Proc. Supplement.

22. P. Jain and H. J. Munczek, Phys. Rev. D **48**, 5403 (1993).

Description of Hadrons in a relativistic Quark Model

Dirk Merten

Helmholtz-Institut für Strahlen- und Kernphysik, Nußallee 14–16, D-53115 Bonn,
Germany

Abstract. A relativistic quark model for hadrons is presented. The model is based on the
Bethe-Salpeter equation in instantaneous approximation with a linear confining potential
and a residual interaction induced by instantons. Some selected results on meson masses,
baryon masses and nucleon form factors are discussed.

Constituent quark models for hadrons should describe many different characteristics of the observed spectra at once: The mass splittings of ground-state mesons and baryons as well as the Regge trajectories up to highly excited states and the obvious shell structure of baryon resonances have to be accounted for. The flavor mixing of the η and the η' and the occurrence of parity doublets (mainly in the N- and Λ-spectra) must be explained. In addition to that form factors and decay observables should be reproduced, if a reasonable description of bound states is achieved. Such an investigation will show, if the notion of the underlying dynamics is reasonable, if the introduced approximations are justified, but also if the concept of constituent quarks is applicable in the whole energy range.

To this end a relativistic treatment is mandatory. It is known that a linear confinement potential leads to linear Regge trajectories and the shell structure. An additional residual interaction has to explain fine and hyperfine splittings. A candidate for this residual interaction is the instanton-induced interaction derived by 't Hooft, which has the special feature to be effectively flavor-dependent and, in contrast to the widely used One Gluon Exchange, solves the $U_A(1)$ problem. A constituent quark model motivated by these ideas has been developed recently for mesons and baryons. It is based on the Bethe-Salpeter equation, a homogeneous integral equation, written symbolically

$$\chi = -i\, G_0\, K\, \chi$$

for the Bethe-Salpeter amplitude χ with the full propagator G_0 of two or three non-interacting quarks and an irreducible interaction kernel K. To solve this equation approximations are necessary. In our approach the propagator is substituted by free constituent quark propagators, where the fermion self energy is parameterized by the effective mass of the constituent. The interaction kernel is assumed to be instantaneous, *i.e.* independent of the relative energies of the quarks in the rest-frame of the bound state. With these approximations the Bethe-Salpeter
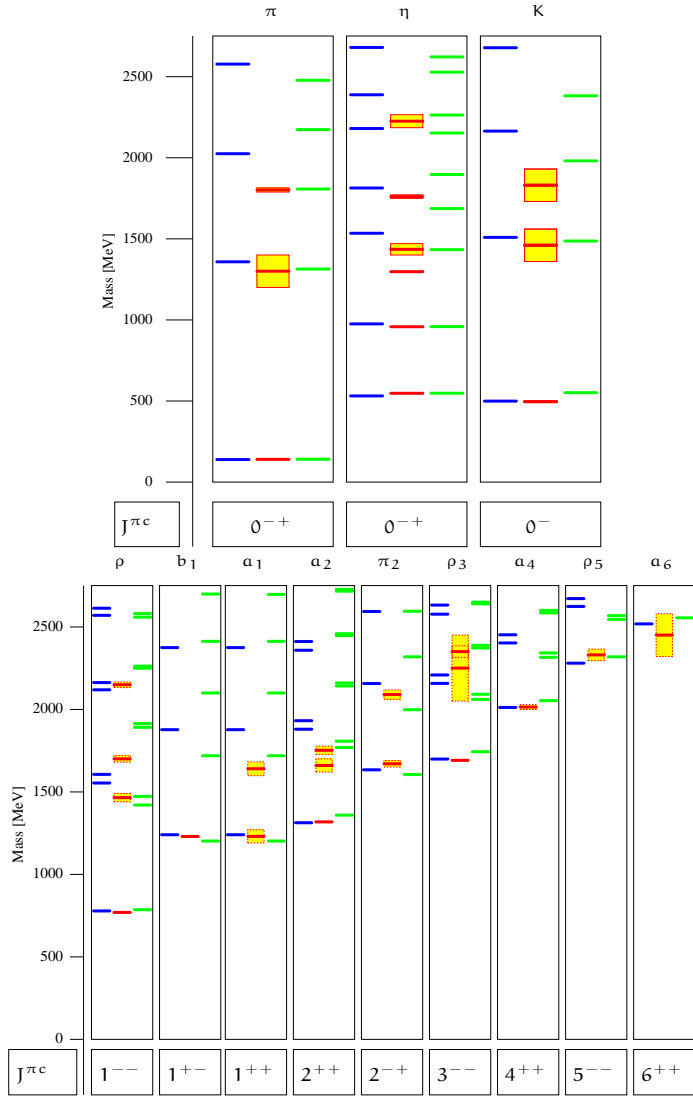
Fig. 1. The spectra of pseudo-scalar and isovector mesons in model $\mathcal{A}$ (left column) and model $\mathcal{B}$ (right column) compared to the experimental values [4] (middle column).

equation reduces to the 3-dimensional Salpeter equation which is solved numerically by expanding the amplitudes in a finite basis. The interaction kernel, as anticipated above, is the sum of a linearly rising confinement potential and a residual interaction induced by instantons. In a relativistic treatment an adequate spinorial structure of the confinement potential has to be specified. Further details of this approach are given in the references cited below. In the following we shall present some selected results.

The model for mesons has been described in [1]. For the spinorial structure of the confining potential two phenomenologically motivated possibilities were

studied, refered to as model $\mathcal{A}$ and $\mathcal{B}$: A linear combination of scalar and time-like vector

$$\frac{1}{2}\left(1\otimes 1-\gamma^0\otimes\gamma^0\right)\qquad(\text{model }\mathcal{A})\,,$$

chosen to minimize spin-orbit splittings generated by the confinement, and the $U_A(1)$ symmetric combination

$$\frac{1}{2}\left(1\otimes 1-\gamma^\mu\otimes\gamma_\mu-\gamma_5\otimes\gamma_5\right)\qquad(\text{model }\mathcal{B})\,.$$

The instanton-induced interaction leads to a short-range flavor-dependent force in the quark-anti-quark system affecting scalar and pseudo-scalar mesons only. Hence, the strength of this interaction (involving two parameters) is adjusted to the pseudo-scalar ground state nonet after the masses of the constituent quarks and the parameters of the confinement have been fitted to the Regge trajectories. The resulting spectra for the pseudo-scalar and the isovector mesons are shown in Fig. 1. Both models allow for a very good description of the $\pi-K-\eta-\eta'$ splitting and the Regge trajectories. In addition to that the radial excitations are reproduced reasonably but slightly better in model $\mathcal{B}$ where the splitting turns out to be smaller. These excitations also lie on approximately linear trajectories which has been pointed out lately by V.V. Anisovich and is shown in Fig. 2 for π and a_0.
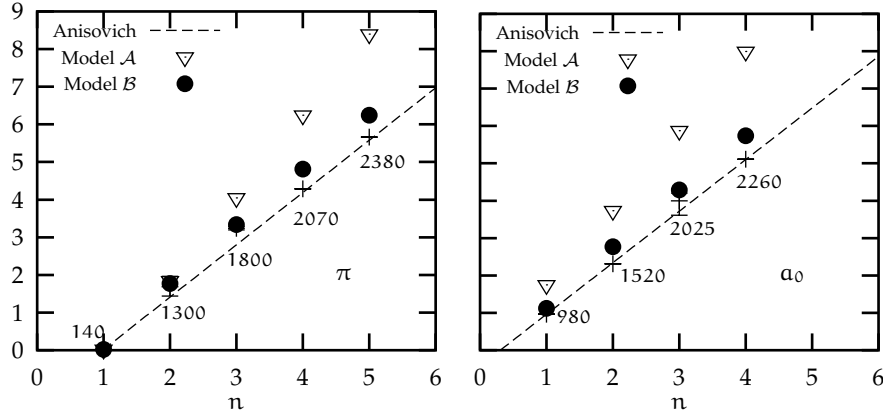

Fig. 2. The masses of radial excitations (in GeV^2) of π and a_0 compared to the experimental values and predictions taken from [1] (see references therein).

This behavior is described nicely with the special spinorial structure of model $\mathcal{B}$ while most of the states in model come out too high. Especially the low-lying $a_0(980)$ can not be accounted for in model $\mathcal{A}$. This demonstrates the relevance of the spinorial structure of the confinement potential.
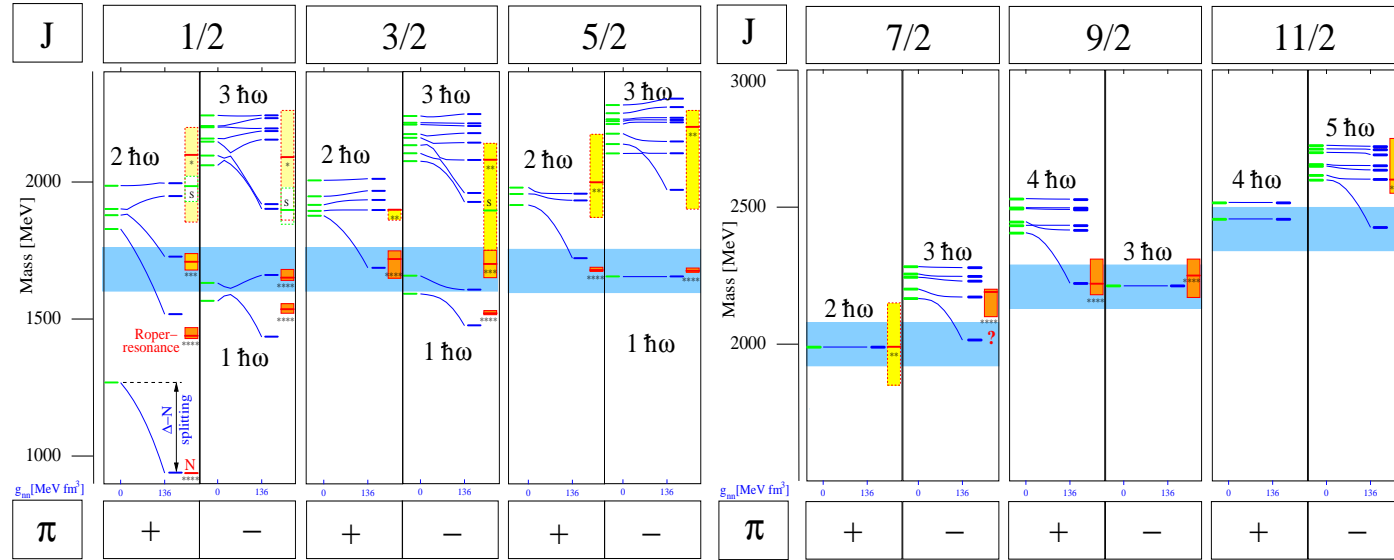
Fig. 3. The calculated masses of nucleon resonances in dependence of the strength g_{nn} of the instanton-induced force (left column, g_{nn} rises from left to right) compared to the experimental values [4] (right column). Parity doublets are stressed by shaded boxes.

The model for baryons was built with the meson model as a guideline and is described in [2]. Confinement is parameterized by a linearly rising potential in the quark pair distance with the spinorial structure

$$\frac{3}{4}\left[\mathbf{1}\otimes\mathbf{1}\otimes\mathbf{1}+\gamma^0\otimes\gamma^0\otimes\mathbf{1}+\text{cycl. perm.}\right]$$

for the offset and

$$\frac{1}{2}\left[-\mathbf{1}\otimes\mathbf{1}\otimes\mathbf{1}+\gamma^0\otimes\gamma^0\otimes\mathbf{1}+\text{cycl. perm.}\right]$$

for the slope, chosen to minimize spin-orbit splittings. The instanton-induced force acts on flavor anti-symmetric scalar di-quarks and thus lowers the octet baryons while the decuplet ground states and the Δ resonances remain unaffected. Hence, the quark masses and confinement parameters have been fitted to the decuplet states and Δ Regge trajectory before the two strengths of the residual interaction are adjusted to the octet-decuplet splitting. But also excited states are significantly influenced by the instanton-induced force as can be seen in Fig. 3 where the effect on the nucleon spectrum is shown. It allows for an almost quantitative description of the low-lying Roper resonance. Furthermore, the occurrence of parity doublets, *e.g.* $F_{15}(1680) - D_{15}(1675)$ and $H_{19}(2220) - G_{19}(2250)$, can be reproduced. This is possible since very selectively some states are lowered by approximately the amount of the splitting of the oscillator shells and become almost degenerated with a state of opposite parity. It is remarkable that the strength of the force adjusted to the octet-decuplet splitting indeed leads to this degeneracy.

The Salpeter amplitudes gained by solving the Salpeter equation are used to calculate electromagnetic current matrix elements according to the prescription of Mandelstam without introducing new parameters (see [3] for further details). The results on static properties of the nucleon are shown in Tab. 1 and agree well with the experimental data.

	Calc.	Exp.		Calc.	Exp.
μ_p	$2.74\,\mu_N$	$2.793\,\mu_N$	μ_n	$-1.70\,\mu_N$	$-1.913\,\mu_N$
$\sqrt{\langle r^2\rangle^p_E}$	0.82 fm	0.847 fm	$\langle r^2\rangle^n_E$	0.11 fm^2	0.113 ± 0.004 fm^2
$\sqrt{\langle r^2\rangle^p_M}$	0.91 fm	0.836 fm	$\sqrt{\langle r^2\rangle^n_M}$	0.86 fm	0.889 fm
g_A	1.21	1.2670 ± 0.0035	$\sqrt{\langle r^2\rangle_A}$	0.62 fm	0.61 ± 0.01 fm

Table 1. Static properties of the nucleon. Experimental data is taken from [4] for the magnetic moments and g_A and from [5] for the mean square radii.

For the calculation of form factors, *e.g.* the magnetic form factors shown in Fig. 4, a correct boost prescription as provided by our relativistic approach is mandatory. We find rather good agreement with the data below a momentum transfer of $Q^2 \approx 0.5$ GeV^2 but above that value the calculated form factors fall off too fast compared to the experiment.

Hence, in summary we find a very successful description of hadron masses in the frame-work of a relativistic quark model adopting an instanton-induced
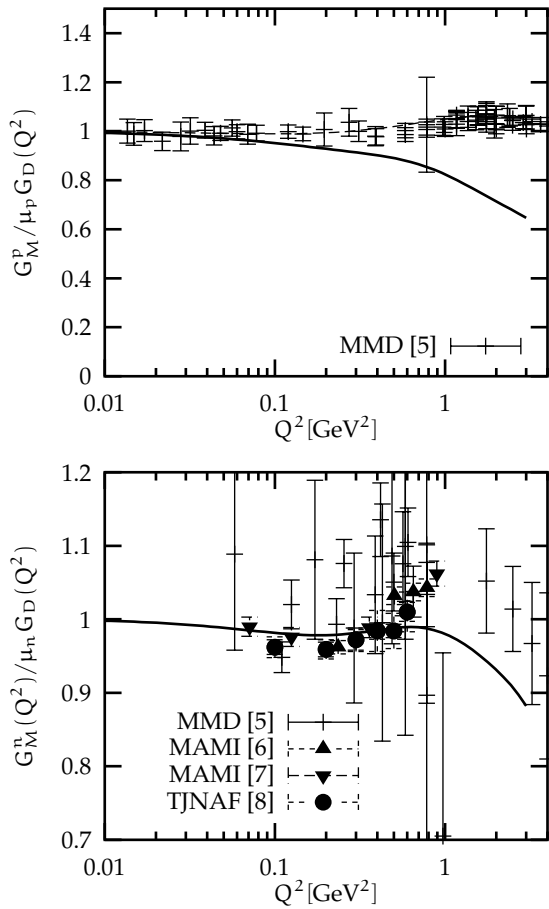
Fig. 4. The magnetic form factors of proton (left) and neutron (right) divided by the experimental dipole parametrization.

interaction, where all the characteristics of the observed spectra mentioned above can be accounted for. In addition to that a reasonable reproduction of nucleon form factors can be achieved.

References

1. M. Koll *et al.*, Eur. Phys. J. A **9** (2000) 73; R. Ricken *et al.*, Eur. Phys. J. A **9** (2000) 221.
2. U. Löring *et al.*, Eur. Phys. J. A **10** (2001) 309; Eur. Phys. J. A **10**, 395 (2001); Eur. Phys. J. A **10** (2001) 447.
3. D. Merten *et al.*, Eur. Phys. J. A **14** (2002) 477.
4. PARTICLE DATA GROUP, D.E. Groom *et al.*, Eur. Phys. J. C **15** (2000) 1.
5. P. Mergell *et al.*, Nucl. Phys. A **596** (1996) 367; V. Bernard *et al.*, J. Phys. G **28** (2002) R1.
6. H. Anklin *et al.*, Phys. Lett. B **428** (1998) 248.
7. G. Kubon *et al.*, Phys. Lett. B **524** (2002).
8. W. Xu, arXiv:nucl-ex/0208007, W. Xu *et al.*, Phys. Rev. Lett. **85** (2000) 2900.

Evolving QCD[*]

H.J. Pirner

Institut für Theoretische Physik der Universität Heidelberg

Abstract. We give an overview of the current theoretical status of proper time renormalization group flow equations applied to QCD. These equations give the evolution of coupling constants in an effective QCD Lagrangian as a function of an infra-red cut-off parameter. This parameter characterizes the resolution with which the system is looked at. Decreasing resolution transforms partonic quarks into constituent quarks and generates pion bound states. The evolution equations can also be applied to finite temperature and finite density QCD.

Quarks and gluons are the ultimate building blocks of hadrons. Their interaction is governed by the QCD coupling which grows dynamically for low energies. With the increasing coupling gluons and quark-antiquark pairs multiply indefinitely. Therefore QCD forms new structures of dominant collective units in the infra-red. The renormalization group is the principal tool to investigate the formation of these new structures. Its importance in quantum field theory can only be compared to the Schrödinger equation in quantum mechanics. In this paper I use the term renormalization group in a wide sense including the evolution of systems of Lagrangians. It may well be that the degrees of freedom change under evolution. Such an approach is not so well researched yet, but the necessity of a theoretical framework for it - especially in QCD - is universally recognized. I will try to give a summary of our work using renormalization group techniques to handle quark degrees of freedom evolving into hadronic bound states.

The quark-hadron transition governs strong interaction physics when the resolution is lowered below 1 GeV. Hadronic physics is well researched up to a mass scale of 1.5 GeV. Its spectroscopy still lacks a clear identification of glueballs and hybrid states. Yukawa models like the sigma model are natural to describe hadron physics at low energies. In order to bridge the gap between quark and meson physics we choose a hybrid approach where the original action contains a four-quark interaction which is bosonized into sigma and pion fields. These mesonic degrees of freedom are not propagating fields in the ultraviolet, i.e., their kinetic term is zero. They couple to the quark fields and mimic the local four-fermion interaction. In principle all the mesonic couplings arising from the Fierz transformation of a local color exchange interaction should be taken into account. Mean field theory shows a basic ambiguity to the possible Fierz transformations [1]. The RG-equations can overcome this problem. At the ultraviolet

scale the meson-quark Yukawa coupling can be set to unity. There is only the mass parameter of the combined sigma and pion fields in the Wigner mode which sets the mass scale for the evolving system. The renormalized Yukawa coupling decreases strongly in the infra-red which makes the evolution infra-red stable. In the approximation with meson loops we have indications that the infra-red evolution has fixed point character. Reversely the divergence of the Yukawa coupling for large scales signals the unsatisfactory high energy behaviour of the hadronic theory. Above the 1 GeV scale the compositeness of hadronic objects becomes important and one has to choose a quark-gluon basis.
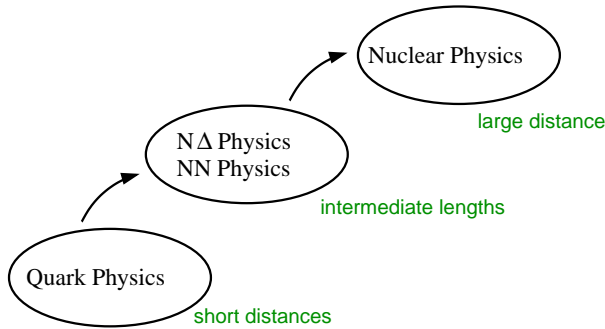

Fig. 1. The traditional separation of quark physics, the physics of the nucleon/delta and nucleon-nucleon interaction and nuclear physics

In Fig. 1 we summarize the traditional approach to hadronic and nuclear physics indicating the hierarchy between quark physics, nucleon-mesonic physics and nuclear physics. A division into these subfields is highly efficient when special topics in a field are researched, because then refined methods can be applied to get maximum insight into a detailed aspect. On the other hand it is refreshing to cross the borderlines of these fields and see how things are connected. Indeed modern high energy experiments in nuclear physics look at nuclei with high resolution in electron nucleus collisions and at high excitation energies in relativistic heavy ion collisions. They naturally relate nuclear physics to quark physics.

The renormalization group connects regions of different length scales and is the appropriate tool for such an interdisciplinary approach. It avoids the appearance of arbitrary cut-off functions when additional quantum corrections appear. Going beyond the large N_c approximation in the Nambu Jona Lasinio (NJL) model one needs to include meson loops which necessitates an additional cut-off in the Schwinger-Dyson approach. The unifying aspect of the renormalization group is shown in Fig. 2 and illustrated by the work here. Starting from the renormalization group in the vacuum, which only tests physics along the resolution axis, I will cover high temperature physics and high density investigations in the same theoretical framework.

Renormalization group flow equations describe the average of an effective action and represent the continuum analogue of a block spin transformation. I
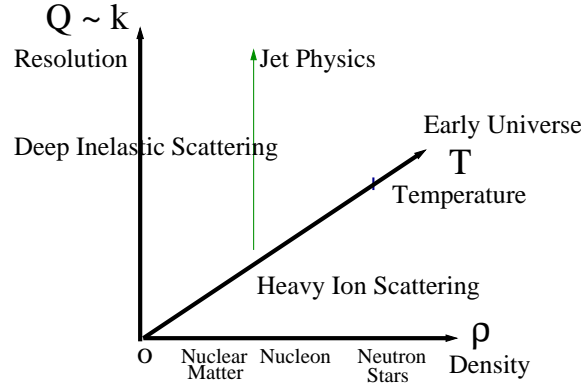
Fig. 2. The renormalization group unifies physics along the three different axis: physics at varying resolution, finite temperature and density

have tried before to use the Monte Carlo renormalization group to extend the lattice gluon action of Wilson into the long distance region [2–4]. This approach introduces new collective variables into the lattice action, namely the colordielectric fields. The resulting QCD action has a strong coupling which is modulated by the colordielectric field and confines. It reproduces results obtained on the finer lattice with an accuracy of 10 %. A large numerical effort is needed to solve a set of overdetermined Schwinger-Dyson equations. Already at that time it was desirable to have an analytic scheme to follow the flow of couplings when high momenta larger than a coarse-graining scale k are integrated out. The flow equations proposed by Wegner and Houghton [5], Polchinsky [6], Wetterich and Berges [7,8] present such a scheme. They are ultraviolet and infra-red finite through the introduction of a scale dependent cut-off function. We use renormalization group flow equations with a heat kernel cut-off [10–12] which we think are more practical. Moreover, they are so simple that they are ideally suited to learn and teach renormalization in field theory. No infinities appear at any time. All integrals can be done analytically and have a simple form. The solution of these RG-equations includes complicated summations of diagrams which are similar to solutions of a coupled set of Schwinger-Dyson equations. The heat kernel regularization method [9] preserves the symmetries of the theory and keeps the physical interpretation of the evolution equations particularly simple for phenomenological applications.

We choose as a starting action at the UV scale the NJL Lagrangian

$$S_{NJL} = \int d^4x [\bar{q}\, i\gamma\partial q + G\, \{(\bar{q}q)^2 + (\bar{q}i\boldsymbol{\tau}\gamma_5 q)^2\}] \tag{1}$$

which is embedded into a linear σ-model with $Z_q = 1$, a vanishing wave function renormalization constant $Z_\Phi = 0$ and an effective potential $U(\Phi^2) = \frac{m^2 \Phi^2}{2}$. We assume the linear σ-model to be a valid description of nature below scales of 1.5 GeV. In this region the gluon degrees of freedom are supposed to be already frozen out. Confinement is not dealt with correctly. The physics is governed by

chiral symmetry, which is spontaneously broken in the infra-red. The Euclidian action of the linear σ-model in generalized form is given by

$$S[\Phi, \bar{q}, q] = \int d^4x \left(Z_q(\Phi^2)\bar{q}\gamma\partial q + \frac{1}{2}Z_\Phi(\Phi^2)(\partial_\mu\Phi^a)(\partial_\mu\Phi^b) \right.$$
$$\left. + \quad g(\Phi^2)\bar{q}Mq + U(\Phi^2) \right). \tag{2}$$

The quark and meson fields are $\bar{q}, q$ and Φ, where $\Phi = (\sigma, \boldsymbol{\pi})$ is the O(4)- and $M = \sigma + i\boldsymbol{\tau}\boldsymbol{\pi}\gamma_5$ the chiral $SU(2)_L \otimes SU(2)_R$-representation of the meson fields. We consider this action to be preserved during the evolution and follow the generalized couplings and the effective potential during evolution by calculating the effective action S_{eff} in a one-loop approximation.

$$S_{eff}[\Phi, \bar{q}, q] = S[\Phi, \bar{q}, q] - \frac{1}{2}\text{Tr} \log S_{\bar{q}q} + \frac{1}{2}\text{Tr} \log \left(S_{\Phi^i\Phi^j} - 2S_{\Phi^iq}S_{\bar{q}q}^{-1}S_{\bar{q}\Phi^j} \right), \tag{3}$$

with

$$S_{\bar{q}q}(x,y) = \left. \frac{\delta^2 S[\Phi, \bar{q}, q]}{\delta\bar{q}(x)\delta q(y)} \right|_{av}, \tag{4}$$

$$S_{\Phi^i\Phi^j}(x,y) = \left. \frac{\delta^2 S[\Phi, \bar{q}, q]}{\delta\Phi^i(x)\delta\Phi^j(y)} \right|_{av}. \tag{5}$$

The first logarithm results from the fermion loop fluctuations, whereas the two terms in the second logarithm are the contributions of the bosonic and the mixed loop, respectively. The derivative of S_{eff} with respect to the evolution scale can be computed after a cut-off function is introduced. For this purpose we represent the fluctuation determinants by Schwinger proper time integrals with the cut-off function $f(k^2\tau) = \left(1 + k^2\tau + \frac{1}{2}(k^2\tau)^2\right) e^{-k^2\tau}$

$$\text{Tr} \log(A) = -\text{Tr} \int_0^\infty \frac{d\tau}{\tau} e^{-\tau A} f(k^2\tau). \tag{6}$$

The heat kernel cut-off function f suppresses all fluctuations with momenta below the cut-off scale k. Going to $k \to 0$ means to include more and more infrared modes. Finally, all modes are included, because of the limiting behaviour $f_{k\to 0} \to 1$. The ultraviolet region is left undisturbed due to the extra τ and τ^2 terms in front of the exponential. Therefore we can extend the τ-integration to the interval $[0, \infty]$. We further replace the masses and couplings of the classical action by the running masses and running couplings of the *effective* action S_{eff}. Generically, we obtain the following evolution equation for S_{eff} which contains its second order derivatives S''_{eff} indicated in Eqs.(4,5):

$$\frac{\partial S_{eff}}{\partial k} = -\frac{1}{2}\text{Tr} \int \frac{d\tau}{\tau} e^{-S''_{eff}(k)} \frac{\partial}{\partial k} f(k^2\tau). \tag{7}$$

This replacement of S'' by S''_{eff} turns the one-loop equation into a renormalization group improved flow equation, which goes beyond the standard one-loop renormalization group running and includes higher loop terms successively

into the proper time integral. Therefore it is capable to include nonperturbative physics in the strong coupling region. The evolution equations are obtained by comparing the derivative on $S_{eff}(k)$ with respect to k with the formal expression of Eq. (2) which contains the generalized couplings and the effective potential as functions of k. The local potential terms are easy to evaluate and lead to nonlinear partial differential equations containing derivatives of the potential with respect to Φ^2. The evolution of the other couplings can be obtained in a derivative expansion which is an expansion in derivatives (momentum) over mass. This expansion is well controlled because of two reasons. Firstly, we approach the infra-red, so momenta become always smaller, we need only few terms in the expansion. Secondly, the infra-red cut-off scale k acts like a mass cut-off, so the expansion is well defined even if the excitations themselves are massless, like the quarks in the ultraviolet or the mesons in the infra-red region.

Let me give an overview of the results we have achieved so far. We have solved in local potential approximation the vacuum evolution, the finite temperature evolution and finite baryon density evolution [10–12]. There are strong similarities between the vacuum evolution as a function of resolution scale and as a function of temperature. Both show the transition from partons to constituent quarks which has also been phenomenologically checked in deep inelastic scattering at fixed energy $\sqrt{s}$ as a function of photon virtuality Q^2 see Ref. [13] and Fig. (2). Numerically, the transition temperature $2\pi T_c$ is about equal to the chiral symmetry breaking scale $k_{\chi sb}$ where the quarks condense in the vacuum. Going from the ultraviolet to the infra-red the strong attractive quark-antiquark interaction leads to a condensation of quark pairs in the vacuum. At the resolution $k_{\chi sb}$ the effective mass parameter of the mesons equals zero. The critical exponents agree with the $0(4)$ critical exponents, but differ from the mean field values [14].

In large N_c approximation we have shown that the renormalization group flow equations are identical to the gap equations of the NJL model [15]. Further it is possible to calculate the eigenmode spectrum of the Euclidean Dirac operator [16] which previously was only known for very small eigenvalues in random matrix theories.

The full equations possess extra complexity via the expansion of all running couplings and wavefunction renormalization parameters in Φ^2. As mentioned above the global form of the meson potential $U(\Phi^2)$ changes from the parabolic shape in the ultraviolet to a mexican hat shape in the infra-red. This evolution leads to a change of the minimum of the effective potential with resolution k. We track all couplings in Taylor series around this running minimum with terms up to 5th order in Φ^2. This leads to 20 coupled non-linear differential equations. Including meson loop terms the infra-red properties of the system depend only on the mass term in the ultraviolet and no longer on the starting ultraviolet cut-off. We have a real fixed point behaviour for the pion decay constant, meson quark coupling, constituent quark mass and quark condensate. In comparison to NJL the flow equations have predictive power since only one mass scale fixes all the other dimensionful parameters.

For finite density [17] the model has similar deficiences as the conventional NJL model. It overbinds and restores the chiral symmetry too early. We have im-

proved the model by including ω-repulsion and plan to do this calculation including loop corrections.

The very successful chiral perturbation theory alone cannot connect to QCD in the ultraviolet. Typically it starts to fail when the resolution scale is of the order of half the ρ mass. Hybrid models like the one presented here containing meson degrees of freedom *and* quarks extend to larger momentum scales, which is a definite advantage. There are, however, two problems: Firstly, the number of mesons in the theory should include also the vector mesons. Secondly, the size of the scalar Yukawa couplings increases dramatically in the ultraviolet, therefore it seems difficult to cross over to the asymptotically free gauge theory of QCD. For nuclei a theory with quarks and nucleons [18] seems to be the most efficient way to describe the transition from purely nucleonic matter to quark matter at high baryon density [19]. Our model like most of the other hybrid models lacks a field theoretic mechanism to avoid the appearance of free quarks as asymptotic states. A major progress would be to capture the smooth infra-red limit of lattice QCD in a field theoretic continuum picture.

References

1. J. Jaeckel and C. Wetterich, arXiv:hep-ph/0207094.
2. H. J. Pirner, Prog. Part. Nucl. Phys. **29** (1992) 33.
3. H. J. Pirner, J. Wroldsen and E. M. Ilgenfritz, Nucl. Phys. **B 294** (1987) 905.
4. B. Grossmann, H. J. Pirner, A. I. Signal, R. Baier and J. Wroldsen, Int. J. Mod. Phys. **A 6** (1991) 2649.
5. F. J. Wegner and A. Houghton Phys. Rev. **A 8** (1973) 401.
6. J. Polchinski, Proc. of the 1992 TASI Elementary Particle physikcs, World. Science 1992, Nucl. Phys. **B 231** (1984) 269.
7. C. Wetterich, Phys. Lett. **B 301** (1993) 90.
8. J. Berges, N. Tetradis and C. Wetterich, Phys. Rep. **363** (2002) 223 [arXiv:hep-ph/0005122].
9. R. Ball, Phys. Rep. **182** (1989) 1.
10. B. J. Schaefer and H. J. Pirner, arXiv:nucl-th/9801067.
11. B. J. Schaefer and H. J. Pirner, Nucl. Phys. **A 660** (1999) 439 [arXiv:nucl-th/9903003].
12. G. Papp, B. J. Schaefer, H. J. Pirner and J. Wambach, Phys. Rev. **D 61** (2000) 096002 [arXiv:hep-ph/9909246].
13. H. G. Dosch, T. Gousset and H. J. Pirner, Phys. Rev. **D 57** (1998) 1666 [arXiv:hep-ph/9707264].
14. B. J. Schaefer, O. Bohr and J. Wambach, Int. Journ. Mod. Phys. **A 16** (2001) 3823.
15. J. Meyer, K. Schwenzer, H. J. Pirner and A. Deandrea, Phys. Lett. **B 526** (2002) 79 [arXiv:hep-ph/0110279].
16. T. Spitzenberg, K. Schwenzer and H. J. Pirner, Phys. Rev. **D 65** (2002) 074017 [arXiv:hep-ph/0201095].
17. J. Meyer, G. Papp, H. J. Pirner and T. Kunihiro, Phys. Rev. **C 61** (2000) 035202 [arXiv:nucl-th/9908019].
18. J. Meyer, K. Schwenzer and H. J. Pirner, Phys. Lett. **B 473** (2000) 25 [arXiv:nucl-th/9908017].
19. K. Schwenzer, J. Meyer and H.J. Pirner preprint in preparation.

N-Δ axial transition form factors [*]

B. Golli[a,b], L. Amoreira[c,e], M. Fiolhais[d,e], and S. Širca[f,b]

[a] Faculty of Education, University of Ljubljana, 1000 Ljubljana, Slovenia
[b] J. Stefan Institute, 1000 Ljubljana, Slovenia
[c] Department of Physics, University of Beira Interior, 6201-001 Covilhã, Portugal
[d] Department of Physics, University of Coimbra, 3004-516 Coimbra, Portugal
[e] Centre for Computational Physics, University of Coimbra, 3004-516 Coimbra, Portugal
[f] Faculty of Mathematics and Physics, University of Ljubljana, 1000 Ljubljana, Slovenia

Abstract. We review some basic properties of the N-Δ transition axial amplitudes and relate them to the strong πNΔ form-factor. In models with the pion cloud we derive a set of constraints on the pion wave function which guaranty the correct behaviour of the amplitudes in the vicinity of the pion pole. Corrections due to the spurious center-of-mass motion are calculated to the leading order in the inverse baryon mass. We give explicit expressions for the amplitudes in the Cloudy Bag Model and show that they rather strongly underestimate the experimental values.

1 Introduction

The weak N-Δ transition amplitudes yield important information about the structure of the nucleon and the Δ, and in particular about the role of chiral mesons since they explicitly enter in the expression for the axial part of the weak current. There exist only very few calculations in quark models [1,2] yet none of them includes the mesonic degrees of freedom. This can be traced back to the difficulty of incorporating consistently the pion field which is necessary to describe the correct low-Q^2 behaviour of the amplitudes. Obviously, this can be done only in the models that properly incorporate the chiral symmetry.

The aim of this work is to study the axial amplitudes of the N-Δ transition in models with quarks and chiral mesons. In Sec. 2 we introduce expressions for the axial helicity amplitudes and relate them to the experimentally measured quantities, $C_i^A, i = 3, 6$, the so called Adler form-factors. We derive the analog of the Goldberger-Treiman relation that relates the leading axial form factor, C_5^A, to the strong πNΔ coupling constant. In Sec. 3 we calculate the amplitudes in a simple isobar model that includes the pion. In Sec. 4 we study some general properties of the axial amplitudes in quark models that include the pion and possibly also its chiral partner, the σ-meson. We derive a set of constraints on the pion field and show that in models that satisfy these constraints the pion pole appears only in the C_6^A form-factor. Furthermore, if the meson self-interaction is absent in the model, i.e. if the pion interacts only with quarks, the pion contributes solely to

---

[*] Talk delivered by B. Golli.

the C_6^A form-factor while the C_4^A and C_5^A form-factors pick up only the contribution from quarks. In most quark models the nucleon and the Δ are calculated as localized states while the expressions for the amplitudes require states with good linear momenta. In Sec. 5 we use the wave packet formalism to derive corrections to the amplitudes calculated between localized states and show that the approximations are valid for momenta that are small compared to typical baryon masses. In Sec. 6 we give explicit expressions for the axial as well as the strong form-factors in the Cloudy Bag Model (CBM) and make a simple estimate of their strengths.

The calculation of the form-factors in the CBM as well as in the linear σ-model that includes besides the pion also the σ-meson is presented and compared to the experimentally measure form-factors in [3,4] and in the contribution of Simon Širca [5] to these Proceedings.

2 Same basic properties of transition amplitudes

2.1 Definition of the helicity amplitudes

The weak transition amplitudes are defined as the matrix elements of the weak interaction Hamiltonian

$$M = \langle\Delta|H|N, W\rangle = W_{a\mu}^{(-)}\langle\Delta|V^{a\mu} - A^{a\mu}|N\rangle \tag{1}$$

where a is the isospin index. For simplicity we shall assume $a = 0$ and will not write it explicitly. For the axial part alone we have:

$$M^A = \sqrt{\frac{4\pi\alpha_W}{2K_0}} \sum_\lambda e_{\mu\lambda}\langle\Delta|A^\mu|N\rangle = \sqrt{\frac{4\pi\alpha_W}{2K_0}} \left[\langle\Delta|A^0|N\rangle - \sum_\lambda \varepsilon_\lambda \cdot \langle\Delta|\mathbf{A}|N\rangle\right] ,$$
$$\tag{2}$$

where

$$K_0 = \frac{M_\Delta^2 - M_N^2}{2M_\Delta} \quad \text{and} \quad 4\pi\alpha_W = \frac{4\pi\alpha}{\sin^2\theta_W} \approx 0.443 . \tag{3}$$

The 4-momentum of the incident weak boson (W) is

$$k^\mu = (k_0, 0, 0, k) , \quad k_0 = \frac{M_\Delta^2 - M_N^2 - Q^2}{2M_\Delta} , \quad k = \sqrt{k_0^2 + Q^2} . \tag{4}$$

The helicity amplitudes are defined as

$$\tilde{S}^A = -\langle\Delta^+(p'), s_\Delta = \tfrac{1}{2}|A_0^0(0)|N^+(p)s_N = \tfrac{1}{2}\rangle , \tag{5}$$

$$\tilde{A}_{\frac{3}{2}}^A = -\langle\Delta^+(p'), s_\Delta = \tfrac{3}{2}|\varepsilon_+ \cdot \mathbf{A}(0)|N^+(p)s_N = \tfrac{1}{2}\rangle , \tag{6}$$

$$\tilde{A}_{\frac{1}{2}}^A = -\langle\Delta^+(p'), s_\Delta = \tfrac{1}{2}|\varepsilon_+ \cdot \mathbf{A}(0)|N^+(p)s_N = -\tfrac{1}{2}\rangle , \tag{7}$$

$$\tilde{L}^A = -\langle\Delta^+(p'), s_\Delta = \tfrac{1}{2}|\varepsilon_0 \cdot \mathbf{A}(0)|N^+(p)s_N = \tfrac{1}{2}\rangle . \tag{8}$$

2.2 The Adler form-factors

Experimentalists measure the so called Adler form-factors defined as [6]:

$$\langle \Delta^+(p') | A_{\alpha(a=0)} | N^+(p) \rangle = \bar{u}_{\Delta\alpha} \frac{C_4^A(Q^2)}{M_N^2} p'_\mu q^\mu u_N - \bar{u}_{\Delta\mu} \frac{C_4^A(Q^2)}{M_N^2} p'_\alpha q^\mu u_N$$

$$+ \bar{u}_{\Delta\alpha} C_5^A(Q^2) u_N + \bar{u}_{\Delta\mu} \frac{C_6^A(Q^2)}{M_N^2} q^\mu q_\alpha u_N + \bar{u}_{\Delta\alpha} \frac{C_3^A(Q^2)}{M_N} \gamma_\mu q^\mu u_N , \quad (9)$$

where $p'_\mu = (M_\Delta; 0, 0, 0)$ and $q^\mu = (\omega; 0, 0, k)$, and $u_{\Delta\alpha}$ is the Rarita-Schwinger spinor:

$$u_\alpha(p, s_\Delta) = \sum_{\lambda',s} C^{\frac{3}{2} s_\Delta}_{1\lambda' \frac{1}{2} s} e_{\alpha\lambda'}(p) u(p, s) . \quad (10)$$

Here

$$e_\lambda^\mu(p) = \left[\frac{\varepsilon_\lambda \cdot \mathbf{p}}{M_\Delta} , \; \varepsilon_\lambda + \frac{\mathbf{p}(\varepsilon_\lambda \cdot \mathbf{p})}{M_\Delta(p_0 + M_\Delta)} \right] , \quad (11)$$

and $u(p, s)$ is the usual bispinor for a spin $\frac{1}{2}$ particle. For the Δ at rest it has a simple form (e.g. [7], 414):

$$e_\lambda^\mu = (0, \, \varepsilon_\lambda) , \qquad u(p, s) = \begin{pmatrix} 1 \\ 0 \end{pmatrix} \chi_{\frac{1}{2} s} , \quad (12)$$

where ε_λ are the polarization vectors. The form-factor C_3^A is small; in models with s-wave quarks and p-wave pions it is even identically 0; we shall therefore assume $C_3^A = 0$ in the further derivations.

The helicity amplitudes can now be easily related to the form factors. For $\alpha = 0$ the evaluation is straightforward, while for $\alpha \neq 0$ we multiply (9) by e_λ^α and use the following relations:

$$e_\lambda^\alpha \bar{u}_\alpha(p, s_\Delta) u_N = \varepsilon_\lambda \sum_{\lambda',s} C^{\frac{3}{2} s_\Delta}_{1\lambda' \frac{1}{2} s} (-\varepsilon_{\lambda'}^*) \bar{u}(p, s) u_N = -C^{\frac{3}{2} s_\Delta}_{1\lambda \frac{1}{2} s_N} , \quad (13)$$

$$e_\lambda^\alpha q_\alpha = -k \delta_{\lambda,0} , \qquad \bar{u}_\mu(p, s_\Delta) q^\mu u_N = -k C^{\frac{3}{2} s_\Delta}_{1\lambda \frac{1}{2} s_N} . \quad (14)$$

We obtain

$$\check{S}^A = - \left[k \frac{C_4^A}{M_N^2} M_\Delta - \omega k \frac{C_6^A}{M_N^2} \right] \sqrt{\frac{2}{3}} , \quad (15)$$

$$\tilde{A}_{\frac{3}{2}}^A = - \left[\frac{C_4^A}{M_N^2} \omega M_\Delta + C_5^A \right] = \sqrt{3} \, \tilde{A}_{\frac{1}{2}}^A , \quad (16)$$

$$\tilde{L}^A = - \left[\frac{C_4^A}{M_N^2} \omega M_\Delta + C_5^A - \frac{k^2}{M_N^2} C_6^A \right] \sqrt{\frac{2}{3}} . \quad (17)$$

The Adler form-factors read

$$C_6^A = \frac{M_N^2}{k^2} \left[-\tilde{A}_{\frac{3}{2}}^A + \sqrt{\frac{3}{2}} \tilde{L}^A \right] , \quad (18)$$

$$C_5^A = -\sqrt{\frac{3}{2}} \left(\tilde{L}^A - \frac{k_0}{k} \tilde{S}^A \right) - \frac{k_0^2 - k^2}{M_N^2} C_6^A \,, \tag{19}$$

$$C_4^A = \frac{M_N^2}{k M_\Delta} \left[-\sqrt{\frac{3}{2}} \tilde{S}^A + \frac{k_0 k}{M_N^2} C_6^A \right] \,. \tag{20}$$

2.3 The off-diagonal Goldberger-Treiman relation

Let us compute the divergence of the axial current between the Δ and N (9). Using (14) we get ($q^2 \equiv -Q^2$):

$$\langle \Delta^+(P) | \partial^\alpha A_\alpha | N^+(p) \rangle = ik \left[C_5^A(q^2) + \frac{C_6^A(q^2)}{M_N^2} q^2 \right] C_{10\,\frac{1}{2}\,\frac{1}{2}}^{\frac{3}{2}\,\frac{1}{2}} \,. \tag{21}$$

In the chiral limit the divergence has to vanish. From the above expression we would conclude that $C_5^A(q^2) = 0$ which is experimentally not the case. Hence $C_6^A(q^2)$ should have a pole at $q^2 = 0$ such that

$$C_6^A(q^2) = -\frac{M_N^2 C_5^A(q^2)}{q^2} \,. \tag{22}$$

As in the nucleon case, we relate this term to the term in the axial current that is responsible for the pion decay: $A_{a\,\mathrm{pole}}^\alpha(x) = f_\pi \partial^\alpha \pi_a(x)$. We can therefore identify the C_6^A-term in (9) with:

$$\bar{u}_{\Delta\mu} \frac{C_6^A(q^2)}{M_N^2} q^\mu q_\alpha u_N = i q_\alpha f_\pi \langle \Delta^+(P) | \pi_0(0) | N^+(p) \rangle \,. \tag{23}$$

Indeed, the pion propagator behaves as q^{-2} in the chiral limit.

In the real world the pion mass is finite and we write the pion field as

$$\langle \Delta^+(P) | \pi_0(0) | N^+(p) \rangle = i \frac{G_{\pi N\Delta}(q^2)}{2M_N} \frac{\bar{u}_{\Delta\mu} q^\mu u_N}{-q^2 + m_\pi^2} \sqrt{\frac{2}{3}} \,. \tag{24}$$

while the vanishing of (21) is replaced by PCAC:

$$\langle \Delta^+(P) | \partial^\alpha A_{\alpha\,a} | N^+(p) \rangle = -m_\pi^2 f_\pi \langle \Delta^+(P) | \pi_a(0) | N^+(p) \rangle \,. \tag{25}$$

Replacing the LHS of (25) by (21) and using (23) and (24) we find

$$i q^\alpha \bar{u}_{\Delta\alpha} u_N \left[C_5^A(q^2) + f_\pi \frac{G_{\pi N\Delta}(q^2)}{2M_N} \frac{q^2}{-q^2 + m_\pi^2} \sqrt{\frac{2}{3}} \right] =$$

$$i q^\alpha \bar{u}_{\Delta\alpha} u_N \frac{G_{\pi N\Delta}(q^2)}{2M_N} \frac{m_\pi^2 f_\pi}{-q^2 + m_\pi^2} \sqrt{\frac{2}{3}} \,. \tag{26}$$

We finally obtain

$$C_5^A(q^2) = f_\pi \frac{G_{\pi N\Delta}(q^2)}{2M_N} \sqrt{\frac{2}{3}} \,, \tag{27}$$

the *off-diagonal Goldberger-Treiman relation*, which – strictly speaking – holds only in the limit $q^2 \to m_\pi^2$. Assuming a smooth behaviour of the amplitudes for q^2 in the vicinity of m_π^2 we can expect (27) to remain valid for sufficiently small q^2 in the experimentally accessible range.

3   The axial current in a simple isobar model with pions

The aim of this section is to derive the amplitudes in a simple model in order to study the contribution of pions to the amplitudes and to analyze the qualitative behaviour of the amplitudes. The derivation in this section is based on the standard derivation of the diagonal Goldberger-Treiman relation and PCAC (see e.g. [7]).

We investigate the axial hadronic current in a model with two structureless fermion fields, the nucleon and the Δ, and the pion field. Since we are interested here only in the nucleon-Δ transition we shall write down explicitly only the pertinent parts of the Lagrangian and of the hadron current. The nucleon and the Δ (at rest) satisfy the Dirac equation

$$(i\gamma_\mu \partial^\mu - E_N)\psi_N = 0 , \qquad (i\gamma_\mu \partial^\mu - M_\Delta)\psi_\Delta = 0 . \tag{28}$$

We assume the following form of the $\pi N\Delta$ interaction

$$\mathcal{L}_{\pi N\Delta} = -iG_{\pi N\Delta}\bar{\psi}_\Delta \gamma_5 T_a \psi_N \pi_a , \tag{29}$$

where we introduce the transition operator $\vec{T}$ (and $\mathbf{\Sigma}$) by

$$\langle \tfrac{3}{2} t_\Delta | T_a | \tfrac{1}{2} t_N \rangle = C^{\frac{3}{2} t_\Delta}_{1a \frac{1}{2} t_N} , \qquad \langle \tfrac{3}{2} s_\Delta | \Sigma_\lambda | \tfrac{1}{2} s_N \rangle = C^{\frac{3}{2} s_\Delta}_{1\lambda \frac{1}{2} s_N} . \tag{30}$$

(Note that γ^μ has a more complicated structure:

$$\gamma = \begin{vmatrix} 0 & \mathbf{S} \\ -\mathbf{S} & 0 \end{vmatrix} , \tag{31}$$

where the generalized Pauli matrices $\mathbf{S}$ act in the space spanned by the $S = \tfrac{1}{2}$ and $S = \tfrac{3}{2}$ subspaces:

$$\mathbf{S} = \begin{vmatrix} \sigma & \mathbf{\Sigma} \\ \mathbf{\Sigma}^\dagger & \sigma_{\Delta\Delta} \end{vmatrix} . \tag{32}$$

The generalized isospin is introduce in the same way.)

The nucleon bispinor can be written as

$$u_N(p) = \sqrt{\frac{E_N + M_N}{2M_N}} \begin{pmatrix} 1 \\ \frac{\mathbf{\Sigma} \cdot \mathbf{p}}{E_N + M_N} \end{pmatrix} \chi_{\frac{1}{2} s_N} \xi_{\frac{1}{2} t_N} \approx \begin{pmatrix} 1 \\ \frac{\mathbf{\Sigma} \cdot \mathbf{p}}{2M_N} \end{pmatrix} \chi_{\frac{1}{2} s_N} \xi_{\frac{1}{2} t_N} , \tag{33}$$

with χ and ξ describing respectively the spin and isospin part of the bispinor, and

$$p^\mu = (E_N, \mathbf{p}) , \qquad E_N = \sqrt{M_N^2 + \mathbf{p}^2} \approx M_N . \tag{34}$$

We assume that Δ is at rest, $p'^\mu = (M_\Delta; 0, 0, 0)$, hence

$$u_\Delta(p') = \begin{pmatrix} 1 \\ 0 \end{pmatrix} \chi_{\frac{3}{2} s_\Delta} \xi_{\frac{3}{2} t_\Delta} . \tag{35}$$

In the model, the transition part of the axial current takes the form:

$$A_a^\mu = g_A^\Delta \bar{\psi}_\Delta \gamma^\mu \gamma_5 \tfrac{1}{2} T_a \psi_N + f_\pi \partial^\mu \pi_a . \tag{36}$$

Using the Dirac equations (28) and the Klein-Gordon equation for the (pertinent part of the) pion field:

$$\left(\partial_\mu \partial^\mu + m_\pi^2\right) \pi_a = -iG_{\pi N\Delta} \bar{\psi}_\Delta \gamma_5 T_a \psi_N \tag{37}$$

we immediately obtain

$$\partial_\mu A_a^\mu = ig_A^\Delta \tfrac{1}{2}(M_\Delta + M_N)\bar{\psi}_\Delta \gamma_5 T_a \psi_N - if_\pi G_{\pi N\Delta} \bar{\psi}_\Delta \gamma_5 T_a \psi_N - f_\pi m_\pi^2 \pi_a \ . \tag{38}$$

In the limit $m_\pi \to 0$ the current is conserved provided

$$\tfrac{1}{2}(M_\Delta + M_N)g_A^\Delta = f_\pi G_{\pi N\Delta} \tag{39}$$

which is the *off-diagonal Goldberger-Treiman relation* (27). The constant g_A^Δ is related to the experimentally measured $C_5^A(0)$ by

$$g_A^\Delta = \frac{2M_N}{M_\Delta + M_N} \sqrt{6}\, C_5^A(0) \ , \qquad C_5^A(0) = 1.22 \pm 0.06 \ . \tag{40}$$

We now evaluate the matrix elements of the transition axial current. In this case the solution of (37) is

$$\langle \Delta(p')|\pi_a(\omega, \mathbf{k})|N(p)\rangle = -i\, \frac{G_{\pi N\Delta}}{2M_N} \frac{\langle \Delta|\,(-\mathbf{\Sigma}\cdot\mathbf{k})\,T_a|N\rangle}{(-\omega^2 + \mathbf{k}^2 + m_\pi^2)} \tag{41}$$

with $\omega = M_\Delta - M_N$, $\mathbf{k} = -\mathbf{p}$. For the time-like component of the current we get

$$\langle \Delta(p')|A_a^0(0)|N(p)\rangle = -k\, \frac{g_A^\Delta}{2M_N} \langle \Delta|\Sigma_0 \tfrac{1}{2}T_a|N\rangle + i\omega f_\pi \langle \Delta(p')|\pi_a|N(p)\rangle$$

$$= -\left[\frac{g_A^\Delta k}{4M_N} + \frac{f_\pi G_{\pi N\Delta}}{2M_N} \frac{\omega k}{(-q^2 + m_\pi^2)}\right] \langle \Delta|\Sigma_0 T_a|N\rangle \ . \tag{42}$$

The spatial part is

$$\langle \Delta(p')|\mathbf{A}_a(0)|N(p)\rangle = g_A^\Delta \langle \Delta|\mathbf{\Sigma}\, \tfrac{1}{2}T_a|N\rangle + ikf_\pi \langle \Delta(p')|\pi_a|N(p)\rangle$$

$$= \tfrac{1}{2}\, g_A^\Delta \langle \Delta|\mathbf{\Sigma}\, T_a|N\rangle - \frac{f_\pi G_{\pi N\Delta}}{2M_N} \frac{\mathbf{k}}{(-q^2 + m_\pi^2)} \langle \Delta|(\mathbf{\Sigma}\cdot\mathbf{k})\,T_a|N\rangle \ . \tag{43}$$

The helicity amplitudes introduced in the first section (for 4-vector momentum transfer $q^\mu = p'^\mu - p^\mu = (\omega; 0, 0, k)$) are now expressed as

$$\tilde{S}^A = \left[k\, \frac{g_A^\Delta}{4M_N} + k\, \frac{f_\pi G_{\pi N\Delta}}{2M_N} \frac{\omega}{(-q^2 + m_\pi^2)}\right] \sqrt{\frac{2}{3}}^2 \ , \tag{44}$$

$$\tilde{A}_{\frac{3}{2}}^A = -\tfrac{1}{2}\, g_A^\Delta \sqrt{\frac{2}{3}} = \sqrt{3}\tilde{A}_{\frac{1}{2}}^A \ , \tag{45}$$

$$\tilde{L}^A = \left[-\tfrac{1}{2}\, g_A^\Delta + \frac{f_\pi G_{\pi N\Delta}}{2M_N} \frac{k^2}{(-q^2 + m_\pi^2)}\right] \sqrt{\frac{2}{3}}^2 \ . \tag{46}$$

Using (39) we are now able to explicitly check that PCAC holds in the model:

$$\langle\Delta^+(p')|\partial_\mu A^\mu_{a=0}|N^+(p)\rangle = -i\left(\omega\tilde{S}^A - k\tilde{L}^A\right)$$
$$= -m_\pi^2 f_\pi \langle\Delta^+(p')|\pi_0|N^+(p)\rangle\ . \tag{47}$$

In this model we can express the Adler form-factors solely in terms of either g_A^A or $G_{\pi N\Delta}$:

$$C_6^A = \frac{1}{\sqrt{6}}\, f_\pi M_N \, \frac{G_{\pi N\Delta}}{-q^2 + m_\pi^2}\ , \tag{48}$$

$$C_5^A = \frac{1}{\sqrt{6}}\, \frac{M_\Delta + M_N}{2M_N}\, g_A^A = \sqrt{\frac{2}{3}}\, \frac{f_\pi G_{\pi N\Delta}}{2M_N}\ , \tag{49}$$

$$C_4^A = -\frac{1}{\sqrt{6}}\, \frac{M_N}{2M_\Delta}\, g_A^A = -\frac{M_N^2}{M_\Delta(M_\Delta + M_N)}\, C_5^A \approx -0.33\, C_5^A\ . \tag{50}$$

The relations derived above show that only C_6^A exhibits the pole behavior while in the other two amplitudes the pole behavior cancels out and the result is the same as if we used only the fermion part of the axial current. In the next section we shall see that this property holds in a vast class of models that fulfill certain virial relations.

4 Helicity amplitudes in models with the pion cloud

We investigate quark models that include the pion and possibly also its chiral partner, the σ-meson. The part of the Hamiltonian that involves pions can be written in the following form:

$$H_\pi = \int d\mathbf{r}\left\{ \tfrac{1}{2}\left[\vec{P}_\pi^2 + (\nabla^2 + m_\pi^2)\vec{\pi}^2\right] + U(\sigma,\vec{\pi}) + \sum_t j_t \pi_t \right\}\ . \tag{51}$$

Here j_t represents the quark pseudoscalar-isovector source term, t is the third component of the isospin, and $U(\sigma,\vec{\pi})$ a possible meson self-interaction term (such as the Mexican hat potential of the linear σ-model). Let $|N\rangle$ and $|\Delta\rangle$ be the ground state and the excited state describing the Δ with $H|N\rangle = E_N|N\rangle$ and $H|\Delta\rangle = E_\Delta|\Delta\rangle$, then we can write the following virial theorems (relations):

$$\langle N|[H,\vec{P}_\pi]|N\rangle = \langle N|H\vec{P}_\pi - \vec{P}_\pi H|N\rangle = 0\ , \tag{52}$$

$$\langle\Delta|[H,\vec{P}_\pi]|\Delta\rangle = 0\ , \tag{53}$$

$$\langle\Delta|[H,\vec{P}_\pi]|N\rangle = (E_\Delta - E_N)\langle\Delta|\vec{P}_\pi|N\rangle = i(E_\Delta - E_N)^2\langle\Delta|\vec{\pi}|N\rangle\ . \tag{54}$$

We have used $\vec{P}_\pi = i[H,\vec{\pi}]$ in the last line. We call (54) the *off-diagonal virial relation (theorem)*. (Note that there is no off-diagonal relation of this type for the σ-field because it is scalar-isoscalar and the matrix elements vanish identically.)

We now evaluate the commutators on the LHS using (51):

$$(-\Delta + m_\pi^2)\langle N|\pi_t(\mathbf{r})|N\rangle = -(-1)^t\langle N|J_{-t}(\mathbf{r})|N\rangle\ , \tag{55}$$

$$(-\Delta + m_\pi^2)\langle\Delta|\pi_t(\mathbf{r})|\Delta\rangle = -(-1)^t\langle\Delta|J_{-t}(\mathbf{r})|\Delta\rangle\ , \tag{56}$$

$$(-\Delta + m_\pi^2 - \omega_*^2)\langle\Delta|\pi_t(\mathbf{r})|N\rangle = -(-1)^t\langle\Delta|J_{-t}(\mathbf{r})|N\rangle\ . \tag{57}$$

We have defined $\omega_* = (E_\Delta - E_N)$ and

$$J_t(\mathbf{r}) = j_t(\mathbf{r}) + (-1)^t \frac{\partial U(\sigma, \vec{\pi})}{\partial \pi_{-t}(\mathbf{r})} \,, \tag{58}$$

and used

$$[\pi_{t'}(\mathbf{r}'), P_{\pi,t}(\mathbf{r})] = i(-1)^t \delta_{t,-t'} \delta(\mathbf{r}' - \mathbf{r}) \,. \tag{59}$$

These relations hold for the exact solutions; in an approximate computational scheme we can use these relations as constraints on the approximate states.

We now show an important property of the axial transition amplitudes which holds for the states that satisfy the above virial relations. Let us split the axial current into two parts:

$$\vec{A}^\alpha = \vec{A}^\alpha_{np} + \vec{A}^\alpha_{pole} \,, \tag{60}$$

$$\vec{A}^\alpha_{np} = \bar{\psi}\gamma^\alpha\gamma_5 \tfrac{1}{2}\vec{\tau}\psi + (\sigma - f_\pi)\partial^\alpha\vec{\pi} - \vec{\pi}\partial^\alpha\sigma \,, \tag{61}$$

$$\vec{A}^\alpha_{pole} = f_\pi\partial^\alpha\vec{\pi} \,. \tag{62}$$

We can now relate the non-pole contribution (61) to the first term in (36) and (obviously) the pole contribution to the second term in (36). Since the off-diagonal virial relation (57) coincides with (41), the evaluation is similar to the derivation presented in the previous section. The pole term (62) contributes only to the longitudinal and the scalar amplitude, hence:

$$C^A_{6(pole)} = -if_\pi \frac{M_N^2}{k} \sqrt{\frac{3}{2}} \langle \Delta^+_{s_\Delta = \frac{1}{2}}|\pi_0(0)|N^+_{s_n = \frac{1}{2}}\rangle \,, \tag{63}$$

$$C^A_{5(pole)} = 0 \,,$$

$$C^A_{4(pole)} = 0 \,.$$

5   Calculation of form-factors between localized states

The amplitudes (5)-(8) are defined between states with good 4-momenta p' and p respectively while in the model calculations localized states are used. We can use such states in our calculation of amplitudes by interpreting them as wave packets of states with good linear momenta:

$$|B(\mathbf{r})\rangle = \int d\mathbf{p}\, \varphi(\mathbf{p})\, e^{i\mathbf{p}\cdot\mathbf{r}}|B(\mathbf{p})\rangle \,. \tag{64}$$

The spin-momentum dependence of $|B(\mathbf{p})\rangle$ is expressed by the bispinor

$$u_B(\mathbf{p}) = \sqrt{\frac{E+M}{2M}} \begin{pmatrix} 1 \\ \frac{\sigma \cdot \mathbf{p}}{E+M} \end{pmatrix} \chi_{spin} \,. \tag{65}$$

Requiring (65) is normalized, $\langle B(\mathbf{p})|B(\mathbf{p})\rangle = 1$, we have

$$\int d\mathbf{r}\langle B(\mathbf{r})|B(\mathbf{r})\rangle = (2\pi)^3 \int d\mathbf{p}\, |\varphi(\mathbf{p})|^2 = 1 \,. \tag{66}$$

We now relate matrix elements between localized states to matrix elements between states with good momenta. We start by a matrix element between localized states:

$$\int d\mathbf{r}\, e^{i\mathbf{k}\cdot\mathbf{r}}\langle\Delta|M(\mathbf{r})|N\rangle = \int d\mathbf{r}\int d\mathbf{p}'\int d\mathbf{p}\, e^{i(\mathbf{k}-\mathbf{p}'+\mathbf{p})\cdot\mathbf{r}}\langle\Delta(\mathbf{p}')|M(\mathbf{r})|N(\mathbf{p})\rangle$$
$$\times\varphi_\Delta^*(\mathbf{p}')\varphi_N(\mathbf{p}). \tag{67}$$

Since the matrix element $\langle\Delta(\mathbf{p}')|M(\mathbf{r})|N(\mathbf{p})\rangle$ does not depend on $\mathbf{r}$ (all $\mathbf{r}$-dependence is contained in the exponential) we can substitute it by its value at $\mathbf{r} = 0$. We then carry out the $\mathbf{r}$ integration yielding $\delta(\mathbf{p}-\mathbf{p}'+\mathbf{k})$, and the above matrix element reads:

$$\int d\mathbf{r}\, e^{i\mathbf{k}\cdot\mathbf{r}}\langle\Delta|M(\mathbf{r})|N\rangle = (2\pi)^3\int d\mathbf{p}\,\langle\Delta(\mathbf{p}+\mathbf{k})|M(0)|N(\mathbf{p})\rangle\,\varphi_\Delta^*(\mathbf{p}+\mathbf{k})\varphi_N(\mathbf{p})\,. \tag{68}$$

From the parameterization of the axial current (9) we can read off the p' and p dependence and plug it into (68). We neglect terms of the order p^2/M^2, e.g. the last term in the expression (11) for $e_\lambda^\mu(p)$. We find:

$$\bar{u}_\alpha(p', s_\Delta = \tfrac{1}{2})q^\alpha u_N(s = \tfrac{1}{2}) = \left[\frac{M_\Delta - M_N}{M_\Delta}p'_3 - k\right]\sqrt{\frac{2}{3}} \tag{69}$$

and

$$\bar{u}_0(p', s_\Delta = \tfrac{1}{2})u_N(s = \tfrac{1}{2}) = \frac{p'_3}{M_\Delta}\sqrt{\frac{2}{3}}\,. \tag{70}$$

We can carry out the integration over $\mathbf{p}$ since $C_i(q^2)$ do not depend on $\mathbf{p}$. We assume $\varphi_\Delta(\mathbf{p}) \approx \varphi_N(\mathbf{p}) \equiv \Pi_{i=1}^3\varphi(p_i)$. A typical integral gives:

$$(2\pi)^3\int d\mathbf{p}\, p_3\,\varphi(\mathbf{p}+\mathbf{k})\varphi(\mathbf{p}) = 2\pi\int dp_3\, p_3\varphi(p_3+k)\varphi(p_3)$$

$$= 2\pi\int dq\,(q-\tfrac{1}{2}k)\,\varphi(q+\tfrac{1}{2}k)\varphi(q-\tfrac{1}{2}k)$$

$$= -\tfrac{1}{2}k\left[1 - \tfrac{1}{2}k^2\int dq\,\varphi'(q)^2 + \dots\right]$$

$$\approx -\tfrac{1}{2}k\left[1 - \tfrac{1}{2}k^2\langle z_{\text{c.m.}}^2\rangle\right]\,, \tag{71}$$

where we have taken into account that φ are normalized and used the relation ($\tilde{\varphi}(z)$ is the Fourier transform of $\varphi(q)$):

$$\int dq\,\varphi'(q)^2 = \int dz\, z^2\tilde{\varphi}(z)^2 = \langle z^2\rangle\,. \tag{72}$$

(Integrating p'_3 we would get $\tfrac{1}{2}k$.) Here $\langle z_{\text{c.m.}}^2\rangle = \tfrac{1}{3}\langle r_{\text{c.m.}}^2\rangle$ is a typical spread of the wave packet describing the center-of-mass motion of the localized state and is of the order of the inverse baryon mass. Clearly, in this approximation it is not meaningful to calculate the form-factor to very high k. We finally obtain

(neglecting terms of the order k^2/M^2):

$$\tilde{S}^A = -\left[k\,\frac{M_\Delta}{M_N^2}\,C_4^A + \frac{k}{2M_\Delta}\,C_5^A - \frac{\omega k}{M_N^2}\,\frac{M_\Delta + M_N}{2M_\Delta}\,C_6^A\right]\sqrt{\frac{2}{3}}\,, \tag{73}$$

$$\tilde{A}_{\frac{3}{2}}^A = = -\left[\omega\,\frac{M_\Delta}{M_N^2}\,C_4^A + C_5^A\right] = \sqrt{3}\,\tilde{A}_{\frac{1}{2}}^A\,, \tag{74}$$

$$\tilde{L}^A = = -\left[\omega\,\frac{M_\Delta}{M_N^2}\,C_4^A + C_5^A - \frac{k^2}{M_N^2}\,\frac{M_\Delta + M_N}{2M_\Delta}\,C_6^A\right]\sqrt{\frac{2}{3}}\,. \tag{75}$$

We now express the experimental amplitudes in terms of the helicity amplitudes as

$$C_6^A = \frac{M_N^2}{k^2}\left[-\tilde{A}_{\frac{3}{2}}^A + \sqrt{\frac{3}{2}}\tilde{L}^A\right]\frac{2M_\Delta}{M_\Delta + M_N}\,, \tag{76}$$

$$C_5^A = -\sqrt{\frac{3}{2}}\left(\tilde{L}^A - \frac{k_0}{k}\,\tilde{S}^A\right)\frac{2M_\Delta}{M_\Delta + M_N} - \frac{k_0^2 - k^2}{M_N^2}\,C_6^A\,, \tag{77}$$

$$C_4^A = \frac{M_N^2}{kM_\Delta}\left[-\sqrt{\frac{3}{2}}\,\tilde{S}^A + \frac{k_0 k}{M_N^2}\,\frac{M_\Delta + M_N}{2M_\Delta}\,C_6^A\right] - \frac{M_N^2}{2M_\Delta^2}\,C_5^A\,. \tag{78}$$

The strong form-factor can be treated in the same way. The general coupling of the pion field to the baryon is written in the form

$$H_{B-\pi} = \int d\mathbf{r}\, J_a^\pi(\mathbf{r})\pi_a(\mathbf{r})\,, \tag{79}$$

where $J_a^\pi(\mathbf{r})$ is the baryon strong pseudoscalar- isovector current. The N-Δ transition matrix element is parameterized as

$$\langle \Delta^+(p')|J_a^\pi(0)|N^+(p)\rangle = -i\bar{u}_{\Delta\mu}\,\frac{G_{\pi N\Delta}(q^2)}{2M_N}\,q^\mu u_N\,, \tag{80}$$

where $q = p' - p$. Using (69) we find

$$\langle \Delta^+(p')|J_a^\pi(0)|N^+(p)\rangle = -i\frac{G_{\pi N\Delta}(q^2)}{2M_N}\left[\frac{M_\Delta - M_N}{M_\Delta}p'_3 - k\right]C_{10\frac{1}{2}\frac{1}{2}}^{\frac{3}{2}\frac{1}{2}}\,. \tag{81}$$

We now use of relation (68) as well as (71) to obtain

$$\frac{G_{\pi N\Delta}(q^2)}{2M_N}\,\frac{M_\Delta + M_N}{2M_\Delta} = \frac{1}{ik}\langle \Delta\|\int d\mathbf{r}e^{i\mathbf{k}\cdot\mathbf{r}}J(\mathbf{r})\|N\rangle\,. \tag{82}$$

6 Helicity amplitudes in the Cloudy Bag Model

The Cloudy Bag Model (CBM) is the simplest example of a quark model with the pion cloud that fulfills the virial constraints (52)-(54) provided we take the usual perturbative form for the pion profiles [8,9]. We also take the N-Δ splitting equal to the experimental value, $\omega \equiv M_\Delta - E_N$. Since the pion contribution to the axial

current has the form of the pole term in (62), only the quarks contribute to the C_5^A and C_4^A amplitudes.

The helicity amplitudes and the Adler form-factors simplify further if we make the usual assumption of the same quark profiles for the nucleon and the Δ. In this case the scalar amplitude picks up only the pion contribution while the quark term is identically zero. The transverse amplitude $\tilde{A}_{\frac{3}{2}}^A = \sqrt{3}\,\tilde{A}_{\frac{1}{2}}^A$ has only the quark contribution while the longitudinal amplitude has both:

$$\tilde{A}_{\frac{3}{2}}^A(Q^2) = -\frac{1}{\sqrt{6}} \int dr\, r^2 \left[j_0(kr)\left(u^2 - \frac{1}{3}v^2\right) + \frac{2}{3}\,j_2(kr)v^2 \right] \langle\Delta\|\sum\sigma\tau\|N\rangle, \tag{83}$$

$$\tilde{L}^A(Q^2) = -\frac{2}{3}\left\{ \frac{1}{2}\int dr\, r^2 \left[j_0(kr)\left(u^2 - \frac{1}{3}v^2\right) - \frac{4}{3}\,j_2(kr)v^2 \right] \right.$$
$$\left. -\frac{\omega_{MIT}}{\omega_{MIT}-1}\frac{m_\pi}{2f_\pi}\frac{j_1(kR)}{kR}\frac{k^2}{(Q^2+m_\pi^2)} \right\} \langle\Delta\|\sum\sigma\tau\|N\rangle, \tag{84}$$

$$\tilde{S}^A(Q^2) = \frac{2}{3}\frac{\omega_{MIT}}{\omega_{MIT}-1}\frac{m_\pi}{2f_\pi}\frac{j_1(kR)}{kR}\frac{\omega k}{(Q^2+m_\pi^2)} \langle\Delta\|\sum\sigma\tau\|N\rangle. \tag{85}$$

Here k and $Q^2 \equiv -q^2$ are related through (4), $\omega_{MIT} = 2.04$, and

$$\langle\Delta\|\sum\sigma\tau\|N\rangle = \sqrt{Z_N Z_\Delta}\left\{ 2\sqrt{2} \right.$$
$$+\frac{\sqrt{2}}{27\pi}\mathcal{P}\int_0^\infty dk\, k^2\,\rho^2(k)\left[\frac{25}{\omega_k^2(\omega_k-\omega)} + \frac{2}{\omega_k(\omega_k^2-\omega^2)} \right]$$
$$\left. +\frac{25\sqrt{2}}{27\pi}\int_0^\infty dk\, k^2\,\rho^2(k)\left[\frac{5}{4\omega_k^3} + \frac{1}{\omega_k^2(\omega_k+\omega)} \right]\right\}, \tag{86}$$

where

$$\rho(k) = \frac{\omega_{MIT}}{\omega_{MIT}-1}\frac{j_1(kR)}{\sqrt{2\pi}\,f_\pi R^3}. \tag{87}$$

and Z_N and Z_Δ are the usual wave-function-renormalization constants [8].

The strong transition form-factor $G_{\pi N\Delta}(Q^2)$ is:

$$\frac{G_{\pi N\Delta}(Q^2)}{2M_N} = \frac{\omega_{MIT}}{\omega_{MIT}-1}\frac{1}{2f_\pi}\frac{j_1(kR)}{kR} \langle\Delta\|\sum\sigma\tau\|N\rangle\frac{2M_\Delta}{M_\Delta+M_N}. \tag{88}$$

Similarly as in (47) we can now explicitly show that PCAC is fulfilled provided the off-diagonal GT relation holds in the model. Since the Lagrangian is invariant under the chiral transformation both relation should hold for the exact solution, but this is of course not obvious for the approximate solution. In the model it is straightforward to evaluate the pertinent quantities at $Q^2 = -m_\pi^2$. We prefer to give here the expressions at $Q^2 = 0$ which take much simpler forms, e.g.:

$$C_5^A(0) = \frac{1}{\sqrt{6}} \int dr\, r^2 \left[j_0(kr)\left(u^2 - \frac{1}{3}v^2\right) - \frac{4}{3}\,j_2(kr)v^2 \right] \langle\Delta\|\sum\sigma\tau\|N\rangle\frac{2M_\Delta}{M_\Delta+M_N}, \tag{89}$$

with $k = K_0$ (see (3)).

The constant (89) can be easily evaluated for the degenerate N and Δ and neglecting pion corrections to $\langle\Delta\|\sum\sigma\tau\|N\rangle$:

$$C_5^A(0) = \frac{1}{\sqrt{6}}\,\frac{3g_A^\circ}{5}\,2\sqrt{2} = 0.755\ , \tag{90}$$

where $g_A^\circ = 1.09$ is the value of the nucleon g_A in the MIT bag model. Clearly, (90) strongly underestimates the experimental value (40). In the same limit, the strong coupling is

$$g_{\pi N\Delta} \equiv G_{\pi N\Delta}(0)\,\frac{m_\pi}{2M_N} = \sqrt{\frac{72}{25}}\,g_{\pi NN}^\circ = 1.39\ . \tag{91}$$

Here $g_{\pi NN}^\circ = 0.82$ is the CBM value without pion correction. Again, (91) strongly underestimates the experimental value of 2.2, though the off-diagonal Goldberger-Treiman relation is exactly fulfilled in this approximation.

In [3] we show that the pion corrections improve the results in particular the ratio of the strong $g_{\pi N\Delta}$ and $g_{\pi NN}$ coupling constants but the value of $C_5(0)$ remains far below the experimental value. A possible solution, described and discussed in [3–5] is to include the contribution of the σ-meson which enters the expression for the axial current (61) and considerably increases the value of C_5^A.

References

1. Jùn Líu, N. C. Mukhopadhyay, and L. Zhang, Phys. Rev. C **52** (1995) 1630
2. T. R. Hemmert, B. R. Holstein, and N. C. Mukhopadhyay, Phys. Rev. D **51** (1995) 158
3. B. Golli, S. Širca, L. Amoreira, and M. Fiolhais, hep-ph/0210014
4. S. Širca, L. Amoreira, M. Fiolhais, B. Golli, to appear in R. Krivec, B. Golli, M. Rosina, S. Širca (eds.), *Proceedings of the XVIII European Conference on Few-Body Problems in Physics*, 7–14 September 2002, Bled, Slovenia; hep-ph/0211290
5. S. Širca, L. Amoreira, M. Fiolhais, and B. Golli, these Proceedings; hep-ph/0211292
6. C. H. Llewellyn Smith, Phys. Rep. **3C** (1972) 261
7. T. Ericson and W. Weise, Pions and Nuclei, Clarendon Press, Oxford 1988
8. A. W. Thomas, Adv. Nucl. Phys. **13** (1984) 1
9. L. Amoreira et al., Int. J. Mod. Phys. **14** (1999) 731

The Spin-Spin splitting of Bottomium – an Estimate based on leptonic decays of vector mesons [*]

D. Janc[a] and M. Rosina[a,b]

[b] J. Stefan Institute, 1000 Ljubljana, Slovenia
[a] Faculty of Mathematics and Physics, University of Ljubljana, 1000 Ljubljana, Slovenia

Abstract. The mass of η_b is estimated to be about 120 MeV below the mass of Υ, similarly as in the case of charmonium. The estimate is based on the experimental fact that the widths $\Gamma_{e^+e^-}$ for Υ and J/ψ are equal (apart from the factor 4 due to quark charges), and the hypothesis that both the spin-spin splitting and $\Gamma_{e^+e^-}$ of vector mesons are proportional to the density at the origin divided by quark mass squared.

1 Introduction

The comparison of the spin-spin splitting in charmonium and bottomium represents a valuable test of our understanding of the effective quark-quark interaction. Since the $b\bar{b}$ ground state, the η_b meson, has not yet been reliably observed, the interest in this state gives a strong motivation to experimentalists. Moreover, since theoretical predictions of the spin-spin splitting $\Delta m = m(\Upsilon) - m(\eta_b)$ vary strongly, this is also a challenge to theorists. (The estimates from perturbative QCD, from potential models and from lattice-inspired potential models lie in the range between 30 and 140 MeV.)

Recently, one candidate for η_b has been reported [1], with its mass $160 \pm 20 \pm 20 \text{GeV}/c^2$ below Υ. Though still inconclusive, such a large difference encourages further studies whether quark models or lattice calculations allow a high value for Δm.

We present a theoretical estimate which is based on general properties of the constituent quark models and depends only weakly on the details of the models.

2 Zero order approximation

2.1 Leptonic decay

The estimate for the mass of η_b is based on the remarkable fact that the partial width $\Gamma_{e^+e^-}(\Upsilon) = 1.32$ keV and $\Gamma_{e^+e^-}(J/\psi) = 5.26$ keV are equal (apart from the factor 4 due to quark charges). Assuming point-like quarks the leptonic decay of vector mesons can be represented by the graph in Fig. 1. The $Q\bar{Q}\gamma$ vertex can be

---

[*] Talk delivered by D. Janc.

expressed as $z_Q e \sqrt{\rho(0)}$ where $z_Q e$ is the quark charge. Then the partial width is described by van Royen - Weisskopf formula:

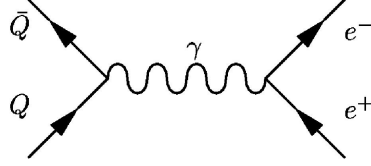$$\Gamma^0_{e^+e^-} = z_Q^2\, \rho(0)\, \frac{16\pi\alpha^2}{m^2}. \tag{1}$$

Fig. 1. The leptonic decay of vector mesons

Since the experimental values of $\Gamma_{e^+e^-}/z_Q^2$ are equal for Υ and J/ψ this fixes the ratio of the densities at the origin: $\rho(0)$ are proportional to m^2 where m is the vector meson mass. We conclude that (up to the assumed order of approximation) $\rho_\Upsilon(0)/m_\Upsilon^2 = \rho_{J/\psi}(0)/m_{J/\psi}^2$.

2.2 Spin-spin splitting

In the nonrelativistic constituent quark model the spin-spin potential between heavy quarks is assumed to be the result of one gluon exchange between quarks which gives

$$\Delta H_{oge} = \frac{4}{3}\frac{2\pi\alpha_s}{3m_Q^2}\delta(\mathbf{r})\sigma_1 \cdot \sigma_2$$

For very heavy quarks the spin dependent part of this interaction can be treated perturbatively and it yields the spin splitting between vector and pseudoscalar meson Δm proportional to $\rho(0)/m_Q^2$. If the quark mass is $m_Q = \frac{1}{2}\,m$, Δm is proportional to $\Gamma_{e^+e^-}/z_Q^2$. Since the latter is equal for bottomium and charmonium, it follows $\Delta m(\Upsilon) = \Delta m(J)/\psi = 117$ MeV. This prediction is within the error of the experimental candidate [1], but we have to wait for new experiments.

3 Corrections

It is well known, that there are large corrections to the van Royen - Weisskopf formula. Apart from first order correction in α_s, there are two additional corrections due to approximations which are implied in Eq (1). First approximation is, that we consider quarks to be point-like and the second is, that we neglect momentum of quarks inside the meson. We can write the partial width as

$$\Gamma_{e^+e^-} = R\Gamma^0_{e^+e^-}$$

where the factor R is 1, if we ignore this correction, or it is $R = (1 - 16\alpha_s/3\pi)$ if we consider just first order corrections. The current values for α_s at charmonium and

bottomium relevant energies are $\alpha_s(3.1\text{GeV})= 0.249 \pm 0.010$ and $\alpha_s(9.46\text{GeV})= 0.178 \pm 0.005$, so neglecting other corrections, we have R = 0.57 and R = 0.70 respectively. It was shown [2] that the refinement due to momentum of quarks inside the meson is also of the same order, and is larger in charmonium as in bottomium. This correction depends on the potential model in which one calculate the meson wave function. If one considers only the first order corrections in α_s and refinements due to quarks momentum, one obtains for both charmonium and bottomium an overall correction to the original van Royen - Weisskopf formula R = 0.85 ± 0.05. Since the factor R is almost the same in bottomium as in charmonium, we can again assume that the densities at the origin are still proportional to m^2.

4   Test – the η_c(2S) meson

We now test the assumptions of our estimation by looking into the charmonium sector, where we estimate the spin splitting between the 2S states η_c (2S) and ψ (2S). There are two very different experimental results about the mass of η_c (2S) state. The old results from 1982 is 3594 ± 5 MeV [4] while the Belle Collaboration reported the observation of η_c(2S) in exclusive $B \to KK_sK^-\pi^+$ decay [3] with the mass 3654 ± 6 MeV. We can estimate the spin splitting from the leptonic decay width of ψ (2S) which is known to a large accuracy $\Gamma_{e^+e^-}(\psi(2S)) = 2.19\pm 0.15$ keV:

$$m_{\psi(2s)} - m_{\eta_c(2S)} = \frac{\Gamma_{e^+e^-}(\psi(2S))}{\Gamma_{e^+e^-}(J/\psi)} \cdot \frac{m_{\psi(2S)}^2}{m_{J/\psi}^2} \cdot \left(m_{J/\psi} - m_{\eta_c}\right) =$$

$$(0.42 \pm 0.06) \cdot 1.41 \cdot 117\text{MeV} = 69\text{MeV} \pm 10\text{MeV}.$$

meson	m[MeV]	$\frac{\Gamma_{e^+e^-}^{exp}}{(3z_q)^2}$ [keV]	$\Delta m_{exp.}$[MeV]	$\Delta m_{predict.}$[Mev]
η_c(1S)	2979.7		117	117 (input)
J/ψ	3096.9	1.32 ± 0.09		
η_c(2S)	$\begin{cases} 3654 \pm 6 \text{ [3]} \\ 3594 \pm 5 \text{ [4]} \end{cases}$		32 ± 6 92 ± 5	69 ± 10
ψ(2S)	3686	0.55 ± 0.04		
η_b(1S)	9300 ± 40		160 ± 40	117
Υ	9460	1.32 ± 0.07		

Table 1. Second column: masses of the heavy mesons from [3] and [4]. Third column: leptonic decay width of vector meson. Fourth column: experimental data for spin-spin splitting. Last column: our prediction on spin-spin splitting.

Since the evaluation of the η_c(2S) mass in [3] is still in progress, we have to wait with our conclusions about our scheme.

References

1. The ALEPH Collaboration: CERN-EP/2002-009 (2002)
2. F. Bissey, J.-J. Dugne and J.-F. Mathiof, Eur. Phys. J **C24** (2002) 101
3. S.-K. Choi et al., (Belle Collaboration), Phys. Rev. Lett. **89** (2002) 102001; Erratum, Phys. Rev. Lett. **89** (2002) 12901
4. C. Edwards et al., Phys. Rev. Lett. **48** (1982) 70

Production and detection of bbūd̄ tetraquarks at LHC? ⋆

M. Rosina[a,b], D. Janc[b], D. Treleani[c], and A. Del Fabbro[c]

[a] Faculty of Mathematics and Physics, University of Ljubljana, Jadranska 19, P.O. Box 2964, 1001 Ljubljana, Slovenia
[b] J. Stefan Institute, 1000 Ljubljana, Slovenia
[c] Dipartimento di Fisica Teorica, Università di Trieste, Strada Costiera 11, Miramare-Grignano, and INFN, Sezione di Trieste, I-34014 Trieste, Italy

Abstract. The bound state of two B mesons (the "tetraquark" bbūd̄) has been shown to be bound by 100 MeV. Therefore it is stable against strong and electromagnetic decay and can decay only weakly. It represents a very interesting four-body problem to test our ideas about the effective quark-quark interactions and about the formation of the bb diquark (which later gets dressed by two light antiquarks into the tetraquark). It represents also a challenge to experimentalists. We shall discuss possible models of its formation, possible characteristic decays and the possibility of detecting it in LHC.

1 Introduction

Different versions of the nonrelativistic constituent quark model agree that the only long-living tetraquark should be bbūd̄ with the I=0, J=1 quantum numbers [1–3]. The predictions of its energy are about 100 MeV below the threshold of BB* and about 60 MeV below the threshold of $B^0 B^-$ (into which it cannot decay anyway due to its quantum numbers). Therefore it can decay only weakly with a lifetime of picoseconds which corresponds to a width of meV. It would be very rewarding to confirm these predictions experimentally.

The estimates of the production and detection rate of the bbūd̄ tetraquark in the present machines are very pessimistic and have for this reason not been published. Therefore we consider the possibility of the production and detection of such a heavy dimeson (tetraquark) in LHC . For production we assume a three-step model.

(i) First, two b-quarks are formed in the process pp $\rightarrow$ bb̄bb̄ by a double parton interaction fusion (g + g $\rightarrow$ b + b̄, (twice)) which is the leading production mechanism [4]. One might wonder why we need a TeV machine to produce GeV particles. The answer is simple. The two colliding protons can be considered as two packages of virtual gluons whose number is huge for low Bjorken-x. Only the number of gluons with x ∼ 0.001 turns out to be sufficient to make tetraquarks

---

⋆ Talk delivered by M. Rosina

detectable.

(ii) In the second step, the two b-quarks join into a diquark.

(iii) In the third step, the diquark gets dressed either with one light quark into the doubly-heavy baryon bbu, bbd or bbs, or with two light antiquarks to become a tetraquark. We shall show that the rates are comparable and that the comparison of the branching ratios may test our understanding of the process.

For the decay we consider two competitive processes, the independent decay of the two B-mesons (for example $B \to D +$ anything), and the direct formation of Υ with its characteristic energy and decay modes. While the former decay is difficult to distinguish from the decay of two completely independent b-quarks, the latter would require some kind of $b \to \bar{b}$ oscillation which is not easily feasible for bound B mesons.

2   Production

2.1   Double $b\bar{b}$ production

The multiple bottom production in a double parton collision was first studied as a possible contamination of the signal for the Higgs boson [4]. Such a double b production is, however, also a promising source of doubly heavy baryons and tetraquarks.

The forward detector LHCb will cover the pseudorapidity region $1.8 < \eta < 4.9$ and will detect the B and $\bar{B}$ hadrons in the low p_T region. By requiring that the two b are produced with $|p_1(j) - p_2(j)| < \Delta$, $j = x, y, z$, we get the cross section $\sigma \approx 0.4(\Delta/\text{GeV})^3$ nb. The cross section is approximately proportional to the momentum volume up to 2 GeV: $d\sigma/d^3p \approx 0.4\text{nb}/\text{GeV}^3$.

We are interested in double-b production in which the two b-quarks are close enough in phase space to synthesize a diquark. In our rough estimate we use wave functions approximated by Gaussians and denote the oscillator parameter of nucleon by B and of diquark by β. The quark model calculation of the diquark gives an effective momentum of each quark 1.04 GeV which correspond to a momentum range $\Delta^3 \approx 10 \,\text{GeV}^3$ (see next subsection) and therefore to a cross section of 4 nb. At the expected luminosity L=0.1 events/(second nb) this corresponds to 1440 interesting bb pairs per hour.

2.2   Formation of the diquark

We assume simultaneous production of two independent b-quarks with momenta $\mathbf{p}_1, \mathbf{p}_2$, modulated with a Gaussian profile of the nucleon size $B = \sqrt{2/3}\sqrt{<r^2>} = 0.69$ fm:

$$\mathcal{N}_B \exp(-\mathbf{r}_1^2/2B^2 + i\mathbf{p}_1\mathbf{r}_1)\mathcal{N}_B \exp(-\mathbf{r}_2^2/2B^2 + i\mathbf{p}_2\mathbf{r}_2)$$
$$\equiv \mathcal{N}_{B/\sqrt{2}} \exp(-\mathbf{R}^2/2(B/\sqrt{2})^2 + i\mathbf{PR})\mathcal{N}_{B\sqrt{2}} \exp(-\mathbf{r}^2/2(B\sqrt{2})^2 + i\mathbf{pr})$$

where the normalization factor $\mathcal{N}_\beta = \pi^{-3/4}\beta^{-3/2}$.

Furthermore, we make an impulse approximation that such a two quarks sate is instantaneously transformed in any of the eigenstates of the two-quark Hamiltonian. Then the probability of the formation of the lowest energy diquark is equal to the square of the overlap $\mathcal{M}$ between the two free quarks and the diquark (with the same centre-of-mass motion). If we approximate the diquark wavefunction with a Gaussian with the oscillator parameter $\beta = 0.23$ fm, we get the overlap

$$
\begin{aligned}
\mathcal{M} &= \int \mathrm{d}^3 r \, \mathcal{N}_{B\sqrt{2}} \exp(-\mathbf{r}^2/2(B\sqrt{2})^2 - i\mathbf{p}\mathbf{r})\mathcal{N}_\beta \exp(-\mathbf{r}^2/2\beta^2) \\
&= \sqrt{\frac{2\sqrt{2}B\beta}{2B^2 + \beta^2}}^3 \exp\left[-(k^2/2)(2B^2\beta^2/(2B^2 + \beta^2))\right]
\end{aligned}
$$

and the production cross section

$$
\begin{aligned}
\sigma &= \int \mathrm{d}^3 p \, \frac{\mathrm{d}\sigma}{\mathrm{d}^3 p} \mathcal{M}^2(k) = \frac{\mathrm{d}\sigma}{\mathrm{d}^3 p} \left(\frac{4\pi\hbar^2}{2B^2 + \beta^2}\right)^{3/2} \\
&\approx \frac{\mathrm{d}\sigma}{\mathrm{d}^3 p} \left(\frac{\sqrt{2\pi}\hbar}{B}\right)^3 = 0.15 \text{nb}.
\end{aligned}
$$

This expression can be interpreted as

$$
\sigma = \frac{\mathrm{d}\sigma}{\mathrm{d}^3 p} \times \Delta^3 \times f_{vol}
$$

where $\Delta^3 = (\sqrt{2\pi}/\beta)^3 \approx 10\,\mathrm{GeV}^3$ is the effective momentum range of the diquark and $f_{vol} = (\beta/B)^3 = (0.23\,\mathrm{fm}/0.69\,\mathrm{fm})^3 = 0.04$ is the volume ratio between the diquark and nucleon. This cross section corresponds to 54 dibaryons/hour.

2.3   Dressing of the diquark into tetraquark

Since the diquark will soon get dressed by two antiquarks or more probably by a single u, d or s quark, we guess a probability f_{dress} to synthesize our tetraquark smaller than 1/4, possibly $f_{dress} \sim 0.1$. This yields a production rate $L\sigma f_{vol}f_{dress} \sim 5 - 6$ events/hour.

The estimate $f_{dress} \sim 0.1$ is supported by the comparison with the dressing of a single quark in the Fermilab experiment [5]:

$$
b \to B^-, B^0, B_s, \Lambda_b = 0.375 \pm 0.015, 0.375 \pm 0.015, 0.160 \pm 0.025, 0.090 \pm 0.028.
$$

Since a heavy diquark acts similarly as a heavy quark, we expect similar branching ratios:

$$
bb \to bbd, bbu, bbs, bb\bar{d}\bar{u} \approx 0.37, 0.37, 0.16, 0.09.
$$

3   Decay and detection

The independent decay of the two B-mesons (for example B $\rightarrow$ D + anything) is difficult to distinguish from the decay of two unbound b-quarks and is therefore not characteristic. Anyway, there are no good two-body decay channels of B mesons to allow the reconstruction of the total energy of the tetraquark; moreover, each separate exclusive decay channel has a low branching ratio of up to a few percent.

We are looking for more characteristic decay channels of the tetraquark – the direct formation of Υ with its characteristic energy and decay mode. This would be a simple two-body channel $\Upsilon + \pi$ with c.m. energy of the tetraquark which means a kinetic energy 876 MeV for both mesons (in the c.m. system). Of course there would be a crowd of other Υ mesons, but few at this energy. The inspiration comes from the $B^0 \rightarrow \bar{B}^0$ oscillation which unfortunately is not feasible for bound B mesons because the BB and B$\bar{B}$ states are not degenerate. The weak transition $b\bar{u} \rightarrow u\bar{b}$ is negligible because of the low CKM amplitudes. New ideas are needed!

The reader may wonder why are we so keen about the $bb\bar{u}\bar{d}$ tetraquark rather than the $cc\bar{u}\bar{d}$ tetraquark which would be easier to produce and detect. The answer is that in all reasonable models so far the cc-tetraquark is unbound. However, a recent measurement at SELEX in Fermilab [6] hints at three ccu (ccd) candidates with masses at 3519 , 3783 (and 3460) MeV. The 3519 MeV ground state can be accomodated into present quark models and does not change the conclusion that the cc-tetraquark is unbound. If the 3460 MeV state is confirmed, it would require a major revision of our quark model calculations (3-body forces ?) and by further stretching parameters T_{cc} might even be bound [7]. But we do not believe it since the 60 MeV isospin splitting is not believable and we rather wait for futher experiments.

References

1. D. Janc and M. Rosina, Few-Body Systems **31**, 1 (2001)
2. B. Silvestre-Brac and C. Semay, Z. Phys. **C57**, 273 (1993)
3. D. M. Brink and Fl. Stancu, Phys. Rev. **D57**, 6778 (1998)
4. A. Del Fabbro and D. Treleani, Phys. Rev. **D61**, 077502 (2000) Phys. Rev. **D63**, 057901 (2001) Nucl. Phys. B **92**, 130 (2001)
5. T. Affolder et al. (CDF Collaboration), Phys. Rev. Lett. **84**, 1663 (2000)
6. M. Mattson et al. (SELEX Collaboration), Phys. Rev. Lett. **89**, 112001 (2002); J. S. Russ (on behalf of the SELEX Collaboration), hep-ex/0209075
7. B. A. Gelman and S. Nussinov, hep-ph/0209095

Axial currents in electro-weak pion production at threshold and in the Δ-region [⋆]

S. Širca[a,b], L. Amoreira[c,d], M. Fiolhais[d,e], and B. Golli[f,b]

[a] Faculty of Mathematics and Physics, University of Ljubljana, 1000 Ljubljana, Slovenia
[b] Jožef Stefan Institute, 1000 Ljubljana, Slovenia
[c] Department of Physics, University of Beira Interior, 6201-001 Covilhã, Portugal
[d] Centre for Computational Physics, University of Coimbra, 3004-516 Coimbra, Portugal
[e] Department of Physics, University of Coimbra, 3004-516 Coimbra, Portugal
[f] Faculty of Education, University of Ljubljana, 1000 Ljubljana, Slovenia

Abstract. We discuss electro-magnetic and weak production of pions on nucleons and show how results of experiments and their interpretation in terms of chiral quark models with explicit meson degrees of freedom combine to reveal the ground-state axial form factors and axial N-Δ transition amplitudes.

1 Introduction

The study of electro-weak N-Δ transition amplitudes, together with an understanding of the corresponding pion electro-production process at low energies, provides information on the structure of the nucleon and its first excited state. For example, the electro-magnetic transition amplitudes for the processes $\gamma^\star p \to \Delta^+ \to p\pi^0$ and $\gamma^\star p \to \Delta^+ \to n\pi^+$ are sensitive to the deviation of the nucleon shape from spherical symmetry [1]. Below the Δ resonance (and in particular close to the pion-production threshold), the reaction $\gamma^\star p \to n\pi^+$ also yields information on the nucleon axial and induced pseudo-scalar form-factors. While the electro-production of pions at relatively high [2] and low [3,4] momentum transfers has been intensively investigated experimentally in the past years at modern electron accelerator facilities, very little data exist on the corresponding weak axial processes.

2 Nucleon axial form-factor

In a phenomenological approach, the nucleon axial form-factor is one of the quantities needed to extract the weak axial amplitudes in the Δ region. There are basically two methods to determine this form-factor. One set of experimental data comes from measurements of quasi-elastic (anti)neutrino scattering on protons, deuterons, heavier nuclei, and composite targets (see [4] for a comprehensive list

---

[⋆] Talk delivered by S. Širca.

of references). In the quasi-elastic picture of (anti)neutrino-nucleus scattering, the $\nu N \to \mu N$ weak transition amplitude can be expressed in terms of the nucleon electro-magnetic form-factors and the axial form factor G_A. The axial form-factor is extracted by fitting the Q^2-dependence of the (anti)neutrino-nucleon cross section,

$$\frac{d\sigma}{dQ^2} = A(Q^2) \mp B(Q^2)\,(s-u) + C(Q^2)\,(s-u)^2\,, \qquad (1)$$

in which $G_A(Q^2)$ is contained in the $A(Q^2)$, $B(Q^2)$, and $C(Q^2)$ coefficients and is assumed to be the only unknown quantity. It can be parameterised in terms of an 'axial mass' M_A as

$$G_A(Q^2) = G_A(0)/(1 + Q^2/M_A^2)^2\,.$$

Another body of data comes from charged pion electro-production on protons (see [4] and references therein) slightly above the pion production threshold. As opposed to neutrino scattering, which is described by the Cabibbo-mixed $V - A$ theory, the extraction of the axial form factor from electro-production requires a more involved theoretical picture [5,6]. The presently available most precise determination for M_A from pion electro-production is

$$M_A = (1.077 \pm 0.039)\,\text{GeV} \qquad (2)$$

which is $\Delta M_A = (0.051 \pm 0.044)\,\text{GeV}$ larger than the axial mass $M_A = (1.026 \pm 0.021)\,\text{GeV}$ known from neutrino scattering experiments. The weighted world-average estimate from electro-production data is $M_A = (1.069 \pm 0.016)\,\text{GeV}$, with an excess of $\Delta M_A = (0.043 \pm 0.026)\,\text{GeV}$ with respect to the weak probe. The $\sim 5\,\%$ difference in M_A can apparently be attributed to pion-loop corrections to the electro-production process [5].

3   N-Δ weak axial amplitudes

The experiments using neutrino scattering on deuterium or hydrogen in the Δ region have been performed at Argonne, CERN, and Brookhaven [7–11]. (Additional experimental results exist in the quasi-elastic regime, from which M_A has been extracted.) For pure Δ production, the matrix element has the familiar form

$$M = \langle \mu\Delta | \nu N \rangle = \frac{G_F \cos\theta_C}{\sqrt{2}}\, j_\alpha \langle \Delta | V^\alpha - A^\alpha | N \rangle\,,$$

where G_F is the Fermi's coupling constant, θ_C is the V_{ud} element of the CKM matrix, $j_\alpha = \overline{u}_\mu \gamma_\alpha (1 - \gamma_5) u_\nu$ is the matrix element of the leptonic current, and the matrix element of the hadronic current J^α has been split into its vector and axial parts. Typically either the Δ^{++} or the Δ^+ are excited in the process. The hadronic part for the latter can be expanded in terms of weak vector and axial form-factors [12]

$$M = \frac{G}{\sqrt{2}} \overline{u}_{\Delta\alpha}(p') \left\{ \left[\frac{C_3^V}{M}\gamma_\mu + \frac{C_4^V}{M^2}p'_\mu + \frac{C_5^V}{M^2}p_\mu \right] \gamma_5 F^{\mu\alpha} + C_6^V j_\alpha \gamma_5 \right.$$
$$\left. + \left[\frac{C_3^A}{M}\gamma_\mu + \frac{C_4^A}{M^2}p'_\mu \right] F^{\mu\alpha} + C_5^A j^\alpha + \frac{C_6^A}{M^2} q^\alpha q^\mu j_\mu \right\} u(p) f(W)\,,$$

where $F^{\mu\alpha} = q^\mu j^\alpha - q^\alpha j^\mu$, $\overline{u}_{\Delta\alpha}(p')$ is the Rarita-Schwinger spinor describing the Δ state with four-vector p', and $u(p)$ is the Dirac spinor for the (target) nucleon of mass M with four-vector p. (In the case of the Δ^{++} excitation, the expression on the RHS acquires an additional isospin factor of $\sqrt{3}$ since $\langle \Delta^{++} | J^\alpha | p \rangle = \sqrt{3} \langle \Delta^+ | J^\alpha | p \rangle = \sqrt{3} \langle \Delta^0 | J^\alpha | p \rangle$.) The function $f(W)$ represents a Breit-Wigner dependence on the invariant mass W of the $N\pi$ system.

The matrix element is assumed to be invariant under time reversal, hence all form-factors $C_i^{V,A}(Q^2)$ are real. Usually the conserved vector current hypothesis (CVC) is also assumed to hold. The CVC connects the matrix elements of the strangeness-conserving hadronic weak vector current to the isovector component of the electro-magnetic current:

$$\langle \Delta^{++} | V^\alpha | p \rangle = \sqrt{3} \, \langle \Delta^+ | J_{EM}^\alpha(T=1) | p \rangle \, ,$$
$$\langle \Delta^0 | V^\alpha | p \rangle = \quad \langle \Delta^+ | J_{EM}^\alpha(T=1) | p \rangle \, .$$

The information on the weak vector transition form-factors C_i^V is obtained from the analysis of photo- and electro-production multipole amplitudes. For Δ electro-excitation, the allowed multipoles are the dominant magnetic dipole M_{1+} and the electric and coulomb quadrupole amplitudes E_{1+} and S_{1+}, which are found to be much smaller than M_{1+} [2,3]. If we assume that M_{1+} dominates the electro-production amplitude, we have $C_5^V = C_6^V = 0$ and end up with only one independent vector form-factor

$$C_4^V = -\frac{M}{W} \, C_3^V \, .$$

It turns out that electro-production data can be fitted well with a dipole form for C_3^V,

$$C_3^V(Q^2) = 2.05 \left[1 + \frac{Q^2}{0.54 \, \mathrm{GeV}^2} \right]^{-2} \, .$$

An alternative parameterisation of C_3^V which accounts for a small observed deviation from the pure dipole form is

$$C_3^V(Q^2) = 2.05 \left[1 + 9\sqrt{Q^2} \right] \exp\left[-6.3\sqrt{Q^2} \right] \, .$$

The main interest therefore lies in the axial part of the hadronic weak current which is not well known.

Extraction of $C_i^A(Q^2)$ from data

The key assumption in experimental analyses of the axial matrix element is the PCAC. It implies that the divergence of the axial current should vanish as $m_\pi^2 \to 0$, which occurs if the induced pseudo-scalar term with C_6^A (the analogue of G_P in the nucleon case) is dominated by the pion pole. In consequence, C_6^A can be expressed in terms of the strong $\pi N\Delta$ form-factor,

$$\frac{C_6^A(Q^2)}{M^2} = f_\pi \sqrt{\frac{2}{3}} \, \frac{G_{\pi N\Delta}}{2M} \, \frac{1}{Q^2 + m_\pi^2} \, ,$$

while C_5^A and C_6^A can be approximately connected through the off-diagonal Goldberger-Treiman relation [13]. In a phenomenological analysis, $C_3^A(Q^2)$, $C_4^A(Q^2)$, and $C_5^A(Q^2)$ are taken as free parameters and are fitted to the data. The axial form-factors are also parameterised in "corrected" dipole forms

$$C_i^A(Q^2) = C_i^A(0) \left[1 + \frac{a_i Q^2}{b_i + Q^2} \right] \left[1 + \frac{Q^2}{M_A^2} \right]^{-2} .$$

In the simplest approach one takes $a_i = b_i = 0$. Historically, the experimental data on weak pion production could be understood well enough in terms of a theory developed by Adler [14]. For lack of a better choice, Adler's values for $C_i^A(0)$ have conventionally been adopted to fix the fit-parameters at $Q^2 = 0$, i. e.

$$C_3^A(0) = 0 , \tag{3}$$
$$C_4^A(0) = -0.3 , \tag{4}$$
$$C_5^A(0) = 1.2 . \tag{5}$$

In such a situation, one ends up with M_A as the only free fit-parameter.

Several observables are used to fit the Q^2-dependence of the form-factors. Most commonly used are the total cross-sections $\sigma(E_\nu)$, and the angular distributions of the recoiling nucleon

$$\frac{d\sigma}{d\Omega} = \frac{\sigma}{\sqrt{4\pi}} \left[Y_{00} - \frac{2}{\sqrt{5}} \left[\tilde{\rho}_{33} - \frac{1}{2} \right] Y_{20} + \frac{4}{\sqrt{10}} \tilde{\rho}_{31} \operatorname{Re} Y_{21} - \frac{4}{\sqrt{10}} \tilde{\rho}_{3-1} \operatorname{Re} Y_{22} \right] ,$$

where $\tilde{\rho}_{mn}$ are the density matrix elements and Y_{LM} are the spherical harmonics. Better than from the $\tilde{\rho}_{mn}$ coefficients, the Q^2 dependence of the matrix element can be determined from the differential cross-section $d\sigma/dQ^2$. In particular, since the dependence on C_3^A and C_4^A is anticipated to be weak at $Q^2 \sim 0$, then

$$\frac{d\sigma}{dQ^2}(Q^2 = 0) \propto (C_5^A(0))^2 .$$

The refinements of this crude approach are dictated by several observations. If the target is a nucleus (for example, the deuteron which is needed to access specific charge channels), nuclear effects need to be estimated. Another important correction arises due to the finite energy width of the Δ. In addition, the non-zero mass of the scattered muon may play a role at low Q^2.

All these effects have been addressed carefully in [15]. The sensitivity of the differential cross-section to different nucleon-nucleon potentials was seen to be smaller than 10 % even at $Q^2 < 0.1 \,\mathrm{GeV}^2$. In the range above that value, this allows one to interpret inelastic data on the deuteron as if they were data obtained on the free nucleon. The effect of non-zero muon mass is even less pronounced: it does not exceed 5 % in the region of $Q^2 \sim 0.05 \,\mathrm{GeV}^2$. The energy dependence of the width of the Δ resonance was observed to have a negligible effect on the cross-section. The final value based on the analysis of Argonne data [9] is

$$C_5^A(0) = 1.22 \pm 0.06 . \tag{6}$$

At present, this is the best estimate for $C_5^A(0)$, although a number of phenomenological predictions also exist [16]. We adopt this value for the purpose of comparison to our calculations. There is also some scarce, but direct experimental evidence from a free fit to the data that $C_3^A(0)$ is indeed small and $C_4^A(0)$ is close to the Adler's value of -0.3 (see Figure 1). We use $C_4^A(0) = -0.3$ in our comparisons in the next section.
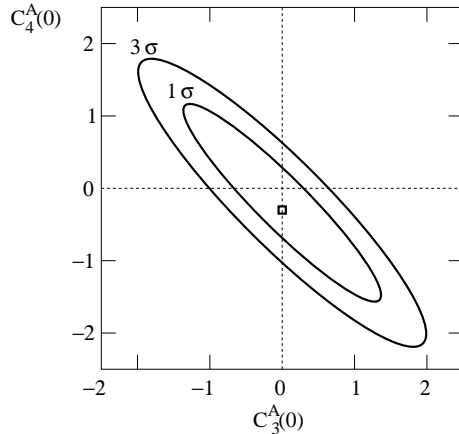

Fig. 1. One- and three-standard deviation limits on $C_3^A(0)$ and $C_4^A(0)$ as extracted from measurements of $\nu_\mu p \rightarrow \mu^- \Delta^{++}$. The square denotes the model predictions by Adler [14]. (Figure adapted after [7].)

4   Interpretation of $C_i^A(Q^2)$ in the linear σ-model

The axial N-Δ transition amplitudes can be interpreted in an illustrative way in quark models involving chiral fields like the linear σ-model (LSM), which may reveal the importance of non-quark degrees of freedom in baryons. Due to difficulties in consistent incorporation of the pion field, the model predictions for these amplitudes are very scarce [17]. The present work [18,19] was partly also motivated by the experience gained in the successful phenomenological description of the quadrupole electro-excitation of the Δ within the LSM, in which the pion cloud was shown to play a major role [20].

4.1   Two-radial mode approach

We have realised that by treating the nucleon and the Δ in the LSM in a simpler, one-radial mode ansatz, the off-diagonal Goldberger-Treiman relation can not be satisfied. For the calculation of the amplitudes in the LSM, we have therefore used the two-radial mode ansatz for the physical baryon states which allows for different pion clouds around the bare baryons. The physical baryons are obtained

from the superposition of bare quark cores and coherent states of mesons by the Peierls-Yoccoz angular projection. For the nucleon we have the ansatz

$$|N\rangle = \mathcal{N}_N P^{\frac{1}{2}} \left[\Phi_N|N_q\rangle + \Phi_{N\Delta}|\Delta_q\rangle\right] ,\tag{7}$$

where $\mathcal{N}_N$ is the normalisation factor. Here Φ_N and $\Phi_{N\Delta}$ stand for hedgehog coherent states describing the pion cloud around the bare nucleon and bare Δ, respectively, and $P^{\frac{1}{2}}$ is the projection operator on the subspace with isospin and angular momentum $\frac{1}{2}$. Only one profile for the σ field is assumed. For the Δ we assume a slightly different ansatz to ensure the proper asymptotic behaviour. We take

$$|\Delta\rangle = \mathcal{N}_\Delta \left\{ P^{\frac{3}{2}} \Phi_\Delta|\Delta_q\rangle + \int dk\,\eta(k)[a^\dagger_{mt}(k)|N\rangle]^{\frac{3}{2}\frac{3}{2}} \right\} ,\tag{8}$$

where $\mathcal{N}_\Delta$ is the normalisation factor, $|N\rangle$ is the ground state and $[\ ]^{\frac{3}{2}\frac{3}{2}}$ denotes the pion-nucleon state with isospin $\frac{3}{2}$ and spin $\frac{3}{2}$. We have interpreted the localised model states as wave-packets with definite linear momentum, as elaborated in [13].

4.2   Calculation of helicity amplitudes

We use the kinematics and notation of [13]. For the quark contribution to the two transverse ($\lambda = 1$) and longitudinal ($\lambda = 0$) helicity amplitudes we obtain

$$\tilde{A}^{(q)}_{s_\Delta\lambda} = -\langle\Delta_{s_\Delta\,\frac{1}{2}}| \int d\mathbf{r}\, e^{ikz}\psi^\dagger\alpha_\lambda\gamma_5\tfrac{1}{2}\tau_0\psi|N_{s_\Delta-\lambda\,\frac{1}{2}}\rangle$$

$$\tilde{A}^{(q)}_{s_\Delta\lambda} = -\tfrac{1}{2}\mathcal{N}_\Delta \int dr\,r^2 \bigg\{$$

$$\left[j_0(kr)\left(u_\Delta u_N - \tfrac{1}{3}v_\Delta v_N\right) + \tfrac{2}{3}(3\lambda^2-2)\,j_2(kr)v_\Delta v_N \right]\langle\Delta_b\|\sigma\tau\|N\rangle$$

$$- c_\eta \left[j_0(kr)\left(u_N^2 - \tfrac{1}{3}v_N^2\right) + \tfrac{2}{3}(3\lambda^2-2)\,j_2(kr)v_N^2 \right]$$

$$\times \left[\tfrac{4}{9}\langle N\|\sigma\tau\|N\rangle + \tfrac{1}{36}\langle N\|\sigma\tau\|N(J=\tfrac{3}{2})\rangle \right] \bigg\} C^{\frac{3}{2}\,s_\Delta}_{\frac{1}{2}\,s_\Delta-\lambda\,1\lambda}\, C^{\frac{3}{2}\,\frac{1}{2}}_{\frac{1}{2}\,\frac{1}{2}\,1\,0} .$$

Here u and v are upper and lower components of Dirac spinors for the nucleon and the Δ, while c_η is a coefficient involving integrals of the function $\eta(k)$ appearing in (8). The reduced matrix elements of $\sigma\tau$ can be expressed in terms of analytic functions with intrinsic numbers of pions as arguments. In all three cases, we take $s_\Delta = \frac{3}{2}$. For the scalar amplitudes, we take $\lambda = 0$ and $s_\Delta = \frac{1}{2}$, and obtain

$$\tilde{S}^{(q)} = -\langle\Delta_{\frac{1}{2}\frac{1}{2}}| \int d\mathbf{r}\, e^{ikz}\psi^\dagger\gamma_5\tfrac{1}{2}\tau_0\psi|N_{\frac{1}{2}\frac{1}{2}}\rangle$$

$$= \tfrac{1}{3}\mathcal{N}_\Delta \int dr\,r^2\, j_1(kr)\,(u_\Delta v_N - v_\Delta u_N)\,\langle\Delta_b\|\sigma\tau\|N\rangle .$$

For the non-pole meson contribution to the transverse and longitudinal helicity amplitudes we assume the same σ profiles around the bare states, but different

for the physical states. Introducing an "average" σ field $\bar{\sigma}(r) \equiv \frac{1}{2}(\sigma_N(r) + \sigma_\Delta(r))$ we obtain

$$
\begin{aligned}
\tilde{A}^{(m)}_{s_\Delta \lambda} &= \langle \Delta_{s_\Delta \frac{1}{2}} | \int d\mathbf{r}\, e^{ikz} \left((\sigma - f_\pi)\nabla_\lambda \pi_0 - \pi_0 \nabla_\lambda \sigma \right) |N_{s_\Delta - \lambda \frac{1}{2}}\rangle \\
&= \frac{4\pi}{3}\left\{ \int dr\, r^2\, j_0(kr) \left[\left((\bar{\sigma} - f_\pi)\left(\frac{d\varphi_{\Delta N}}{dr} + \frac{2\varphi_{\Delta N}}{r} \right) - \frac{d\bar{\sigma}}{dr}\,\varphi_{\Delta N} \right) \right] \right. \\
&\quad \left. + (3\lambda^2 - 2) \int dr\, r^2\, j_2(kr)\left[\left((\bar{\sigma} - f_\pi)\left(\frac{d\varphi_{\Delta N}}{dr} - \frac{\varphi_{\Delta N}}{r} \right) - \frac{d\bar{\sigma}}{dr}\,\varphi_{\Delta N} \right) \right] \right\} \\
&\quad \times C^{\frac{3}{2}\,s_\Delta}_{\frac{1}{2}\,s_\Delta - \lambda\,1\lambda}\, C^{\frac{3}{2}\,\frac{1}{2}}_{\frac{1}{2}\,\frac{1}{2}\,1\,0}\,,
\end{aligned}
$$

where $\varphi_{\Delta N} = \langle \Delta | \pi | N \rangle$. To compute the scalar amplitude, we make use of the off-diagonal virial relation derived in [13] and define

$$
\sigma^P(r) = \int_0^\infty dk\, k^2 \sqrt{k^2 + m_\sigma^2}\, \sqrt{\frac{2}{\pi}}\, j_0(kr)\, \sigma(k)\,.
$$

We obtain

$$
\begin{aligned}
\tilde{S}^{(m)} &= -\langle \Delta_{\frac{1}{2}\frac{1}{2}} | \int d\mathbf{r}\, e^{ikz}\left((\sigma - f_\pi)P_{\pi 0} - P_\sigma \pi_0 \right) |N_{\frac{1}{2}\frac{1}{2}}\rangle \\
&= -\frac{8\pi}{3} \int dr\, r^2\, j_1(kr) \left\{ \frac{1}{2}\left(\sigma_N^P(r) - \sigma_\Delta^P(r) \right) \varphi_{\Delta N}(r) - (\bar{\sigma}(r) - f_\pi)\,\omega_* \varphi_{\Delta N}(r) \right\}\,.
\end{aligned}
$$

By using

$$
\tilde{A}_{s_\Delta \lambda} = \left(A^0 - (3\lambda^2 - 2)A^2 \right) C^{\frac{3}{2}\,s_\Delta}_{\frac{1}{2}\,s_\Delta - \lambda\,1\lambda}\, C^{\frac{3}{2}\,\frac{1}{2}}_{\frac{1}{2}\,\frac{1}{2}\,1\,0}\,,
$$

the quark and non-pole meson contributions to the transverse amplitudes can finally be broken into $L = 0$ and $L = 2$ pieces,

$$
\tilde{A}^A_{\frac{3}{2}} = \sqrt{\frac{2}{3}}\left(A^0 - A^2 \right)\,, \tag{9}
$$

$$
\tilde{A}^A_{\frac{1}{2}} = \frac{1}{\sqrt{3}} \tilde{A}^A_{\frac{3}{2}} = \frac{\sqrt{2}}{3}\left(A^0 - A^2 \right)\,, \tag{10}
$$

$$
\tilde{L}^A = \frac{2}{3}\left(A^0 + 2A^2 \right)\,, \tag{11}
$$

and inserted into (76), (77), and (78) of [13]. The pole part of the meson contribution is

$$
C^A_{6\,(\text{pole})}(Q^2) = f_\pi \frac{G_{\pi N \Delta}(Q^2)}{2M_N} \frac{M_N^2}{m_\pi^2 + Q^2} \sqrt{\frac{2}{3}}\,.
$$

The strong $N\Delta$ form-factor $G_{\pi N \Delta}$ can be computed through

$$
\frac{G_{\pi N \Delta}(Q^2)}{2M_N} \frac{M_\Delta + M_N}{2M_\Delta} = \frac{1}{i\,k}\langle \Delta \parallel \int d\mathbf{r}\, e^{i\mathbf{kr}}\, J(\mathbf{r}) \parallel N \rangle\,,
$$

where the current J has a component corresponding to the quark source and a component originating in the meson self-interaction term (see (58) of [13]),

$$J_0(\mathbf{r}) = j_0(\mathbf{r}) + \frac{\partial U(\sigma, \vec{\pi})}{\partial \pi_0(\mathbf{r})} \;.$$

4.3   Results

Fig. 2 shows the $C_5^A(Q^2)$ amplitude with the quark-meson coupling constant of $g = 4.3$ and $m_\sigma = 600\,\text{MeV}$ compared to the experimentally determined form-factors. The figure also shows the $C_5^A(Q^2)$ calculated from the strong $\pi N\Delta$ form-factor using the off-diagonal Goldberger-Treiman relation.
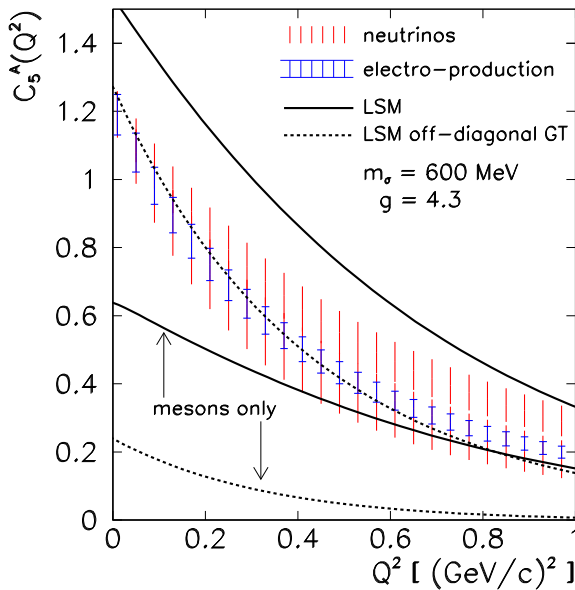
Fig. 2. The amplitude $C_5^A(Q^2)$ in the two-radial mode LSM. The experimental uncertainty at $Q^2 = 0$ is given by Eq. (6). The error ranges are given by the spread in the axial-mass parameter M_A as determined from neutrino scattering experiments (broader range, [11]) and from electro-production of pions (narrower range, Eq. (2)). Full curves: calculation from helicity amplitudes (9), (10), and (11); dashed curves: calculation from $G_{\pi N\Delta}$.

The magnitude of $C_5^A(Q^2)$ is overestimated in the LSM, with $C_5^A(0)$ about 25 % higher than the experimental average. Still, the Q^2-dependence follows the experimental one very well: the M_A from a dipole fit to our calculated values agrees to within a few percent with the experimental M_A. On the other hand, with $C_5^A(Q^2)$ determined from the calculated strong $\pi N\Delta$ form-factor, the absolute normalisation improves, while the Q^2 fall-off is steeper, with $M_A \approx 0.80\,\text{GeV}$. Since the model states are not exact eigenstates of the LSM Hamiltonian, the discrepancy between the two calculated values in some sense indicates the quality

of the computational scheme. At $Q^2 = -m_\pi^2$ where the off-diagonal Goldberger-Treiman relation is expected to hold, the discrepancy is 17 %. The disagreement between the two approaches can be attributed to an over-estimate of the meson strength, a characteristic feature of LSM where only the meson fields bind the quarks.

Essentially the same trend is observed in the "diagonal" case: for the nucleon we obtain $g_A = 1.41$. The discrepancy with respect to the experimental value of 1.27 is commensurate with the disagreement in $C_5^A(0)$. The overestimate of g_A and $G_A(Q^2)$ was shown to persist even if the spurious centre-of-mass motion of the nucleon is removed [21]. An additional projection onto non-zero linear momentum therefore does not appear to be feasible.

The effect of the meson self-interaction is relatively less pronounced in the strong coupling constant (only ~ 20 %) than in $C_5^A(Q^2)$. Both $G_{\pi N\Delta}(0)$ and $G_{\pi NN}(0)$ are over-estimated in the model by ~ 10 %. Still, the ratio $G_{\pi N\Delta}(0)/G_{\pi NN}(0) = 2.01$ is considerably higher than either the familiar SU(6) prediction $\sqrt{72/25}$ or the mass-corrected value of 1.65 [22], and compares reasonably well with the experimental value of 2.2. This improvement is mostly a consequence of the renormalisation of the strong vertices due to pions.
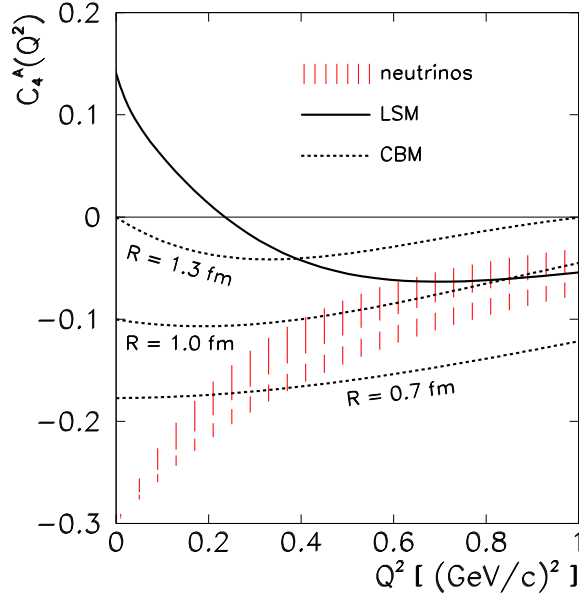

Fig. 3. The amplitude $C_4^A(Q^2)$ in the two-radial mode linear σ-model, with model parameters and experimental uncertainties due to the spread in M_A as in Fig. 2, and in the Cloudy-Bag Model (see below for discussion). Experimentally, $C_4^A(0) = -0.3 \pm 0.5$ (see [7] and Fig. 1). For orientation, the value for $C_4^A(0)$ is used without error-bars.

The determination of the $C_4^A(Q^2)$ is less reliable because the meson contribution to the scalar component of this amplitude [13] is very sensitive to small variations of the profiles. However, the experimental value is very uncertain as well.

Neglecting the non-pole contribution to the scalar amplitude and $C_6^A(Q^2)$ (with the pole contribution canceling out), $C_4^A(Q^2)$ is fixed to $-(M_N^2/2M_\Delta^2)\,C_5^A(Q^2)$. At $Q^2 = 0$, this is in excellent numerical agreement with (4). In the LSM, the non-pole contribution to $C_6^A(Q^2)$ happens to be non-negligible and tends to increase $C_4^A(Q^2)$ at small Q^2, as seen in Fig. 3. An almost identical conclusion regarding $C_4^A(Q^2)$ applies in the case of the Cloudy-Bag Model, as shown below.

The C_6^A amplitude is governed by the pion pole for small values of Q^2 and hence by the value of $G_{\pi N\Delta}$ which is well reproduced in the LSM, and underestimated by $\sim 35\,\%$ in the Cloudy-Bag Model. Fig. 4 shows that the non-pole contribution becomes relatively more important at larger values of Q^2.
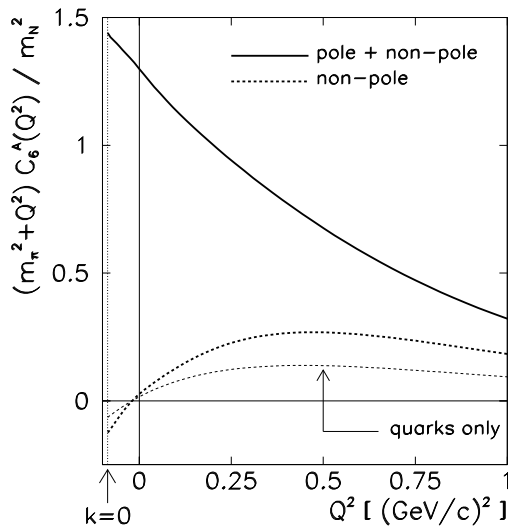

Fig. 4. The non-pole part and the total amplitude $C_6^A(Q^2)$ in the two-radial mode linear σ-model. Model parameters are as in Fig. 2.

5   Interpretation of $C_i^A(Q^2)$ in the Cloudy-Bag Model

For the calculation in the Cloudy-Bag Model (CBM) we have assumed the usual perturbative form for the pion profiles using the experimental masses for the nucleon and Δ. Since the pion contribution to the axial current in the CBM has the form $f_\pi \partial^\alpha \boldsymbol{\pi}$, only the quarks contribute to the $C_4^A(Q^2)$ and $C_5^A(Q^2)$, while $C_6^A(Q^2)$ is almost completely dominated by the pion pole (see contribution by B. Golli [13]). With respect to the LSM, the sensitivity of the axial form-factors to the non-quark degrees of freedom is therefore almost reversed.

In the CBM, only the non-pole component of the axial current contributes to the amplitudes, and as a result the $C_5^A(0)$ amplitude is less than 2/3 of the experimental value. The behaviour of $C_5^A(Q^2)$ (see Fig. 5) is similar as in the pure MIT Bag Model (to within 10 %), with fitted $M_A \sim 1.2\,\text{GeV}\,\text{fm}/R$. The off-diagonal

Goldberger-Treiman relation is satisfied in the CBM, but C_5^A from $G_{\pi N\Delta}$ has a steeper fall-off with fitted $M_A \sim 0.8\,\mathrm{GeV\,fm}/R$.
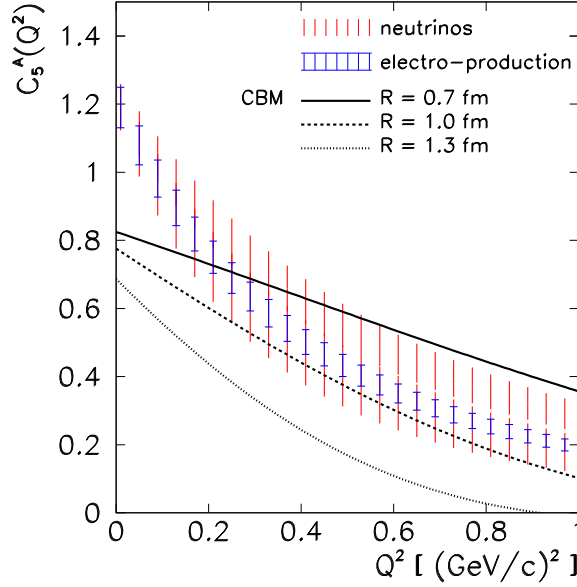

Fig. 5. The amplitude $C_5^A(Q^2)$ in the Cloudy-Bag Model for three values of the bag radius. Experimental uncertainties are as in caption to Fig. 2.

The large discrepancy can be partly attributed to the fact that the CBM predicts a too low value for $G_{\pi NN}$, and consequently $G_{\pi N\Delta}$. We have found that the pions increase the $G_{\pi N\Delta}/G_{\pi NN}$ ratio by $\sim 15\,\%$ through vertex renormalisation. The effect is further enhanced by the mass-correction factor $2M_\Delta/(M_\Delta + M_N)$, yet suppressed in the kinematical extrapolation of $G_{\pi N\Delta}(Q^2)$ to the SU(6) limit. This suppression is weaker at small bag radii R: the ratio drops from 2.05 at $R = 0.7\,\mathrm{fm}$ to 1.60 (below the SU(6) value) at $R = 1.3\,\mathrm{fm}$.

The determination of the $C_4^A(Q^2)$ is less reliable for very much the same reason as in the LSM. The non-pole contribution to $C_6^A(Q^2)$ tends to add to the excessive strength of $C_4^A(Q^2)$ at low Q^2, as seen in Fig. 3. Never the less, the experimental data are too coarse to allow for a meaningful comparison to the model. For technical details regarding the calculation in the CBM, refer to [13].

References

1. A. M. Bernstein, to appear in Proceedings of the VII Conference on Electron-Nucleus Scattering, June 24-28, 2002, Elba, Italy.
2. K. Joo et al., Phys. Rev. Lett. **88** (2002) 122001;
   J. Volmer et al., Phys. Rev. Lett. **86** (2001) 1713;
   D. Gaskell et al., Phys. Rev. Lett. **87** (2001) 202301;
   V. Frolov et al., Phys. Rev. Lett. **82** (1999) 45.

3. Th. Pospischil et al., Phys. Rev. Lett. **86** (2001) 2959;
   C. Mertz et al., Phys. Rev. Lett. **86** (2001) 2963;
   S. Choi et al., Phys. Rev. Lett. **71** (1993) 3927.
4. A. Liesenfeld et al., Phys. Lett. B **468** (1999) 20.
5. V. Bernard, N. Kaiser, U.–G. Meißner, Phys. Rev. Lett. **69** (1992) 1877;
   V. Bernard, N. Kaiser and U.–G. Meißner, Phys. Rev. Lett. **72** (1994) 2810.
6. V. Bernard, L. Elouadrhiri, U.–G. Meißner, J. Phys. G: Nucl. Part. Phys. **28** (2002) R1.
7. S. J. Barish et al., Phys. Rev. D **19** (1979) 2521.
8. P. Allen et al., Nucl. Phys. B **176** (1980) 269.
9. G. M. Radecky et al., Phys. Rev. D **25** (1982) 1161.
10. T. Kitagaki et al., Phys. Rev. D **34** (1986) 2554.
11. T. Kitagaki et al., Phys. Rev. D **42** (1990) 1331.
12. C. H. Llewellyn Smith, Phys. Rep. **3C** (1972) 261.
13. B. Golli, L. Amoreira, M. Fiolhais, S. Širca, these Proceedings; hep-ph/0211293
14. S. Adler, Ann. Phys. **50** (1968) 189.
15. S. K. Singh, M. J. Vicente-Vacas, E. Oset, Phys. Lett. B **416** (1998) 23;
    L. Alvarez-Ruso, S. K. Singh, M. J. Vicente-Vacas, Phys. Rev. C **57** (1998) 2693;
    L. Alvarez-Ruso, S. K. Singh, M. J. Vicente-Vacas, Phys. Rev. C **59** (1999) 3386;
    L. Alvarez-Ruso, E. Oset, S. K. Singh, M. J. Vicente-Vacas, Nucl. Phys. A **663**/**664** (2000) 837c.
16. N. C. Mukhopadhyay et al., Nucl. Phys. A **633** (1998) 481.
17. Jùn L´iu, N. C. Mukhopadhyay, L. Zhang, Phys. Rev. C **52** (1995) 1630.
18. S. Širca, L. Amoreira, M. Fiolhais, B. Golli, to appear in R. Krivec, B. Golli, M. Rosina, S. Širca (eds.), *Proceedings of the XVIII European Conference on Few-Body Problems in Physics*, 7–14 September 2002, Bled, Slovenia; hep-ph/0211290
19. B. Golli, S. Širca, L. Amoreira, and M. Fiolhais, submitted for publication in Phys. Lett. B, hep-ph/0210014.
20. M. Fiolhais, B. Golli, S. Širca, Phys. Lett. B **373** (1996) 229.
21. M. Rosina, M. Fiolhais, B. Golli, S. Širca, Proceedings of the "Nuclear and Particle Physics with CEBAF at Jefferson Lab" Meeting, November 3–10, 1998, Dubrovnik, Croatia, Fizika B **8** (1999) 383.
22. T. R. Hemmert, B. R. Holstein, N. C. Mukhopadhyay, Phys. Rev. D **51** (1995) 158.